Production of Transportation Fuel Range Middle Distillates via Fischer-Tropsch Synthesis with Integrated Product Upgrading under Supercritical Phase Conditions

by

Sihe Zhang

A dissertation submitted to the Graduate Faculty of
Auburn University
in partial fulfillment of the
requirements for the Degree of
Doctor of Philosophy

Auburn, Alabama
May 5th, 2013

Approved by

Christopher B. Roberts, Committee Chair, Dean of Engineering
Mario R. Eden, Chair of Chemical Engineering
Ram B. Gupta, Graduate Program Chair of Chemical Engineering
Sushil Adhikari, Assistant Professor of Biosystem Engineering
Tom Gallagher, Associate Professor of School of Forestry and Wildlife Sciences

Abstract

There has been a great deal of contemporary interest in the utilization of a variety of carbonaceous feedstocks to produce readily usable transportation fuels via synthesis gas (syngas, a mixture of H_2 and CO). Specifically, Fischer-Tropsch synthesis (FTS) can be used to convert synthesis gas into hydrocarbon products and oxygenates. In Fischer-Tropsch synthesis, a set of surface-catalyzed polymerization reactions take place which convert syngas into hydrocarbons and oxygenates with a broad range of carbon chain lengths and type, typically over an iron or cobalt based catalyst. With appropriate product separation and upgrading procedures, these FTS products can be further processed and converted into high quality fuels and value-added chemicals. Utilization of supercritical fluid (SC) media in FTS (SC-FT) has been demonstrated to provide certain benefits including a reduction in the selectivity towards CH_4 and CO_2 as a result of the enhanced heat transfer that the supercritical solvent offers compared to gas phase FTS (GP-FT). In addition, the improved hydrocarbon solubilities in the SC medium can further result in prolonged catalyst life and activity maintenance.

The objective of this work is to explore and demonstrate the effect of integration of product upgrading reactions (such as oligomerization and hydrocracking) subsequent to FTS in a single pass operation and the benefits of introducing supercritical fluid media into these heterogeneous reactions. In chapter 1, a background introduction is given with respect to Gas-To-Liquid (GTL) technology, FTS, FTS product upgrading reactions, and the utilization of supercritical fluid media as reaction solvent.

In chapter 2, the catalytic performance results are presented for each individual reaction, namely the FTS reaction, oligomerization reaction and hydrocracking reaction, separately. A traditional precipitated iron-based low temperature FTS catalyst (since iron-based FTS catalysts are more feasible for a wider range of inlet syngas H_2/CO ratio than cobalt-based FTS catalysts) was prepared and evaluated under gas phase conditions (GP-FT). The catalytic oligomerization activity of amorphous silica alumina (ASA) has been examined to convert the light olefin FTS products into middle distillate range hydrocarbons. A Pd/ASA (1.0 wt.%) hydrocracking/isomerization catalyst has been made using wetness impregnation method, to alter the long-chain FTS hydrocarbons into shorter fuel range products.

In chapter 3, the performance of FTS with direct subsequent product upgrading has been evaluated using a newly designed reactor system. A vertical fixed bed reactor system with three catalyst beds arranged sequentially has been designed and used to incorporate Fischer-Tropsch synthesis in the first bed, oligomerization in the second bed and hydrocracking/isomerization in the third bed (FTOC). In addition, the reactor system performance has been examined under both gas phase and supercritical phase conditions. The gas phase FTOC (GP-FTOC) results of this study have shown a reduction of olefin selectivity and a marked enhancement of branched-paraffins. Furthermore, wax in C_{26+} range was decreased in GP-FTOC operation compared to GP-FT operation. Also, a considerable amount of branched paraffins and aromatics were generated in the gasoline/kerosene range in GP-FTOC. The work in this chapter also has examined the utilization of supercritical hexane as the reaction medium in SC-FT and supercritical phase FTOC (SC-FTOC) where the use of this supercritical solvent medium resulted in a significant reduction in both methane selectivity and carbon dioxide selectivity as well as a well maintained catalyst activity compared to the analogous gas phase operations. Significant quantities of aldehydes and

cyclo-parafins were collected as reaction intermediates in SC-FT and in SC-FTOC, respectively, though these species were not observed in appreciable amounts in the traditional gas phase operation.

To improve our understanding of the reactions that take place in each of these upgrading beds, detailed studies were performed and reported in chapter 4. FTS plus oligomerization (FTO) and FTS plus hydrocracking/isomerization (FTC) have been investigated using a dual reaction bed experimental apparatus. This particular study provided a detailed evaluation of effect that each of the product upgrading reactions had on the FTS products that were produced in the first reactor bed. Significantly improved CO conversion has been observed in supercritical phase FTO (SC-FTO) compared to the CO conversion that was obtained from gas phase FTO (GP-FTO). Similarly, greatly enhanced CO conversion has been shown to occur in supercritical phase (SC FTC) compared to the value of CO conversion that was obtained from the gas phase FTC operation (GP-FTC). Moreover, the selectivity toward CO_2 and CH_4 was greatly reduced under supercritical phase conditions compared to gas phase operation which is consistent with previously documented observations for the use of a supercritical solvent in FTS. The liquid product distribution obtained from GP-FTC exhibited a substantial enhancement in the amount of branched hydrocarbon products generated as well as a markedly decreased heavy wax selectivity. This result indicates that the isomerization and cracking activity is significant in the hydrocracking/isomerization stage in GP-FTC. Analysis of the liquid products that were obtained from SC-FTC also reveals that a high degree of activity towards the hydrogenation reaction occurred in the hydrocracking/isomerization stage. Characterization of each of the catalysts employed in each of these catalytic stages (FTS, oliomerization, and hydrocracking/isomerization) were performed using BET surface area and pore volume analysis as well as SEM microscopy.

Moreover, the phase behavior of the FT reaction mixtures under these supercritical phase conditions has also been studied and described within this dissertation, presented in chapter 5. Experiments to determine the critical point loci of different model SC-FTS reaction mixtures have been performed using a high pressure, variable-volume view cell system. Specifically, the critical point loci of the mixtures of syngas + hexane (with different syngas/hexane ratios), syngas + hexane + tetradecane (which serves as a typical FTS paraffin product), and syngas + hexane + tetradecane + H_2O (which is an important FTS side product that can significantly affect the phase behavior of the SC-FTS reaction mixture) have been carefully measured in order to understand the effects of these FTS reaction and product species on the phase behavior of these highly nonideal mixtures.

Finally, in chapter 6, a series of future investigations have been proposed that will further improve the feasibility of this multi-bed reactor system. These proposed studies include determination of the optimal operational parameters of each of the catalytic reaction bed of this multi-bed system, optimization of the multi-bed catalytic system by further modification of the catalyst system employed catalyst system as well as more elaborate evaluation of the FTS fuels derived.

Acknowledgments

My sincere appreciation and gratitude goes to Dr. Christopher B. Roberts, my research advisor, for his scientific support, professional suggestions, inspiring guidance, generous encouragement, and being an incentive model for my future career and life.

I am grateful to my committee members: Dr. Mario Eden, Dr. Ram Gupta and Dr. Sushil Adhikari and Dr. Tom Gallagher for their consistent assistance and professional suggestions. Brian Schweiker and Kenneth Hornsby provided frequent help without which this work would have been impossible to be finished. I would also like to thank former members of Dr. Roberts' research group: Dr. Xiwen Huang, Dr. Nimir Elbashir and Dr. Ed Durham for their pioneering contribution in setting up this catalysis and supercritical fluid processing laboratory; Dr. Juncheng Liu, Dr. Kendall Hurst, Dr. Steve Saunders and Dr. Deborah Bacik for their help in broadening my academic knowledge and scientific techniques; as well as current group members Rajeshwar Chinnawar, Jie Zhong, David Roe, Charlotte Stewart, Pranav Vengsarkar, Jennifer Boice and former undergraduate research assistant Michael Columbus for their invaluable scientific discussions and technical support. I would like to thank my colleague, friend and husband Rui Xu for his continuous support and encouragement.

I am very grateful to my parents Zhang, Yamin and Ma, Ling to whom I dedicate this work. Their endless love and support have paved the way for my life and career.

Table of Contents

List of Tables

List of Figures

List of Abbreviations

GTL   Gas to Liquid

CTL   Coal to Liquid

BTL   Biomass to Liquid

XTL   Carbonaceous source to Liquid

FT or FTS   Fischer-Tropsch Synthesis

SC   Supercritical phase

GP   Gas phase

FTOC   Fischer-Tropsch Synthesis with integrated oligomerization and hydrocracking/isomerization

FTO   Fischer-Tropsch Synthesis with oligomerization

FTC   Fischer-Tropsch Synthesis with hydrocracking/isomerization

EIA   U.S. Energy Information Administration

DOE   U.S. Department of Energy

AU   Auburn University

Chapter 1   Introduction

1.1   Introduction to Gas-To-Liquid Technology and the History of Fischer-Tropsch Synthesis

1.1.1   Gas-To-Liquid Technology

Worldwide energy and chemical production is primarily based on crude oil. In the past four decades, there has been intense interest in finding guaranteed domestic alternatives to crude oil to meet domestic energy demands, due to persistently high oil prices, heavy economic and energy dependence on oil, political uncertainty in certain oil rich countries of the world, etc. According to the Energy Information Administration (EIA), although crude oil is still the leading energy source, coal and natural gas are fast growing components in the worldwide energy production portfolio, as shown in Figure 1.1.
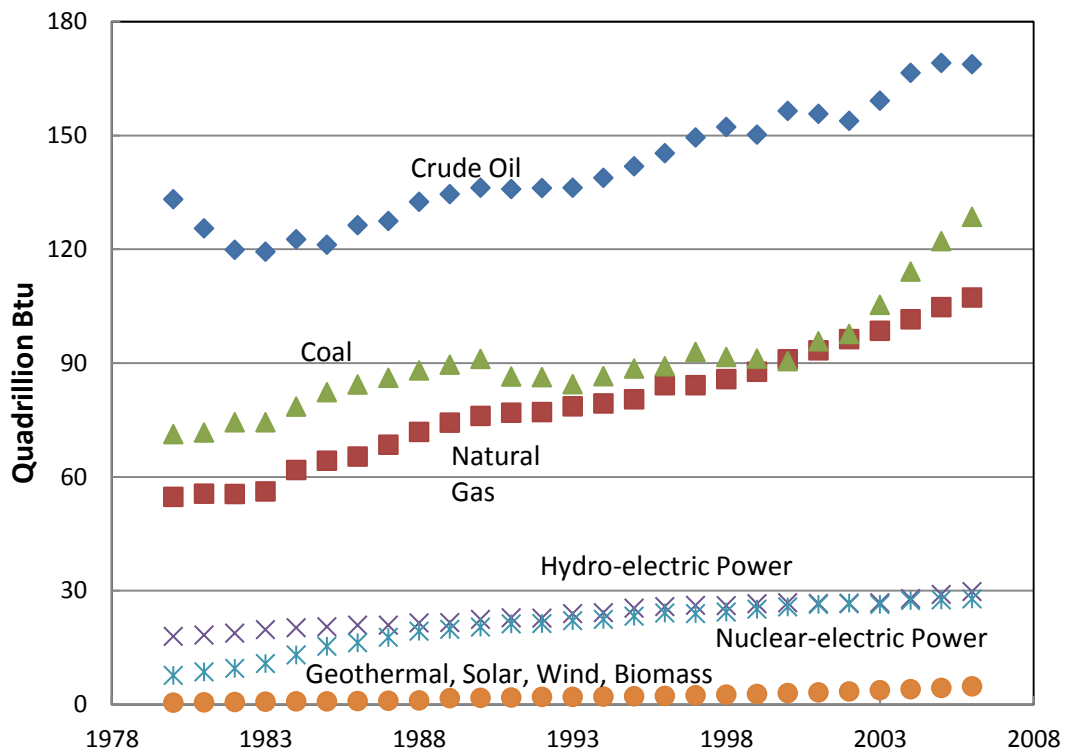
Figure 1.1   World primary energy production by source from 1980 to 2006 (EIA 2012)

In the United States, energy production using coal and natural gas have both surpassed crude oil since 1987 (Figure 1.2). While energy production by coal continues to increase, energy production using both natural gas and crude oil experienced peaks around the 1970's and fell afterwards. However, natural gas utilization for energy production started to increase again since the mid 1980's and later exceeded crude oil for energy production, while crude oil utilization for energy production has shown a gradual decrease during this same period. Energy production using renewable sources has grown rapidly since the 1980's, though it is still far from surpassing the use of crude oil yet.
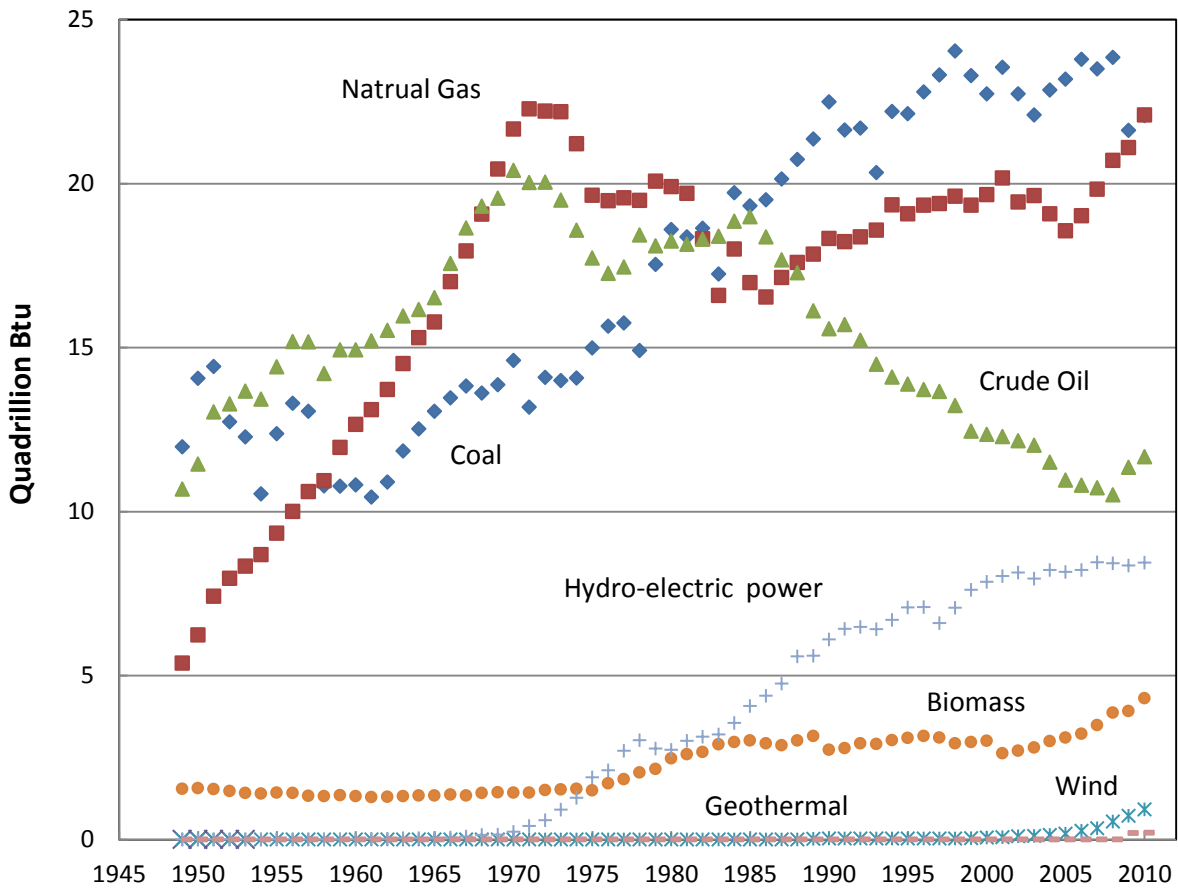
Figure 1.2   U.S. primary energy production by source from 1949 to 2010 (EIA 2012)

Extensive research and continuous improvements in technologies have been utilized to obtain value from resources like natural gas and coal. Gas-to-Liquid (GTL) technology provides an alternative for the utilization of natural gas in producing liquid products compared to the conventional natural gas liquefaction technology that produces liquefied natural gas (LNG). GTL has grown rapidly and has been projected by some to reach a comparable scale or even surpass the LNG industry. This technology can utilize a number of different feedstocks such as coal, biomass, etc. So GTL, and Coal-to-Liquid (CTL), Biomass-to-Liquid (BTL), organic waste to liquid, can be collectively called XTL. XTL technology can be used to produce ultra-clean (low sulphur, low aromatics) transportation fuels, and value-added chemical intermediates, as shown in the following figure.
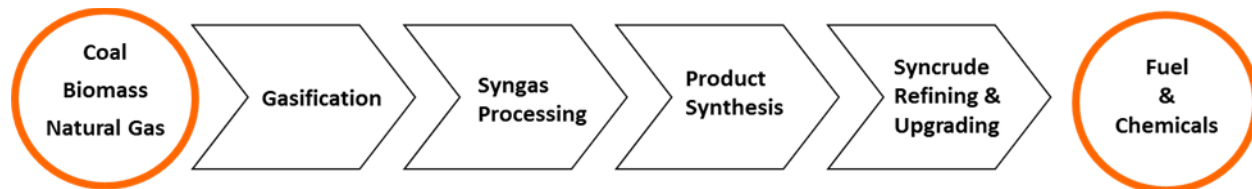
The most widely used approach for conversion of natural gas, coal and biomass to fuels, additives and chemicals is through gasification and gas processing to synthesis gas (syngas: a mixture of H_2 and CO with a variety of H_2/CO ratios). Then, via various product synthesis routes, such as Fischer-Tropsch synthesis (FTS) or methanol synthesis, syngas can be converted into a wide spectrum of desired products including gasoline, jet fuel, diesel, methyl tertiary butyl ether (MTBE), alcohols, etc. A flow diagram is shown to give a demonstration of the broad series of syngas applications in Figure 1.3.
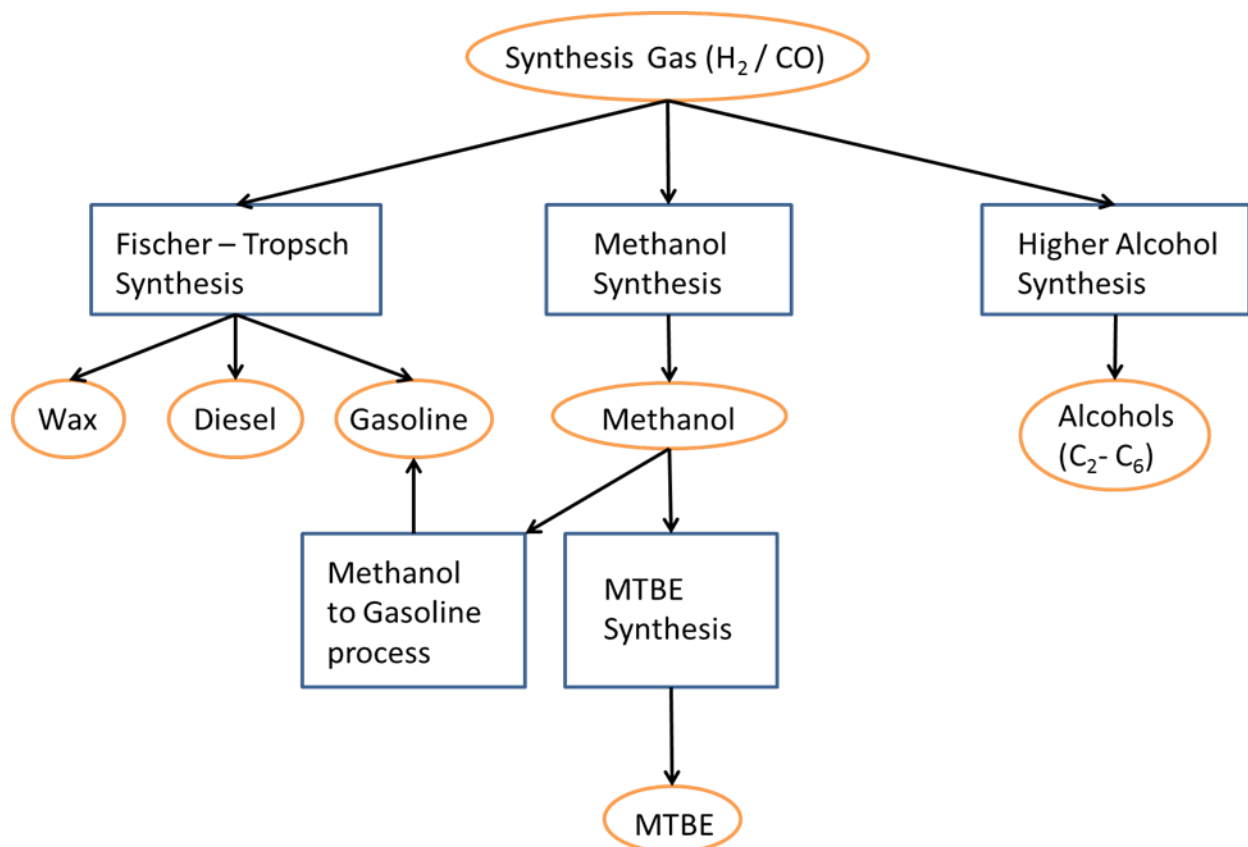
Figure 1.3   Application of synthesis gas on production of fuels, additives and chemicals (MTBE: methyl tertiary butyl ether)

When using natural gas as the carbonaceous source, there are several approaches for its gasification, including steam reforming ($CH_4 + H_2O \rightarrow CO + 3H_2$), dry reforming ($CH_4 + CO_2 \rightarrow 2CO + 2H_2$), or partial oxidation ($CH_4 + \frac{1}{2}O_2 \rightarrow CO + 2H_2$). Considering the economic scale, steam reforming is the best for small scale projects due to no oxygen plant needed, while partial oxidation is the best for larger scale industrial practice for the reason that economies of scale make an oxygen plant economically viable in that case, however, a CO_2 removal process is required (Steynberg & Dry 2004). Due to the syngas being derived from various carbonaceous materials (coal, natural gas or biomass), syngas needs to be processed through to remove various contaminants including a desulfurization step that bring the sulfur content below the maximum sulfur allowable level (10 parts per billion) for the subsequent conversion stages. Unfortunately,

this sulfur removal cannot be adequately achieved by iron oxide sorbents nor molecular sieves (Steynberg & Dry 2004). CoMo and NiMo can be used to convert most sulfur compounds into H_2S (and most halogenates into HX). Zinc oxide can afford an effective absorbance of H_2S (and some activity to convert COS into H_2S, too). There are other issues regarding syngas purity, including nitrogenates, BTX (benzene, toluene, and xylene), tar and particulates (Hamelinck *et al.* 2004).

Fischer-Tropsch technology can be described as a surface-catalyzed polymerization process used to convert C_1 species monomers, formed in situ from synthesis gas (H_2 and CO), into hydrocarbon products and oxygenated hydrocarbons with a broad range of carbon chain lengths and functionalities (Iglesia 1997). Most of the group VIII metals, including Ru, Fe, Co, Ni, have been determined to possess varying degrees of catalytic activity towards the hydrogenation of carbon monoxide (into hydrocarbons and oxygenated hydrocarbons) (Dry 2002). With appropriate separation, upgrading and hydro-processing, these products can be further converted into high quality fuels and chemicals (De Klerk 2009). Compared to crude-oil-derived transportation fuels, FT-derived fuels have some excellent features, such as the absence of sulphur, nitrogen and low aromatic concentration (although the low aromatic content can also be issues relative to elastomer swelling in engines and density) (Steynberg & Dry 2004). What makes FTS unique in the heterogeneous catalysis field is the significant emphasis place on the avoidance of undesirable by-products rather than optimizing production of a single desired-product. Over the course of seven decades of industrial experience, the key challenge to boost industrial application of FT for producing transportation fuels and chemicals involves increasing the economic feasibility, especially for the gasification and syngas preparation/conditioning part, particularly when compared to the relatively low petro-fuel costs (Steynberg & Dry 2004).

For an XTL plant, power generation (the XTL plant must be at least electrically self-sufficient) and hydrogen generation (which must be sufficient for FTS and the sequential product upgrading) are the other major issues (Steynberg & Dry 2004). When considering the economic monetary distribution, taking a GTL plant as an example, using cheap stranded gas it would cost approximately \$20/bbl, of which 25% for the gas, 25% for the operations and 50% for the capital (Steynberg & Dry 2004). As estimated by another group based on using oxygen-blown autothermal reforming, the cost distribution would be 15% for the gas, 21% for the operations and 64% for the capital (28% reforming, 24% FTS system, 23% oxygen plant, 13% product enhancement and 12% power recovery), the energy efficiency would be 65% and carbon efficiency would be 75% (Wilhelm *et al.* 2001).

Using coal as the carbonaceous source, the energy and carbon efficiency would be lower (Eilers *et al*. 1990). This results from the fact that the coal H/C ratio is much lower than that in natural gas leading to higher CO_2 selectivity during gasification and consequently lower efficiency and higher capital cost. Variance of ash levels for different coals calls for discrepant designs of the gasifier. Additionally, the sulfur level in coal is higher than in natural gas, thus regenerable sulfur sorbents are more viable than the sacrificial ones in CTL plants (Steynberg & Dry 2004).

Though biomass is similar to coal, there are more unresolved issues for gasifying biomass, including high tar selectivity, intense ash formation, moisture reduction, and fibrous materials size reduction (Higman & van der Burgt 2003). Biomass preparation (size and moisture reduction), gasification and syngas purification require the majority (around 75%) of the capital cost in BTL through FTS. Dryer biomass can result in more energy efficient gasification however lower H / C ratio in the generated syngas (Hamelinck et al. 2004). Moisture reduction

processes are an energy intensive step and the cost increases remarkably when pushing the moisture content below 10% moisture. An estimated cost of the BTL diesel is approximately $3.40 / gallon, with the capital cost breakdown being 21% for biomass treatment, 18% for gasifier, 18% for syngas cleaning, 15% for oxygen plant, 1% for water-gas-shift (WGS, $CO + H_2O \rightarrow CO_2 + H_2$) reaction, 6% for FTS system, 7% for gas turbine, 11% for heat recovery / steam generation, 4% for other (Faaij *et al*. 2002).

1.1.2   Brief History of Fischer-Tropsch Synthesis

The first successful attempt to hydrogenate CO with H_2 was made by Sabatier and Sanderens, in 1902, by delivering mixtures of H_2 and CO / CO_2 over a Co / Ni catalyst at atmospheric pressure and 200 °C - 300 °C (Keim, 1983). BASF's trial on alkali activated Co / Os catalysts at T > 300 °C and p > 100 bar in 1913 is considered the origin of methanol synthesis. In 1923, Franz Fischer (1877 - 1947) and Hans Tropsch (1889-1935) made an important contribution by discovering high hydrocarbon productivity and selectivity in the conversion of coal-derived syngas. This process was carried out at lower pressure (~ 7bar) on Fe / ZnO and Co / Cr_2O_3 catalysts. Fischer and Tropsch published their hydrocarbon synthesis work in 1926, and henceforth the process has been called Fischer-Tropsch Synthesis (FTS) (Keim 1983, Keim 1986, Khodakov *et al*. 2007). In 1934, the first commercial FT process was licensed by Ruhrchemie, Germany, and in two years the first large-scale FT plant was operational in Braunkohle-Benzin, Germany (Khodakov *et al*. 2007). In 1938, the FT capacity in Germany was approximately 8,000 barrels per day (BPD) (Khodakov *et al.* 2007). In 1943, the production of FT products reached 12,000 BPD worldwide (9 German, 1 French, 4 Japanese and 1 Manchurian facility) (Keim 1986). After World War II, ARGE (Arbeitsgemeinschaft Ruhrchemie and Lurgi) realized their large-scale process with a fixed bed FT reactor in South Africa. In 1950, a 5,000

BPD natural gas FT facility was open in Brownsville, TX (Steynberg & Dry 2004). In 1955, the Sasol One plant was built in Sasolburg in South Africa, utilizing coal as the feedstock with a capacity of 3,000 BPD. Sasol Two and Sasol Three were commissioned for production in 1980 and 1982, respectively. Coal was the major carbon source for both of the plants, with a capacity of 25,000 BPD, separately (Keim 1986, Khodakov *et al*. 2007, Steynberg & Dry 2004). Intensive research and development programs started to flourish in the 1980's due to global concerns about sustainability and diversity of fuel source. As concerns about atmospheric carbon dioxide concentrations emerged, biomass-based FTS was considered as an attractive alternative. For countries with abundant natural gas, FTS using natural gas is promising and economically appealing. In South Africa in 1992, the 12,500 BPD Sasol Mossgas (now PetroSA) plant began operation utilizing natural gas as feedstock (Khodakov *et al*. 2007). The Shell Bintulu plant came into operation in 1993 with capacity of 12500 BPD (Khodakov *et al*., 2007). In 2007, Sasol started their partnership with Qatar Petroleum with a GTL venture, Oryx GTL, in Qatar for a production of 35,000 BPD. In 2009 Sasol started to develop a GTL plant in Nigeria with Chevron and the Nigerian National Petroleum Corporation, aiming to start operation by 2013 (Sasol webpage). A feasibility study is under way to establish a GTL plant in Uzbekistan by Sasol (in partnership with Petronas and Uzbekneftegaz), with an estimated capacity of 15 million tons of GTL product per year (Sasol webpage, Sasol facts 2011). In China, the feasibility study for a CTL plant at the Ningdong Energy and Chemicals base has been completed by Sasol Synthol International (SSI) (Sasol webpage, Sasol facts 2011). The project will be undertaken with Sasol's partner in China, the Shenhua Ningxia Coal Group, and now awaiting for the Chinese Government's approval. In the meantime, Sasol is conducting a pre-feasibility study into a CTL plant in India. Long-term access to the Talcher coalfield in Orissa has been guaranteed by

the Indian government to the SSI and Tata Group joint venture (Sasol webpage, Sasol facts 2011).

1.2 Fischer-Tropsch Reactor and Catalysts

1.2.1 Commercial Fischer-Tropsch Reactor

There are two modes of FTS operation: High Temperature Fischer Tropsch (HTFT) (300 ℃ - 350 ℃, 20 - 40 bars, H_2 / CO « 2) and Low Temperature Fischer Tropsch (LTFT) (200 ℃ - 240 ℃, 20 - 45 bars, H_2 / CO = 1.7 - 2.15). There have been four types of FT reactor configurations used commercially:

Tubular fixed bed reactor

Circulating fluidized bed reactor

Slurry phase reactor

Fluidized bed reactor

For HTFT, two types of fluidized bed reactors have been employed, the circulating fluidized bed (CFD) reactor (1950 to present) and the Sasol Advanced Synthol (SAS) reactor (1989 to present) for production of light alkenes and gasoline. Fused iron catalysts are utilized as HTFT catalysts. For LTFT, both Tubular Fixed Bed Reactor (TFBR) (pre-WWII to present) and Sasol Slurry Phase Distillate reactor (SSPD, 1993 to present) are used for the FTS with supported cobalt based catalysts or precipitated iron base catalysts (Dry 2002, Steynberg & Dry 2004, Boucher 2008).

In HTFT operation, there are two phases (solid catalyst phase and bulk gas phase) and no liquid phase is present outside the catalyst particles in the HTFT fluidized bed reactors, because the presence of the liquid phase will markedly decrease operability by increasing particle agglomeration thus sacrificing fluidization. Therefore, the low carbon chain growth probability

9

(which indicates the reaction tendency towards heavy products, as will be explained later) is kept low at 0.7, and consequently resulting the light olefins and gasoline being the major products of the HTFT process (Steynberg & Dry 2004). There are a number of advantages of fluidized bed operation, such as its high heat exchange rates (resulting from the high degree of turbulant flow patterns), the reactor operates at high temperature with large throughputs of feed gas. The reactor can be kept virtually isothermal and the operation conditions are controlled precisely so that no excessive liquid product will condense in the catalyst pores. (Steynberg & Dry 2004, Steynberg et al. 1999). For HTFT, a fused magnetite based catalyst, with K_2O and structural promoters such as Al_2O_3, etc., is the only viable catalyst (Steynberg et al. 1999).

Due to advanced technology the Sasol incorporated in the SAS reactor, the production capacity of the Secunda plant (Sasol) increased from 5.1 million tons per year to 7.1 million tons per year. The SAS catalyst size is typically 5-100μm and the SAS reactor can be operated between 20 and 40 bar and is run at around 340 ºC. The sixteen CFB reactors in Secunda (Sasol, each with a capacity of 7500 BPD) were all replaced by eight SAS reactors (four 8m diameter reactors, each with a capacity of 11 000 BPD and four 10.7m diameter SAS reactors, each with a capacity of 20 000 BPD) between 1995 and 1999. There are still three Synthol CFB reactors installed at the Sasol Mossgas (now PetroSA) plant (natural gas based, Mossel Bay, South Africa), each with a capacity of 8000 BPD (Steynberg et al. 1999). The advantages of the SAS reactors over the CFB reactors are: (1) the construction costs are 40% lower due to SAS's smaller size and the required support structure is much simpler with only 5% cost of that of CFB; (2) more cooling coils can be installed in the reactor increasing the capacity and pressure flexibility; (3) higher production for a given amount of catalyst can be achieved due to a greater percentage of catalyst being involved in the reaction (the quantity of catalyst which comes into

contact with the feed gas in the reactor for the SAS reactor is about twice that for the CFB reactor); (4) a low rate of on-line catalyst replacement by fresh catalyst can be incorporated to maintain high conversion thus lower the overall catalyst consumption; (5) lower gas and catalyst velocity in the SAS reactors lengthens the time between maintenance inspections, resulting in enhanced production rates and lowers maintenance costs (Jager *et al*. 1990; Steynberg *et al*. 1999, Steynberg & Dry 2004). Investigations into using the slurry bed for HTFT showed that it is not feasible due to continuous media cracking at high temperature (Steynberg *et al.* 1999, Steynberg 2003).

For LTFT operation, two reactor types have been utilized: fixed bed and slurry bed (Steynberg & Dry 2004). The catalyst used for Sasol TFBR and SSPD LTFT processes is a precipitated and promoted iron-based catalyst. Shell's TFBR Fischer- Tropsch plant in Malaysia uses a cobalt-based catalyst (Jager & Espinoza 1995). Using either iron-based catalyst or cobalt-based catalyst, LTFT generates majorly wax and middle distillates (Steynberg & Dry 2004). The wax has high value (higher value as wax than used for fuel production) and can be sold or cracked back into diesel (Steynberg & Dry 2004, Espinoza *et al*. 1999, Jager & Espinoza 1995).

The original reactors for FTS were packed bed reactors, which were later developed into tubular fixed bed reactors (TFBR) in Germany in 1927. ARGE fixed bed reactors were commissioned by Sasol in 1955 (Jager & Espinoza 1995), consisted of 2050 tubes with length of 12m, and a diameter of 5cm, using an iron-based catalyst. The reaction takes place in the tubes while on the shell side steam is generated to remove the reaction heat (Steynberg & Dry 2004). Due to the FTS reactions' exothermal nature, in the reaction tubes axial and radial temperature profiles exist. Sufficient heat removal was a big challenge for the design and operation of these reactors. The catalyst replacement is cumbersome and labor intensive, causing considerable

downtime, while the product selectivities largely depend on the aging of catalyst (Jager & Espinoza 1995). Additionally, carbon formation, which is enhanced by elevated temperature on particular catalytic hot spots in the TFBR, can lead to catalyst break up which in turn causes blockages and necessity of catalyst replacement (Jager & Espinoza 1995). Product selectivity is also temperature dependent, as will be discussed later (Steynberg & Dry 2004). Pressure drop across the packed bed alters from 3 to 7 bar (depending on the operating pressure level) (Jager & Espinoza 1995).

Initial investigation of slurry bed reactors for FTS began in the WWII by Kolbel and co-workers (Kolbel & Ralek 1980). It took over 40 years to bring slurry bed reactors commercialized until an effective filtration process was developed (Jager & Espinoza 1995, Espinoza *et al*. 1999). In the Sasol slurry phase reactor the syngas is distributed from the bottom of the reactor through the wax media/product mixture in which catalyst particles (40-150µm) are suspended (Steynberg & Dry 2004, Jager & Espinoza 1995). There are many advantages to the slurry bed reactor system compared to the TFBR: 1). the slurry phase reactor cost is only a quarter of the traditional TFBR system; 2). the slurry bed can offer near isothermal operation due to the churning of gas bubble and liquid media, which is desirable for better temperature management; 3). slurry bed system gives a lower pressure drop and thus the lower gas compression cost; and 4). lower catalyst consumption rate and longer reactor run time (Espinoza *et al*. 1999, Jager & Espinoza 1995, Steynberg 1999, Duvenhage & Shingles 2002). The disadvantage is that the whole catalysts body can be easily deactivated by catalyst poisoning from impurities entering the reactor (unlike in TFBR only the heading part of catalyst is affected). The development cost of slurry bed reactor is in order of magnitude of that of TFBR (Agee & Espinoza 2010). Shell's Middle Distillate Synthesis (SMDS) process still employs

TFBR. Typical product distributions for HTFT (on fused iron) and LTFT (on precipitated iron) in different reactors are shown in Table 1.1 (Jager & Espinoza 1995).

Table 1.1   Product distributions by type and carbon number range using different reactors for Fischer-Tropsch synthesis (Jager & Espinoza 1995)

Process	HTFT		LTFT			
Reactor	Sasol Advance Synthol		Tubular Fixed Bed Reactor		Slurry Bed Reactor	
Product Range	C_5 - C_{10}	C_{10} - C_{14}	C_5 - C_{10}	C_{10} - C_{14}	C_5 - C_{10}	C_{10} - C_{14}
Paraffins	13%	15%	53%	65%	29%	44%
Olefins	70%	60%	40%	28%	64%	50%
Oxygenate	12%	10%	7%	7%	7%	6%
Aromatics	5%	15%	0%	0%	0%	0%

1.2.2   Fischer-Tropsch Catalyst

Among the group VIII metals, ruthenium followed by cobalt, iron and nickel are the most active metals for the hydrogenation of carbon monoxide (Vannice 1975). Nickel catalysts produce too much methane at low operation pressure while generating volatile nickel carbonyl (which indicates a loss of nickel catalyst from reactor) at high operation pressure. Ruthenium is very expensive and rare. Thus, cobalt and iron are the only viable industrial choices of FT catalysts (Steynberg & Dry 2004). Since cobalt is much more active than iron, plants aiming for

diesel fuel production will probably use cobalt based catalysts. While for the production of the high value linear alkenes, iron based catalyst in HTFT operation using fluidized reactors will be the catalyst choice. In LTFT operation, iron-based catalysts are more profitable for coal-derived syngas conversion due to its viability for low H_2/CO ratio. This work will focus on LTFT operation and LTFT catalysts. Supported cobalt based catalysts exhibit high hydrogenation activity (producing mainly linear paraffins) and better abrasion resistance with longer catalysts' life compared to coprecipitated iron-based FT catalysts (Dry 1989, Ducreux *et al*. 1998). Co catalyst shows negligible water-gas-shift (WGS, $CO + H_2O \rightarrow CO_2 + H_2$) activity. Iron based FT catalyst produces CO_2 via WGS reaction while supported Co-based FT catalyst will produce water when forming monomers or during carbon chain growth, which is a major difference between cobalt-based catalyst and iron-based catalyst (Berge & Everson 1997).

1.2.2.1   Cobalt Based Low Temperature Fischer-Tropsch Synthesis Catalyst

There were many early attempts to prepare cobalt based catalysts suitable for the production of liquid fuels. The early tested catalysts typically were unsupported oxides, such as pure cobalt oxide, cobalt chromium oxide, cobalt-zinc oxide, cobalt-copper oxide, etc (Jager & Espinoza 1995). The high cost of cobalt leads to the application of high surface area supports to increase metal dispersion (metallic cobalt offering the activity for FTS) thus resulting in higher exposed surface area per certain mass of cobalt (Khodakov *et al*. 2007, Steynberg & Dry 2004). However there is a minimum crystal size limitation that smaller than which the cobalt crystal will be converted into inert oxide under normal FT conditions (Schanke *et al*. 1996, Hilmen *et al*. 1999, Berge *et al.* 2000). Silica, alumina, silica-alumina, zeolites, titania, zirconia, magnesia, molecular sieves, etc. have been intensively investigated as catalyst supports with a cobalt loading of 10 to 30 g per 100g of support (Iglesia *et al.* 1993, Oukaci *et al.* 1999, Jacob *et al.*

2002, Steynberg & Dry 2004). The influence of variation in metal/support ratio, particle size, structure, porosity, pore size and distribution, refractory ability, acidity/basicity, etc. has been studied. A number of sophisticated techniques have been applied to provide sufficient characterization of catalysts, such as X-ray diffraction (XRD), transmission electron microscopy (TEM), scanning electron microscope (SEM), BET surface area test, and extended X-ray absorption fine structure (EXAFS) (Iglesia 1997, Jacob *et al*. 2002, Xiong *et al*. 2008, Martínez *et al.* 2003, Morales & Weckhuysen 2006, Steynberg & Dry 2004, Bezemer *et al*. 2006, Wilson & Groot 1995).

In general, the cobalt catalysts preparation procedures are similar using an incipient wetness technique: a cobalt precursor salt is dissolved in a solvent (usually water) to make a precursor solution, which is then used to fill the pore volume of the selected support. After certain drying procedures, the support has been impregnated with the precursor salt. This can then be calcined to make cobalt oxide, and finally reduced to make elemental cobalt (Khodakov 2007).

Incipient wetness impregnation method use any viable salt that contains the aimed metal, while "viable" is determined by the solubility and decomposition of the salt. The higher the solubility of the salt in the solvent (usually water) is, the higher metal loading ratio can be attained by a single time impregnation. This makes chlorides and nitrates the most common choices. Whether or not impregnated precursor is easy to decompose into metal or metal oxide is the other concern, which makes chlorides infeasible. Consequently, nitrates are the most common precursor salt impregnated onto pre-treated supports together with promoters (Khodakov 2007). After promotion with different types of promoters (which will be explained into details), the supported and decorated catalyst is usually carried through a calcination process

with specific temperature program in a certain carrier gas (such as protecting gas for prevention of reoxidation). Then, the catalyst can be used in the reaction, normally following a reduction process. One example of the reduction is that by using hydrogen, the reduction can be carried out at 360 ºC for 14 hours. The FT reaction, following the reduction process, using thus made cobalt catalyst can run at 220 ºC, 15 bar with syngas (a typical H_2/CO ratio of 2/1 or higher) (Steynberg & Dry 2004).

It is known that the distribution of cobalt crystallite size, metal loading percentage, and reaction conditions, such as pressure, have significant impacts on supported cobalt catalysts, and consequently, the FT reactions (Iglesia 1997, Jacobs *et al*. 2002, Steynberg & Dry 2004). Commercial cobalt catalysts typically have a cobalt loading percentage no higher than 20% (Oukaci *et al*. 1999, Iglesia *et al*. 1993, Steynberg & Dry 2004). Niemela *et al*. compared the cobalt precursors using a cobalt nitrate and two cobalt carbonyls for the preparation of Co catalysts supported on silica. On the reduced catalysts, the hydrogen chemisorptions, CO desorption, XRD and X-ray photoelectron spectroscopy (XPS) measurements indicated that the dispersion of Co metal decreased in the order $Co_2(CO)_8 > Co_4(CO)_{12} >> Co(NO_3)_2$ and therefore the carbonyl derived catalysts had a higher initial FT activity (Niemela et al. 1996). Bartholomew concluded that with high dispersion and low cobalt loading, the turn-over-frequency (TOF, the rate of reaction per active site) increases with an increase in loading percentage (Bartholomew 1985). This statement is consistent with Iglesia's conclusion (Iglisia 1997). Additionally C_{5+} selectivity is enhanced by an increase in metal loading in the range of 1%-15% (Iglisia 1997). They argued that an increase in TOF was observed to yield less methane selectivity and a higher degree of olefin readsorption (Bartholomew 1985, Iglisia 1997). The lowest methane selectivity using supported cobalt catalysts is 5% (Steynberg & Dry 2004).

Iglesia claimed that the FT reaction was structure-insensitive and dispersion-insensitive based on experimental data comparing cobalt and cobalt/ruthenium on a variety of supports (A1$_2$O$_3$, SiO$_2$, TiO$_2$, SiO$_2$-modified TiO$_2$, and MgCr$_2$O$_4$, the ratio of surface cobalt to total cobalt atoms ranging from less than 1% to 12%) at conditions endorsing chain growth (C$_{5+}$ selectivity > 80%, tubular packed-bed reactor, 473 K, 2000 kPa, H$_2$/CO=2.05, 55-65% CO conversion) (Iglesia 1997). Iglesia also concluded that cobalt dispersions (ratio of surface cobalt to total cobalt atoms) above 0.15-0.20 (5-6 nm crystallite diameters) were difficult to achieve during catalyst synthesis (Iglesia 1997). The dispersion rate was difficult to retain during recurring oxidative regenerations at high temperatures, which would eventually require the removal of deactivating deposits during long-term operation. In addition, he reasoned that small cobalt metal crystallites (< 5-6 nm diameter) were tend to reoxidize and deactivate rapidly in the presence of water at typical FTS conditions, which is consistent with Schanke, Hilmen and Berge's conclusion (Schanke *et al*. 1996, Iglesia 1997, Hilmen *et al*. 1999, Berge *et al.* 2000). All of the above conclusions indicate that remarkable enhancements in volumetric productivities are unlikely to be attained by increasing cobalt dispersions above 0.15. However, for catalysts with cobalt dispersions of 0.10-0.15 at higher cobalt concentrations (40-50% wt.), the catalyst productivity can be enhanced notably (Iglesia 1997).

Davis' group demonstrated that the cobalt dispersion yield using different supports is: alumina > titania > silica (Jacobs *et al*. 2002). Alumina shows a strong interaction with cobalt which results in high cobalt dispersion, while the weaker interaction between silica and cobalt leading to easier cobalt oxide reduction. Davis' group also testified that higher surface area support brings about higher dispersion notwithstanding harder catalyst reduction (Jacobs *et al*. 2002).

Catalyst promoters are primarily split into three categories: structural promoters, electronic promoters and synergistic promoters (Morales & Weckhuysen 2006). Structural promoters can increase the number and stability of active sites without changing the behavior of the active sites, in this case, affecting the cobalt dispersion by modifying the cobalt-support synergy (Cornils *et al.* 2002). Structural promotion typically falls into one or more of the three types: stabilizing the support, gluing the active metal particle onto support or leading to an increment in dispersion (Morales & Weckhuysen 2006).

Electronic promoters change selectivity of the active sites or the activity (or TOF). Electronic promotion can be interpreted as in ligand effects: the promoter element altering the electronic environment of an active site (in this case an active cobalt site). Consequently it results in electronic donation or withdrawal that usually leads to an increased intrinsic turnover frequency and/or variation in product selectivity. It may also lead to a receded deactivation by changing the adsorption/desorption affinities of the reagents and/or reaction products (Morales & Weckhuysen 2006).

Synergistic promotion effects were brought up by Morales & Weckhuysen to indicate the promoter elements activity, which indirectly influence the behavior of catalytic active element by altering the local feed composition, etc. or changing the overall product distribution (though normally promoters are not considered to be catalytically active, it is not always the case) (Morales & Weckhuysen 2006). For cobalt FT catalyst, Morales and Weckhuysen also concluded the following four reactions which are affected by synergistic promotions effects: 1. Water-gas shift reaction, 2. hydrogenation/dehydrogenation reactions, 3. coke burning during regeneration, 4. H_2S adsorption reaction (Morales & Weckhuysen 2006).

Promoters, such as the noble metals, (Pd, Pt, Ru, Rh, etc.) have been studied extensively

for their beneficial effect on cobalt-based LTFT catalyst activity to facilitating cobalt reduction (Iglesia *et al.* 1993, Iglesia 1997, Adachi *et al.* 1996, Jacobs *et al.* 2002). In addition, zirconia (ZrO_2) has been described as promoting both de-coking and H_2S absorption, supporting catalyst stabilization and cobalt gluing, and as a decorating electronic promoter (Morales & Weckhuysen 2006). In the presence of alumina, on the zirconia supported Co catalyst has been shown to suppress methane selectivity and to increase C_{5+} selectivity (Rohr *et al.* 2000). Manganese can enhance cobalt catalyst activity for FTS when using carbon nanofibers as supports (Bezemer *et al.* 2006). Manganese oxide can be used as a structural promoter by increasing cobalt dispersion and as a decorating electronic promoter and a synergistic promoter (for Water-Gas-Shift, $CO + H_2O \rightarrow CO_2 + H_2$) (Morales & Weckhuysen 2006). It has been reported that lanthanum oxide can support catalyst stabilization during reaction, suppress ethane selectivity and enhance the olefin content slightly. Table 1.2 lists a summary of the promotion effects on the cobalt FT catalyst performances by using different elements reported in the literature (Morales & Weckhuysen 2006).

Table 1.2   Summary of promotion by different element over cobalt FT catalyst (reproduced with permission from Elsevier through Rights Link) (Morales & Weckhuysen 2006)

Promotion type	Influence on catalyst				Element reported in literature
	Promotion mode	Activity	Selectivity	Stability	
Structural	Support stabilization	√		√	Mg, Si, Zr, Nb, Rh, La, Ta, Re, Pt
	Cobalt gluing	√		√	B, Mg, Zr
	Cobalt dispersion increase	√		√	Ti, Cr, Mn, Zr, Mo, Ru, Rh, Pd, Ce, Re, Ir, Pt, Th
Electronic Decorating	Decorating cobalt surface	√	√	√	B, Mg, K, Ti, V, Cr, Mn, Zr, Mo, La, Ce, Gd, Th
	Cobalt alloying	√	√	√	Ni, Cu, Ru, Pd, Ir, Pt, Re
Synergistic Hydrogenation/	Water gas shift	√	√		B, Mn, Cu, Ce
	Hydrogenation/ dehydrogenation		√		Cr, Pt, Pd
	Coke burning			√	Ni, Zr, Gd
	H_2S adsorption			√	B, Mn, Zn, Zr, Mo

To improve C_{5+} selectivity, catalyst life and overall activity, a large number of patents have been published that addressed preparation techniques. This includes the kneading technique compared with impregnation, and the impregnation of cobalt in the external portion of the support particle ("egg-shell" type), or "encapsulated" catalyst particles in permeable meshes (Jager & Espinoza 1995, Sun *et al.* 2002, Kim *et al.* 2008,).

At sufficiently high partial pressure of CO, the reaction rate using cobalt FT catalyst is

independent of pressure (assuming constant syngas composition) while the rate using iron

catalyst is proportional to hydrogen partial pressure (This will be explained in the following

kinetics portion). There is an optimum operation pressure for diesel production (at an operation

pressure lower than 20 atm). Figure 1.4 presents the effect of pressure on the product distribution

of cobalt catalyzed FTS (Pichler 1952). Other than that, higher pressure results in suppressed

methane selectivity (van der Laan & Beenackers 1999), increased oxygenate selectivity (van der

Laan & Beenackers 1999, Steynberg & Dry 2004) and an increase in wax selectivity (Steynberg

& Dry 2004, Jager & Espinoza 1995). It is widely acknowledged that increasing the operation

temperature can enhance the catalytic activity and the methane selectivity while suppressing the

heavy product selectivity (van der Laan & Beenackers 1999). An increase in the reaction

temperature also increases the selectivity towards isomers while the alcohol selectivity decreases.

Isomerization reaction will be enhanced extensively by increasing temperature, which results in

higher branching degree and more secondary products (van der Laan & Beenackers 1999).
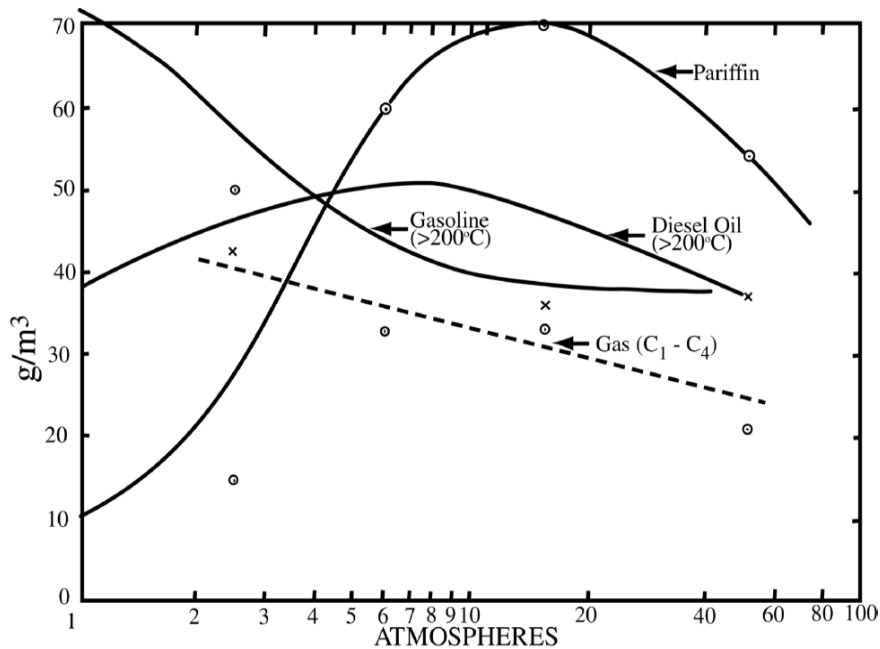
Figure 1.4   Effect of pressure on the FTS selectivity of cobalt catalyst (Pichler 1952)

Cobalt catalysts are generally more resistant to deactivation than iron catalysts (Khodakov *et al*. 2007). The deactivation of cobalt FT catalysts can be caused by: 1). Poisoning (sulfur, halogens, nitrogenates, etc.) (Steynberg & Dry 2004, Khodakov *et al*. 2007), 2). oxidation (cobalt spheres smaller than a 4.4 nm diameter are likely to be oxidized by water as stated previously, however under realistic FT conditions, bulk cobalt will not be oxidized) (Iglesia 1997), 3). active metal sintering (loss of active sites, a prominent source of deactivation) (Das *et al*. 2003), 4). carbide formation (Ducreux *et al*. 1998). and 5). waxing (which will cover the active sites and increase in the product diffusion resistance) (Khodakov *et al*. 2007). In addition, Chen *et al* identified cobalt silicate species and considered their formation as one mode of deactivation (Chen *et al*. 2001).

1.2.2.2 Iron Based Fischer-Tropsch Catalyst

Iron based FT catalyst offers an attractive complement to Co based catalysts stemming from their tendency to produce products with higher olefinic concentration (Schulz 1999). Iron based catalysts can be primarily separated into two types: fused iron based catalysts for HTFT and precipitated iron based catalysts for LTFT, further into two types: supported and unsupported (or self-supported). The precipitated iron based catalyst used in the Slurry Bed Reactor process is similar to that used in the TFBR (ARGE reactors), except that the size are different (one is power and one is pellet, respectively) (Steynberg & Dry 2004). In the fixed bed reactor little or no catalyst's break-up happens. However, for high throughput slurry reactor there is some break-up which can lead to clog and deficiency in the wax/catalyst separation unit. To diminish the catalyst's break-up, the spray dried (a common approach to obtain catalyst particles of the desired size range) catalyst is calcined at approximately 400 ºC to 500 ºC to enhance its

mechanical strength. This causes a 15% decrease in the BET area of the unreduced catalyst but does not lead to loss of the activity to the final operating catalyst (Davis 2003, Steynberg & Dry 2004).

One example of catalyst given by Dry contains 25g SiO_2 5g Cu and 5g K per 100g Fe (Anderson and Boudart, *Ed*s. 1981). When the Fe/Si ratio is over 4, the silica is not considered as a standard support but rather as a binder and as a spacer, the latter of which impeding sintering of the iron oxide (Steynberg & Dry 2004). Though iron catalysts are usually self-supported, supports such as SiO_2, are also frequently added to improve thermal and mechanical stability (Steynberg & Dry 2004, Pham & Datye 2000). Silica is generally accepted as one of the best supports. Zinc has been used as a spacer by Iglesia's group, which has been claimed to be beneficial on the catalyst's activity (Li *et al*. 2002). Our group studied the function of zinc with our collaborator Dr. Mohindar Seehra in West Virginia University, and found that the zinc forms a composite oxide with iron. A far smaller crystal size was thus generated with comparable catalytic activity compared to a zinc-free catalyst.

In precipitation of iron solution (usually iron nitrate) with an alkaline solution, controllable variables include the species of iron solution, alkaline solution, concentration of solutions, order and rate of solution addition, and synthesis temperature, solution pH value, etc. (Anderson and Boudart, *Eds*. 1981). After precipitation and addition of promoters, the catalyst is then washed, filtered, dried and pre-treated for use in the FT reactor. An example of a bench scale continuous precipitated iron catalyst synthesis procedure is offered by Iglesia's group: A solution of iron nitrate (Aldrich, 99.9+%, 3.0 M) and zinc nitrate (Aldrich, 99.9+%, 1.4 M) at the Zn/Fe atomic ratio of 0.1 is added at a constant rate into water at 353 K ($\sim$100 cm^3) at a rate of 120 cm^3h^{-1}. Ammonium carbonate solution (Aldrich, 99.9%, 1M) is added to maintain the solution mixture

pH at 7 ± 0.1, until desired amount of precipitate is obtained. Then the precipitate is washed five times with doubly distilled deionized water (~200 cm^3/g each time, to remove ions from the slurry), then dried in ambient air at 393K overnight, and calcined in flowing dry air at 623K for 1h. The catalyst is then promoted with K, Cu, and Ru by incipient wetness impregnation method.

Aqueous solutions of K_2CO_3 (Aldrich, 99.99%, 0.16M), $Cu(NO_3)_2$ (Aldrich, 99.99%, 0.16M), and/or $Ru(NO)(NO_3)_x(OH)_y$ (x+y = 3) (Aldrich, dilute nitric acid solution, Ru 1.5%) at certain concentrations (depends on the Fe/Zn-oxide pore volume and salts' solubilities) are used to achieve the desired K/Fe, Cu/Fe, and Ru/Fe atomic ratios (e.g. K/Fe = 0.02, Cu(Ru)/Fe = 0.01). The impregnated paste is then dried at 373K in ambient air and then calcined in flowing dry air at 673K for 4h (Li *et al*. 2002).

The choice and concentration of promoters are substantial in influencing the methane selectivity and hydrocarbon selectivity. Typically, alkali promoters will be applied to enhance basicity which is related to modification of selectivity. For example, commercial iron catalysts all are composed of up to 3% (wt. %) of potassium as a chemical promoter to enhance electro-donor effect of iron active sites (Steynberg & Dry 2004). It can help to lower the metal-hydrogen bond and metal-oxygen bond strength, while achieving easier CO adsorption and C-O bond dissociation (Dry *et al*. 1969). Consequently, all carbon consuming reactions are enhanced. When K_2O concentration is increased from 0% to 3% (wt. %), the wax selectivity increases from 5% to 63% (on a hydrocarbon basis) (Dry 1981). It has been proven that alkali promoters (e.g. potassium) will also lead to enhanced olefin selectivity, higher carbon chain propagation probability (α) and suppressed methane selectivity. In theory, all of the alkali metals can be used, following the promotion ability in the order of Li < Na < K < Rb < Cs < Fr resulting from their basicity. Mark Dry demonstrated that the activity of iron catalysts promoted with alkali metals is:

Li (40), Na (90), K (100), and Rb (90) regarding K promotion effect as 100 as the base. The drop from K to Rb is attributed to a side-effect of high wax selectivity (Dry 1981). However, Davis' group argued that however K offers the best promotion, Rb, Cs and Li should be regarded as inhibitors (Ngantsoue-Hoc *et al*. 2002). They also studied alkaline earth metals promotion effects, proving that all the alkaline earth metals were uniformly not as good as potassium (Ngantsoue-Hoc *et al*. 2002).

Copper is another regularly presented metal when promoting iron-based LTFT catalyst as a promoter to enhance reduction of iron oxide in the catalyst reduction step (Steynberg & Dry 2004). Copper remarkably affects the time before the catalyst attains the maximum activity but controversy still surrounds its impact on other catalyst properties However, it is not used with cobalt catalysts because the resulting catalyst shows bad activity maintenance (O'Brien *et al*. 1997). Manganese is found to be beneficial to the catalyst activity and olefin selectivity of iron-based FT catalyst. It is also reported to suppress methane formation and to assist activity loss resistance (Morales & Weckhuysen 2006). Ruthenium is also good for increasing activity (this is explained as a promotion of nucleation of smaller domains) while palladium enhances WGS activity and decreases olefinicity (Li *et al*. 2002, Luo *et al*. 2004, Pham & Datye 2000).

Special treatments can be made prior to the drying and calcinations of iron paste. For example, to increase the pore volume and surface area of the catalyst, a low surface tension liquid, such as ethanol, can be added into the iron paste before the first drying step. By washing using ethanol, the water in and around iron past can be replaced. However, by doing this the catalyst abrasion resistance could be undermined, which is a drawback when using in a slurry bed reactor (Li *et al*. 2002). For TFBR, the catalyst is appropriately re-shaped before loading, and for slurry bed reactors, specific drying techniques are employed to make catalyst powder.

The powder is heated to improve mechanical strength. It is widely understood that the active

form of the iron FT catalyst in the reactor is iron carbide, so a reduction and carbonization step is

often applied before use. Iglesia's group showed the extent of carburization (FeC_x concentration,

atom %) is higher on samples promoted with Ru or Cu than on samples only containing Fe/Zn/K,

as shown in Figure 1.5 (Li et al. 2002). In slurry reactors, catalyst powder is used instead of

catalyst pallets in fix bad reactors, in addition, catalyst activity are higher than that in fixed bed

reactors (Steynberg & Dry 2004).
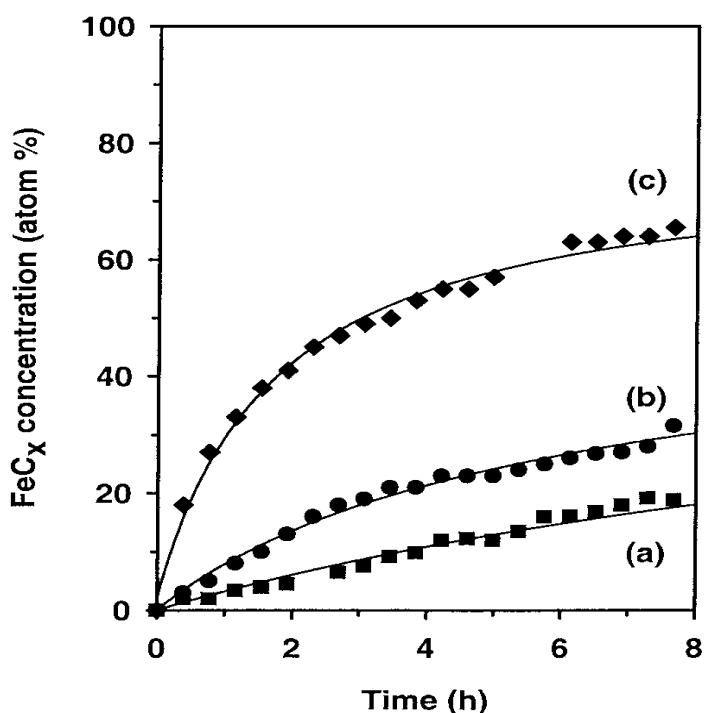
Figure 1.5 Iron carbide concentration as a function of time during in situ X-ray absorption
spectroscopy (XAS) measurement of Fe-based FT catalyst samples in synthesis gas (a) Fe-
Zn-K, (b) Fe-Zn-K-Cu, (c)Fe-Zn-K-Ru (Li et al. 2002).

Mark Dry reported that an iron-impregnated oxide-supported catalyst is not as good as

precipitated iron catalysts (Dry 1981). However, the potassium partitioning between the iron and

silica, which results in lessened promotion effect, makes the comparison difficult. Bukur's group

showed that for impregnated catalyst, silica is superior to alumina as a support, and that

supported catalyst offers a more paraffinic and lighter product distribution than the precipitated catalysts (Bukur & Sivaraj 2002). However this may be at least partly due to the potassium partitioning.

The fused iron catalyst used for HTFT is often prepared by melting magnetite (a solid solution of wustite FeO and hematite Fe_2O_3, depending on the iron ore) with structural promoters such as MgO or Al_2O_3 (forming high melting point oxides, acting as spacers to inhibit sintering and to results in high surface area in HTFT iron catalysts.) Other structure promoters include the oxides of Ca, Mn, and Ti (Dry 1981). Chemical promoters such as K_2O and some other alkali promoters such as Li, Na are added during the molten bath to modify the basicity of catalyst. The iron catalyst activity and the selectivity in the FT reaction are highly dependent on basicity of the catalyst surfaces (Steynberg & Dry 2004). Increasing alkali level results in higher conversions (Steynberg & Dry 2004). The HTFT iron catalyst is made into a fine powder for fluidized bed reactor use. The reasons for catalyst deactivation and selectivity shift with time on stream are concluded by Steynberg & Dry: 1. the loss of the small loose alkali silicate promoter particles (by scouring and break-up of catalyst particles in high velocity movement in fluidized reactor bed), 2. the poisoning of the alkali/Fe sites by sulphur compounds from the feed gas, 3. (probably the most important one) enhanced carbon deposition at high temperature on the more active alkali/Fe centers. (Steynberg & Dry 2004)

Increasing the reaction temperature increases the conversion, the methane selectivity, skeletal isomerization, carbon deposition, while decreasing heavy product selectivity and alcohol selectivity (van de Laan and Beenackers 1999). Mark Dry claimed that for iron-based LTFT catalyst, operation pressure has little effect on the product distribution (Dry 1981). Increasing pressure resulting in increased oxygenates selectivity and a decline in methane selectivity is

27

generally accepted (van de Laan and Beenackers 1999, Steynberg and Dry 2004). The olefin selectivity is not dependent on pressure change. Increasing pressure will suppress the coking rate since it is proportional to the ratio of partial pressure of CO to partial pressure of H_2 for HTFT (Steynberg and Dry 2004). An enhancement in syngas ratio (H_2/CO) will lead to increased methane selectivity, chain branching and suppressed chain growth and declined olefin selectivity and oxygenates formation (Van de Laan and Beenackers 1999). Increased syngas space velocity results in decreased conversion (shortening residence time), methane formation and enhanced olefin selectivity and oxygenates formation (Van de Laan and Beenackers 1999). In LTFT, the catalyst activity declines and the selectivity towards shorter chain products increases with time on-stream (Steynberg & Dry 2004).

The reaction rate is suppressed by water generation for iron catalysts, and some researchers argue that the FT reaction and WGS reaction use the same active sites (Luo *et al*. 2007). Due to high WGS activity, the usage ratio (consumption rate of H_2 / consumption rate of CO) is more flexible for an iron catalyst than a cobalt catalyst. This makes iron-based FT catalyst more appropriate for biomass-derived syngas conversion (Steynberg & Dry 2004). For both iron and cobalt catalysts, sulfur is a strong poison, posing a major challenge for the gas purification process in XTL. However, iron catalysts are more sulfur tolerable than cobalt catalysts. In table 1.3, a brief comparison between cobalt-based LTFT catalyst and iron-based LTFT catalyst is listed.

Table 1.3   Brief comparisons between cobalt-based FT catalyst and iron-based FT catalyst

Parameter	Cobalt catalyst	Iron catalyst
Cost	Expensive	Inexpensive
WGS reaction	Negligible (more noticeable at high conversion)	Significant
Flexibility	Less flexible (significant influence of T* and p* on hydrocarbon selectivity)	Flexible
Sulphur tolerance	<0.1 ppm	< 0.2 ppm
H_2/CO usage ratio	2.0 ~ 2.15	0.5 ~ 2.5
Attrition resistance	Good	Poor

(*: T, temperature; *p*, pressure.)

1.3   Fischer-Tropsch Reaction Mechanism and Kinetics

1.3.1   Fischer-Tropsch Reaction Mechanism

FTS is a surface catalyzed polymerization process involving several reaction categories listed in Table 1.4 (Adesina 1996). The products generated in LTFT include hydrocarbons and oxygenates. Specifically, hydrocarbon products are prevailing, involving normal paraffins, normal olefins (mostly terminal), branched paraffins and branched olefins. There is low selectivity towards dienes and aromatics, too. The prevailing oxygenates include alcohols (mostly linear and terminal, aldehydes (mostly linear), ketones (mostly methyl-), carboxylic acids (mostly linear), and esters (mostly linear). There is very low selectivity towards acetals, furans and phenols, too (Steynberg & Dry 2004). All of these products are primary or secondary products, generated in FT primary reactions and secondary reactions, forming a complicated

mixture. There is a tremendous amount of work that has focused on determining the primary products, which is very important in determination of the reaction pathways and mechanism. One method to identify the primary products is to decrease the conversion towards zero and then to examine the product selectivity. The primary product should be the one(s) that is still present. The main primary products have been generally accepted to be normal paraffins, 1-olefins, and perhaps 2-olefins (Steynberg & Dry 2004, Madon *et al*. 1991, Iglesia 1997). Our group observed significant amount of aldehydes in the supercritical phase FTS, which lead to some changes to the traditional opinions (Durham *et al*. 2010).

Table 1.4 Reactions in the Fischer-Tropsch Synthesis (Adesina 1996)

Main reactions	
1. Paraffins	$(2n+1)H_2 + nCO \rightarrow C_nH_{2n+2} + nH_2O$
2. Olefins	$2nH_2 + nCO \rightarrow C_nH_{2n} + nH_2O$
Side reactions	
3. Water-Gas-Shift (WGS)	$CO + H_2O \leftrightarrow CO_2 + H_2$
4. Carbide formation	$yC + xM \leftrightarrow M_xC_y$
5. Alcohols	$2nH_2 + nCO \rightarrow C_nH_{2n} + 2O + (n-1)H_2O$
6. Boudouard reaction	$2CO \rightarrow C + CO_2$
7. Catalyst reduction and oxidation	$M_xO_y + yH_2 \leftrightarrow xM + yH_2O$ $M_xO_y + yCO \leftrightarrow xM + yCO_2$
8. Coking	$H_2 + CO \rightarrow C + H_2O$

Generally, the polymerization process can be sorted into the following steps:

1. Reactant adsorption

2. Chain initiation

3. Chain growth

4. Chain termination

5. Product desorption

6. Readsorption and further reaction

For each intermediate, there are two possibilities: 1) chain growth by monomer addition and 2) chain termination to a product. When assuming that the chain propagation is only by the addition of a monomer, rather than a dimer, oligomer, or polymer, the FTS polymerization process can be understood as shown in Figure 1.6. The propagation probability, also called chain growth factor α_i, is the probability of that a carbon chain containing i carbons grows longer (terminating as a product with carbon number from i+1 to ∞). The termination probability β_i, on the other hand, refers to the probability that a carbon chain containing i carbons terminates to a product with i carbons. The sum of α_i and β_i must equal 1. When calculating the product distribution, if the probability of chain growth (α) is independent of the existing chain length, it will be much simpler. Fortunately, when calculating under this assumption, the agreement of the observed and predicted value is good enough to support this assumption (C_1 and C_2 products are excluded) (Dry 1981, 1996).
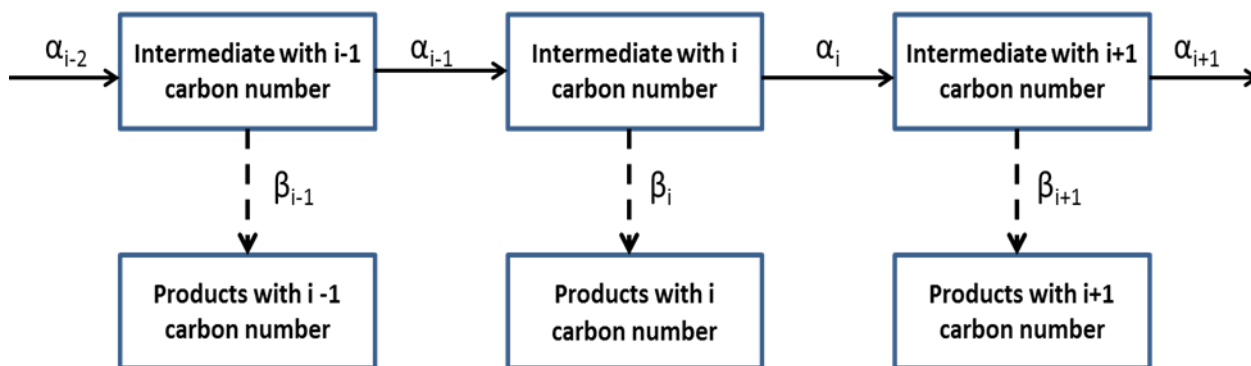
Figure 1.6   Fischer-Tropsch synthesis stepwise carbon chain growth by monomer addition

Despite extensive work in investigating the mechanism of FTS, it is still a controversial topic. Some main arguments involve:

1. CO molecule dissociates into C and O atoms and then C atom is hydrogenated.

2. CO molecule inserts directly into carbon chain, hydrogenated subsequently.

3. CO molecule is hydrogenated on catalyst's surface into "CHO" or "HCOH" and joins the "open end" of carbon chain to reach electronic balance.

Four mechanisms are frequently discussed: the alkyl mechanism, the alkenyl mechanism, the CO insertion mechanism, and the Enol mechanism.

1.3.1.1   The Alkyl Mechanism

1i). CO chemisorbs dissociatively

1ii). C hydrogenates to CH, CH_2, and CH_3

2). The chain initiator is CH_3 and the chain propagator is CH_2

3i). Chain termination to alkane is by α-hydrogenation

3ii). Chain termination to alkene is by β-dehydrogenation

Fischer and Tropsch suggested a mechanism in 1926, which was modified in 1939 and 1949 by Craxford, called the carbide mechanism. It proposed the surface metal carbide is formed

32

first and then hydrogenated into various species (that agglomerate into hydrocarbon and oxygenates) (Steynberg & Dry 2004). Macromolecules are formed from methylene groups (-CH_2-) by the carbide hydrogenation, and then due to hydrocracking, the macromolecules produce molecules with lower molecular weight. This mechanism was widely accepted, but some researchers recognized it as inconsistent with thermodynamic data for the hydrogenation of carbides at the temperatures used for the synthesis (Kummer & Emmett 1952). Investigation on iron carbide using ^{14}C cast further doubt on this theory, based on the experimental results showing no more than 30% produced methane from the hydrogenation of the ^{14}C carbide (Kummer and Emmett 1953, Hall *et al*. 1960). Controversy was raised by Bell questioning Emmett's results. Bell argued that this result might come from some of the chemisorbed carbon atoms still being intermediates (Bell 1981). In addition, the alkyl mechanism does not account for the production of oxygenates (reaction with OH groups). Besides, there are two predominant weaknesses of the alkyl mechanism: the high energy barrier for CO dissociation (Blyholder and Lawless 1991, Inderwildi *et al*. 2008, Dai & Yu 2008, Zhou *et al*. 2009) and sp^3-sp^3 coupling (Long *et al*. 1997, Liu & Hu 2002). In spite of these problems, the alkyl mechanism (aka. carbide mechanism) has been deemed as the major propagation mechanism for all FT catalysts (Van Der Laan & Beenackers 1999, Steynberg & Dry 2004) or just for cobalt (Davis 2001).

1.3.1.2 The Alkenyl Mechanism

1i). CO chemisorbs dissociatively

1ii). C hydrogenates to CH, CH_2

1iii). CH and CH_2 react to form $CHCH_2$

2i). Chain initiator is $CHCH_2$ and chain propagator is CH_2

2ii). The olefin in the intermediate shifts from the 2 position to the 1 position

3). Chain terminates to alkene is by α-hydrogenation

It is obviously indicated that via this mechanism a large amount of internal olefins will be produced. Some researchers argue that this mechanism does not contribute to the chain growth mechanism in the FTS. As is the case with the alkyl mechanism, the alkenyl mechanism starts with the CO dissociation into C and O with the oxygen making no contribution to the mechanism beyond that point. Thus, if these are the propagation mechanisms of the reaction, oxygenate formation requires a separate step, which will involve the reactions with OH groups (van Der Laan & Beenackers 1999, Steynberg & Dry 2004)

1.3.1.3   The CO Insertion Mechanism

1i). CO chemisorbs non-dissociatively

1ii). CO hydrogenates to $CH_2(OH)$

1iii). $CH_2(OH)$ hydrogenates and eliminates water, forming CH_3

2i). Chain initiator is CH_3, and propagator is CO

2ii). Chain propagation produces RC=O

2iii). RC=O hydrogenates to CHR(OH)

2iv). CHR(OH) hydrogenates and eliminates water, forming CH_2R

3i). CH_2CH_3R terminates to alkane by α-hydrogenation

3ii). CH_2CH_3R terminates to alkene by β-dehydrogenation

3iii). CHR(OH) terminates to aldehyde by dehydrogenation

3iv). CHR(OH) terminates to alcohol by hydrogenation

This mechanism is also considered a modification of the carbide mechanism. CO inserts into a metal-methyl/methylene carbon bond, and is then hydrogenated to intermediate alcohol/alkene. Alcohols can eliminate oxygen to form the alkenes. Methylene group is

considered the initiator of hydrocarbon chain growth, and is also the precursor for methane. This mechanism is viewed as a revival of the carbide theory, with the restriction that carbide formation is limited to the surface/near surface layer (Davis 2001). Dry proposed a more elaborate version in 1993, noting the steps involving surface C hydrogenation are rate-controlling while the other reactions are assumed to be at equilibrium (Dry 1993, Davis 2001). This surface carbide mechanism is considered a better choice for a cobalt catalyst, depending on which limited mechanistic data are available (Davis 2001).

1.3.1.4   The Enol Mechanism

1i). CO chemisorbs non-dissociatively

1ii). CO hydrogenates to $CH(OH)$ and $CH_2(OH)$

2i). Chain initiator is $CH (OH)$ and chain propagator is $CH (OH)$ and $CH_2(OH)$

2ii). Chain propagation is by dehydration and hydrogenation to $CR(OH)$

3i). chain termination to aldehyde is by desorption

3ii). Chain termination to alkane, alkene, and alcohol, is by hydrogenation

This enol mechanism is proposed by Eidus in 1976, which suggests adsorbed (as a whole) CO molecule is hydrogenated to enol, $M=CH(OH)$. Then further hydrogenation occurs to eliminate oxygen and to from a methylene group. Propagation occurs at the formation of a C-C bond by elimination of water. Work using ^{14}C labeled alcohols or alkenes by Emmett et al. were able to provided strong corroboration for this theory. It is indicated that the labeled alkene or alcohol could serve to initiate chain growth when the reaction pressure is at atmospheric pressure (Kummer & Emmett 1952, 1953, Hall *et al*. 1960,). Davis *et al*. showed that at medium pressure, the synthesis under slurry phase conditions confirmed Emmett's observation. Additionally, both Emmett and Davis observed that ethanol was 50-100 times as rapid as ethene in the

incorporation process when these two reactants convert at the same reaction conditions (Tau *et al*. 1991, Srinivasan *et al*. 1996). From this result, Davis concluded that for an iron catalyst, this Enol mechanism is more suitable (Davis 2001).

The differences among these four mechanisms can be summarized into the difference in types of the monomers and the initiators. Table 1.5 shows the comparison among monomers and initiators of these mechanisms.

Table 1.5   Comparison of mechanisms in terms of types of monomers and initiators

		Initiator	
		Hydrocarbon	Oxygenates
Monomer	Hydrocarbon	Alkyl[a]/Alkenyl[b]	
	Oxygenates	CO insertion[c]	Enol[d]

a: Alkyl mechanism
b: Alkenyl mechanism
c: CO insertion mechanism
d: Enol mechanism)

1.3.2   Anderson-Schulz-Flory Model

To determine the mechanism of FT reactions, the selectivity data is important. Flory was the first to investigate the synthetic behavior of non-homogenous material given the polymerization nature of the FT process, proposing the first FTS chain-growth model. A series of studies afterwards led to the current well known Anderson-Shultz-Flory (ASF) product

distribution model (Herrington1946, Anderson 1950, Henrici-Olive 1976). The polymerization reaction starts from the formation of an initiator. The first major assumption is that the chain growth is by addition of one monomer at a time. The second major assumption is that the growth and termination rates are independent of the chain length, yielding the chain growth probability (α) as following:

$$\alpha = \frac{rp_i}{(rp_i + rt_i)} = \frac{\sum_{i+1}^{n} Ni}{\sum_{i}^{n} Ni}$$

$$\alpha = N_{i+1} / N_i = R_p / (R_p + R_t)$$

Where R_p and R_t are the propagation rate and termination rate, respectively. rp_i and rt_i are the propagation rate and termination rate for a hydrocarbon (or oxygenated hydrocarbon) with i carbon number in the carbon chain. N is the molar rate (concentration) of product on the surface of the catalyst, and i is the carbon number of the carbon chain. n is the biggest number the carbon number can achieve in the reaction for hydrocarbons. The weight fraction of a chain of length i, W_i, can be measured as a function of the chain growth probability.

$$W_i = i \, \alpha^{i-1}(1 - \alpha)$$

The logarithmic relation is as follows:

$$\ln (W_i / i) = i\ln \alpha + \ln((1 - \alpha)/ \alpha)$$

According the ASF assumptions, the plot of $\ln(W_i/i)$ v.s. i should be a straight line for all hydro carbon products, and α can be determined from the slope of this straight line. According to these equations, heavier hydrocarbons are produced as α increases (as shown in Figure 1.6). There are also reported data showing deviation from ASF behavior, which has been demonstrated as possessing two distinct reaction pathways with different chain growth factor α (Steynberg &Dry 2004). Chain growth kinetics, however, are often considered dependent on

chain size and result in non-Flory carbon number distribution on Co, Ru, and Fe catalysts (Pichler & Schulz 1967, Vanhove *et al*. 1984, Iglesia 1991, Iglesia *et al.* 1993, Madon *et al*. 1991, Madon *et al*. 1992).

1.3.3 Fischer-Tropsch Synthesis Kinetics

Mark Dry proposed the following FTS kinetic equations for iron-based FT catalysts and cobolt-based FT catalysts (Steinberg & Dry 2004). The numerators of both equations, for the two different catalysts, are the same, involving partial pressure of hydrogen and carbon monoxide. The denominators of both equations include partial pressure of CO, which is consistent with CO's general status being a catalyst poison. Water inhibits the reactivity of iron-based FT catalysts, but not cobalt-based FT catalyst.

Iron-based FT catalyst $\qquad r = \frac{m\, P_{H_2} P_{CO}}{P_{CO} + a P_{H_2 O}}$ (1.1)

Cobalt-based FT catalyst $\qquad r = \frac{m\, P_{H_2} P_{CO}}{(1 + b P_{CO})^2}$ (1.2)

From the above equations, when an iron catalyst is at low conversion ($P_{H_2O} \approx 0$), the reaction rate is only a function of hydrogen partial pressure. The kinetic equations imply that water inhibits iron but not cobalt. For cobalt catalyst, when the CO partial pressure is very high, $(1 + b P_{CO})^2 \rightarrow (b P_{CO})^2$, the reaction rate is proportional to the ratio of P_{H_2}/P_{CO}. Both denominators involve partial pressure of CO, indicating CO's general status being a (reversible) catalyst poison. Both kinetic equations indicate hydrogenation as the rate-limiting step.

The Fischer Tropsch reaction is generally regarded as kinetically controlled (opposed to thermodynamically controlled) due to simulations having shown that thermodynamically methanation is preferred to heavy product formation (Steynberg & Dry 2004). However, Diane Hildebrandt's group argued the overall product distribution is possibly thermodynamically

affected (Masuku *et al*. 2010) and the olefinicity at each carbon number (Lu *et al*. 2010).

1.4   Application of Supercritical Fluid as Reaction Media in Fischer-Tropsch Synthesis

1.4.1   The Concept of Utilization of Supercritical Fluid in Fischer-Tropsch Synthesis

There have been a very large number of research studies that have utilized supercritical fluids (SCF) in reactions, separations and material processing studies involving food, pharmaceutics, biochemicals and oil (Johnston & Penninger, *Eds*. 1989). A supercritical fluid (SCF) is a substance that is heated above its critical temperature and compressed beyond its critical pressure such that it exists in a single fluid phase. SCFs exhibit thermo-physical properties that are intermediate between those of a liquid and a gas, such as a liquid-like density and gas-like transport properties. SCFs offer the possibility of carrying out chemistry and chemical technologies in a sustainable manner (energetically, environmentally or economically "green") (Hauthal 2001). The major advantages of using SCF as a unique reaction medium include: 1) offering single phase operation, 2) high concentrations of reactants and products can be achieved due to high miscibility of gases in SCFs compared to liquid solvents (Abbaslou *et al*. 2009), 3) The ability of a SCF to dissolve non-volatile materials is similar as that of liquid solvents, 4) superior mass transfer and heat transfer properties can be obtained in SCFs compared to gas phase due to high diffusivity and low viscosity, and 5) large variations in density (and density dependent properties) in the near-critical range can be imparted by modest temperature and/or pressure changes, thereby enabling the feasibility of tuning the reaction environment and enabling easy separation of dissolved chemicals from the SCFs, (6) in situ extraction of non-volatile materials and low-volatile products from catalyst pores as a result of the low surface tensions of SCFs (Abbaslou *et al*. 2009, Lang, *et al*. 1995, Subramaniam 2001, Frew *et al*. 1988, Baiker 1999).

Fischer-Tropsch synthesis is a set of classical heterogeneous reactions , involving CO, H_2, CO_2 and light hydrocarbons in gas phase, hydrocarbon products in liquid phase and catalysts in solid phase. Traditional gas phase fixed-bed FTS reactors are susceptible to "hotspots" which result from excessive heat released by the FT reactions causing local overheating of the catalyst and increased methane formation (Lang *et al.* 1995, Steynberg & Dry 2004, Elbashir *et al.* 2010). Blockage of the catalyst surface and pores by heavy product condensation is another issue for fixed bed FTS. In combination, these two issues result in low conversion and catalyst deactivation. To improve the heat transfer from the catalysts to the cooling medium, high gas space velocity (to guarantee turbulent flow) and narrow tube diameters (to shorten the distance between the catalysts and the tube walls) are applied. Recycling a portion of the reactor tail gas is commonly practiced to enhance the fresh gas feed conversion (Steynberg & Dry 2004).

Slurry phase FTS reactors were commissioned as an alternative to gas phase fixed-bed reactors, offering better operating temperature uniformity and enhanced heavy hydrocarbon extraction (as a result of the existence of a liquid phase and hence higher product solubility) (Lang *et al.* 1995, Hauthal 2001). However, low rate of reactant mass transfer into the catalyst surface and pores is an apparent drawback. In addition, the simplicity of gas phase FTS is attractive. Thus, there is a need for a mode of FTS that offers gas-like transport properties and liquid-like thermal capacity and solubility. Therefore, the application of SCF solvent medium seems to be an appealing alternative for FTS.

The use of supercritical fluids as reaction media in FTS has been concentrated on LTFT. Fujimoto's group pioneered the investigation of FTS using SCF as a reaction medium in 1989 (Yokata & Fujimoto 1989). They proposed the following criteria for choosing the reaction media for FTS (Yokata & Fujimoto 1989, Fan & Fujimoto 1999):

1. The critical point (temperature and pressure) of the supercritical reaction media should be slightly lower than the operation temperature and pressure (especially when aiming for a single phase operation).

2. The supercritical reaction media should be stable under the reaction conditions and should be an inert in the reaction and to the catalysts.

3. The supercritical reaction media should exhibit high solubility for hydrocarbons, which will enhance the extraction of products (e.g. wax) from the surface of the catalysts and also enhance the readsorption of reaction intermediates.

LTFT operation temperature falls in the range of 220 ºC to 250 ºC while the total operation pressure is the sum of the partial pressure of the reactants, products and the media, and these values limit the selection of the media materials. Researchers have performed many studies using different SCF media: CO_2 (Benoit 2008), propane (Abbaslou *et al*. 2001, Bukur *et al*. 1997, Yan *et al*. 1998), pentane (Fan & Fujimoto 1999, Yan *et al*. 1998, Tsubake *et al.* 2002, Jacobs, *et al.* 2003, Linghu *et al.* 2004, Huang *et al*. 2004, Shi, *et al.* 2005, Irankhah & Haghtalab 2008), hexane (Yokota & Fujimoto 1989, Fan & Fujimoto 1999, Linghu *et al*. 2004, Huang *et al*. 2004, Yokota & Fujimoto 1991, Huang & Roberts 2004, Elbashir & Roberts 2005, Elbashir *et al*. 2005, Bukur 2006), heptanes (Linghu *et al*. 2004, Irankhah, A. Haghtalab 2008), octane (Liu *et al.* 2006, Tang *et al.* 2008), decane (Linghu *et al.* 2004, Liu *et al*. 2006), dodecane (Liu *et al*. 2006), hexadecane (Yokota & Fujimoto 1989, 1991, Yokota *et al*. 1991, Liu *et al*. 2006). The critical properties of some of the investigated media are listed in Table 1.6, from which hydrocarbons with carbon number of 5 and 6 are considered the most viable to be used as solvents in supercritical Fischer-Tropsch synthesis (SC-FTS) considering their consistency with the above-listed criteria. The critical temperature of both propane and CO_2, 97 ºC and 31 ºC respectively,

are much lower than the LTFT operation temperature, which will result in non-desirable media density. For iron-based FT catalysts, CO_2 and H_2O are not inert, being active in the water gas shift reaction and the reverse reaction (Dry 2002). For cobalt-based FT catalysts, large amounts of water at high temperature and pressure can be poisonous (Steynberg & Dry 2004). Roberts' group reported that the phase behavior of the SC-FTS reaction mixture (composed of reactants, products, and SCF media) is quite different from the pure SCF media, and the critical temperature and pressure are both higher in the reactor effluent than those of the neat media (Elbashir & Roberts 2005). Davis' group suggested that a mixture of hexane and pentane as a solvent should offer favorable media density (Jacobs *et al*. 2003, Shi *et al*. 2005). However, in that study they added large amounts of inert gas which can also affect the phase behavior of the reaction mixture. Fujimoto *et al.* reported that for different desired products (e.g. light hydrocarbons, middle distillates or wax, olefin, paraffins), different SCF media should be employed (Fan & Fujimoto 1999).

Table 1.6 Critical properties of hydrocarbon solvents in supercritical phase Fischer-Tropsch synthesis compared to critical properties of CO_2 and H_2O (NIST, Chemistry Webbook, http://webbook.nist.gov/chemistry/)

Solvent	Critical Temperature, T_c (°C)	Critical Pressure, P_c (bar)	Critical Density, $\bar{P}_c$ (g/cm³)
Carbon dioxide	30.9	73.75	
Water	373.9	220.6	
Propane (C_3H_8)	96.6	42.5	0.224
n-Butane (C_4H_{10})	151.6	38.0	0.227
n-Pentane (C_5H_{12})	196.7	33.6	0.232
n-Hexane (C_6H_{14})	233.3	29.7	0.233
n-Heptane (C_7H_{16})	266.6	27.8	0.235
n-Decane ($C_{10}H_{22}$)	344.8	21.1	0.229

1.4.2 Comparison between Supercritical Phase Fischer Tropsch Synthesis and Traditional Fischer Tropsch Synthesis

Compared to traditional FTS, the advantages of SC-FTS, as reported by several researchers, are summarized as follows (Jacobs *et al*. 2003, Fujimoto 1991, Huang 2003, Durham *et al*. 2008, Bukur 1997, Lang *et al*. 1995, Bukur 2005, Elbashir *et al*. 2003, 2004, 2005, 2009).

One advantage of the supercritical solvents is that they can enhance the mass transfer in the reaction mixture, for both the gaseous reactants and the liquid products. The SCF helps to decrease the diffusion resistance, which is a problem for the gas phase operation when the catalysts' pores filled with wax. By measuring activation energy for FTS in different media, nitrogen (23kcal/mol) > hexane (21kcal/mol) > hexadecane (17kcal/mol), Fujimoto's group determined that the reduced activation energy indicated lower diffusion resistance (Yokota & Fujimoto 1991). In addition, suppressed methane selectivity, enhanced wax selectivity and olefin

selectivity were observed as a result of lower Thiele Modulus in SC-FTS than GP-FTS (consequently, a lower H_2/CO ratio on the catalysts' active sites) (Yan *et al*. 1998). Another observation is that the SCF increases the products extraction from the catalyst pores. The degree of products extraction varies with the choice of the reaction media. By comparing the ratio of collected hydrocarbons with and without media extraction after an FT run, hexane showed a lower capacity than hexadecane, but with a heavier product distribution, while nitrogen as a medium exhibited a much worse products extraction performance (Yokota *et al*. 1991).

Another advantage of the supercritical solvents is that supercritical solvents can assist in maintaining better thermal uniformity so as to prevent the formation of the catalytic hot spots that result from the highly exothermic nature of the FTS reaction on the catlayst. Smaller variations in temperature in SC-FTS than GP-FTS has been reported by detecting catalyst bed axial temperature distribution (Fan & Fujimoto 1999, Yokota & Fujimoto 1991, Huang & Roberts 2003). Additionally, for fix-bed reactor design, narrower radial temperature distribution (though not measured in SC-FTS) is an opportunity that would allow for using larger diameter reactor tubes and simpler heat-exchange design.

The third advantage of the supercritical solvents is that supercritical solvents can help maintain catalyst performance. Roberts' group demonstrated that the FTS catalysts' activity, surface area, pore volume and metallic state (of cobalt-based catalysts, hcp in SC-FTS and fcc in GP-FTS) were better maintained in SC-FTS than in GP-FTS (Huang *et al*. 2004, Elbashir *et al*. 2005). In addition, the catalyst can be reactivated using SC-FTS after GP-FTS operation (Durham et al. 2008). Haghtalab's group reported similar observation: less loss of catalysts' surface area, pore volume and average pore diameter in SC-FTS than in GP-FTS (Irankhah & Haghtalab 2008).

The specific influence of utilizing SCF media over FTS conversion remains uncertain. When comparing between SC-FTS and GP-FTS, higher (Lang *et al*. 1995, Irankhah & Haghtalab 2008, Tang et al. 2008), lower (Yokota & Fujimoto 1989, Yokota *et al*. 1991) and similar (Bukur *et al*. 2005, Linghu *et al*. 2007) conversion has all been observed by different groups of researchers.

With respect to selectivity, SC-FTS provides improved performance over GP-FTS. Reduced methane formation has been universally observed (Yokota & Fujimoto 1989, Yang *et al*. 1998, Jacobs *et al*. 2003, Huang & Roberts 2003, Elbashir *et al*. 2005, Tang *et al*. 2008, Durham *et al*. 2008). Suppressed CO_2 selectivity was reported partly resulting from enhanced heat management (Yang *et al*. 1998, Durham *et al*. 2008). In SC-FTS, olefin selectivity at the lower carbon numbers has been reported to decrease or was not affected (Lang *et al*. 1995, Huang & Roberts 2003), while olefin selectivity at the higher carbon numbers showed an increasing trend (Lang *et al*. 1995, Bukur *et al*. 1997, Yokota *et al*. 1991, Huang & Roberts 2003, Durham *et al*. 2008). Selectivity towards 2-olefin has been suppressed in SC-FTS due to the solvents timely extraction of products from catalyst active sites, preventing secondary reactions such as carbon-carbon double bond isomerization and hydrogenation (Lang *et al*. 1993, Bukur *et al*. 1997). Due to the same reason, significant amounts of aldehydes were collected and observed in SC-FTS (using hexanes as the media) when using a precipitated iron-based FT catalyst, indicating that aldehyde is one of the primary FT products (olefins are both primary and secondary products) (Durham *et al*. 2010). With regards to hydrocarbon distribution, some studies demonstrated an enhancement of propagation probability (α) / diesel-wax selectivity (Huang & Roberts 2003, Huang *et al*. 2004, Elbashir 2005) while some others claimed no difference (Jacobs *et al*. 2003, Yokota & Fujimoto 1991, Bukur *et al*. 2005). There are also

reported data deviations from ASF behavior (Tsubake *et al.* 2002, Huang et *al*. 2003, Elbashir *et al*. 2005). Upon which, Fujimoto's group determined that re-adsorbed olefin initiated chain growth (Tsubake *et al*. 2002). On the other hand, Davis' group, concluded that olefin-readsorption and propagation was not a significant influence on the chain length distribution based on investigations that involved adding olefins to the reaction mixture (Shi *et al*. 2005).

1.4.3 Effect of Operation Parameters over Supercritical Phase Fischer-Tropsch Synthesis

SC-FTS's responses to the variations of operational parameters are similar to GP-FTS, but milder in general.

Roberts' group showed that increasing operation temperature in SC-FTS process can enhance conversion and suppress propagation probability and olefinicity (in the range of 220 ºC to 240 ºC) (Huang *et al*. 2004). Fujimoto's group reported similar conclusion in both pentane and hexane media respectively: increased reaction temperature leads to increased conversion, methane selectivity and CO_2 selectivity with decreased propagation probability and olefinicity (Linghu *et al*. 2004, Linghu *et al*. 2007). Haghtalab's group showed similar results (Irankhah & Haghtalab 2008). All of these works used supported cobalt catalysts. However, Bukur's group reported that temperature showed inconsistent effects on olefinicity (Bukur *et al*. 1997).

Roberts' group demonstrated that by increasing pressure up to 65 bar, the conversion can be increase in supercritical hexanes, while beyond 65 bar to 80 bar, the trend showed the reverse (Huang & Roberts 2003). A reasonable cause for this is that very high pressure can result in high density and higher diffusion resistance for the reactants. Propagation probability can be elevated too by increasing reaction pressure (Huang & Roberts 2003). Haghtalab's group reported similar results (Irankhah & Haghtalab 2008).

Increasing the syngas ratio (H_2/CO) can enhance the conversion and methane selectivity

while generally (and weakly) increasing CO_2 selectivity (Irankhah & Haghtalab 2008), increase light product selectivity (Huang *et al*. 2004), 2-olefin selectivity (Bukur *et al*. 1997) and suppress heavy product (Huang *et al*. 2004) formation and olefin content (Bukur *et al*. 1997). By increasing conversion, olefin selectivity(Bukur *et al*. 1997, Linghu *et al*. 2004), is reduced while 2-olefin selectivity (Bukur *et al*. 1997), methane selectivity (Linghu *et al*. 2004, Irankhah & Haghtalab 2008), CO2 selectivity(Linghu *et al*. 2004, Irankhah & Haghtalab 2008) and propagation probability (Linghu *et al*. 2004) is elevated. Roberts' group also demonstrated that the product distribution shifted towards a lighter product spectrum when increasing the syngas flow rate while keeping the media rate constant (Huang *et al*. 2004).

1.4.4   Future Work for Supercritical Phase Fischer-Tropsch Synthesis

As proposed by Roberts' group (Elbashir & Roberts 2005) and Elbashir's group (Elbashir *et al*. 2009), due to complexity of the SCF-FTS process, fundamental understanding is required with respect to the phase behavior of the reactant-solvent/reactant-product-solvent mixtures and the interrelationship of phase behavior of the reaction mixture and FTS performance (such as conversion, selectivity and product distribution). In chapter 5, preliminary investigation results of locating the critical point loci of model SC-FTS reaction mixtures have been reported.

Despite the benefits from the utilization of SCF media for FTS, this technology has not been commercialized in industry yet due to perceived high capital and operating costs for maintaining high pressure, separation and recycling of the large amount of SC media, etc. Elbashir *et al* outlined the future work for developing a pilot scale SC-FTS plant as follows (Elbashir *et al*. 2010).

1. Optimization of reaction parameters, including temperature, pressure, solvent, solvent to reactant ratio, etc.

47

2. Using pressure drop for separation and recycling unreacted reactant and supercritical fluid media.

3. Optimization of the overall process, integrating advanced process techniques and dynamic control systems.

4. Evaluation the synthesized process and system.

1.5   Fischer-Tropsch Products Refining and Upgrading for Fuel Production

Naphtha, transportation fuels (gasoline, jet fuel and diesel), and wax are the desired products of FTS plants. Middle distillate, a mixture of hydrocarbons in the range of jet fuel (C_8 - C_{16}) and diesel (C_{12} - C_{22}), and naphtha are often sold to producing valuable chemicals as a feedstock. However, the raw products coming out of FT reactors are distributed over a wide spectrum including a wide range of hydrocarbons and oxygenates. As a result, a refining process takes place immediately after the FTS unit. The refining process is directly linked to profit production. Numerous studies involving FT refining technology and techniques have been done by both academic researchers and commercial companies. The related technologies include: oligomerization, isomerization, alkylation, hydrotreating, cracking, aromatization, catalyst reforming, coking, alcohol dehydration, etc. (Dry 2003, de Klerk 2008, de Klerk 2010).

For a typical refining process of the raw FTS products, unconverted CO, H_2 and light gaseous products (C_1-C_4) are separated from the products mixture and recycled to the FTS unit or other processes. Then the residual syncrude (the liquid portion of FTS products) is separated by distillation into naphtha, distillates and wax. Hydrogenation of naphtha produces primarily paraffins, part of which is further isomerized to increase branching to enhance fuel quality. The other portion of hydrogenated naphtha is processed into the catalytic reforming unit to increase aromatic content as required for different purposes (e.g. to enhance energy density). The

distillates are hydrotreated, to form desired fuels or chemical feedstock. The wax stream is cracked into distillates and naphtha. C_1-C_4 gaseous hydrocarbons are by-produced within the whole syncrude refining process. Once separated, they are transported for recycle or other uses (de Klerk 2008).

There are two major problems for fuel production via FTS: low fuel fraction selectivity and unsatisfying fuel quality. As mentioned previously, the FTS products follow the Anderson-Shultz-Flory (ASF) product distribution model, which is unselective towards each individual product or product fraction. According to the literature, the maximum gasoline (C_5 - C_{11}) selectivity that can be reached is up to 42% at a propagation probability (α) of 76%, while the diesel (in the hydrocarbon range of C_{12} - C_{18}, however there are others that refer to C_{12} - C_{22}) selectivity is 22% with an α value of 87% (Steynberg & Dry 2004). Both oligomerizing light olefins into longer chain hydrocarbons and cracking heavy waxes into fuels can be employed to increase the selectivity. For fuel quality issues, which are concerns for both gasoline and diesel fraction, poor cold-flow properties (cloud point, pour point, cold filter plugging point, etc.) which result from the low content of branched compounds and low aromatic content that leads to low density are primary concerns. Additionally, FT gasoline suffers from low octane number (which describes the tendency of fuels to self-ignition during compression prior to the desired position of the piston in the cylinder as appropriate for valve and ignition timing) (Steynberg & Dry 2004, de Klerk 2008).

1.5.1 Oligomerization

Oligomerization is the process that describes the conversion of monomers (in this case, the FT hydrocarbons containing double bond) into longer chain polymers. There are two ways to realize oligomerization of olefins: thermal oligomerization and catalytic oligomerization.

Thermal oligomerization is a radical based conversion process, taking place in the temperature range of 320 ºC - 400 ºC while the catalytic oligomerization temperature is from 130 ºC to 250 ºC (de Klerk 2005). 1-Olefins are more reactive than internal olefins. The oligomerization generated heavier hydrocarbons present a low degree of branching. For thermal oligomerization, operating conditions had only a minor influence (temperature had minimal effect on the product distribution and quality while pressure only influences the reaction rate in the gas-phase reactions). The quality of produced motor gasoline, distillate and lubricating oil is determined by the feed (de Klerk 2005). Oxygenates existing in the FT product does not influence the process. Carbon formation is not a significant issue (0.4mg/g of catalyst) (de Klerk 2005). No aromatics are made via the process, neither does skeletal isomerization occur. The dissociation energies indicate that severance of C-C bonds, instead of C-H bonds, produces the intermediate radical. The double bond isomerization to linear internal olefins prior to oligomerization greatly suppressed the reaction rate. The disadvantage of the slow reaction rate at $0.1 \text{mol} \cdot \text{s}^{-1} \cdot \text{m}^3$ can be offset by limiting the refining environment to be feed-specific in olefin-rich feed (Steynberg & Dry 2004, de Klerk *et al*. 2004, de Klerk 2005, 2006, 2007).

A solid acid catalyst is generally employed in the catalytic olefin oligomerization. UOP uses solid phosphoric acid (SPA) as a standard catalyst. For FT processing, both SPA and ZSM-5 are utilized as oligomerization catalysts by Sasol's Conversion of Olefins to Distillates (COD) and Mobil's Olefins to Gasoline and Distillates (MOGD) (Steynberg & Dry 2004, de Klerk 2006).

SPA and ZSM-5 can be used to target different product fractions. SPA produces good gasoline but poor diesel while ZSM-5 yields high quality diesels (de Klerk 2006). SPA requires water in the feed. The catalyst is supported on quarts or Kieselguhr (silica) with an upper

temperature limit of 245ºC and a lower hydration limit of 110% H_3PO_4. High moisture yields

higher gasoline selectivity with an inconsistent effect on product branching. When the catalyst is

under-hydrated, it loses activity while becoming brittle and disintegrates (Prinsloo 2006).

Hydration rate is traditionally expressed in terms of phosphoric acid (H_3PO_4) content which

merely refers to the active/liquid phase. A SPA catalyst claiming a hydration level (or acid

strength) of 100% H_3PO_4 does not imply the it has 100% pure H_3PO_4, however, it only refers to a

state of dryness where the active phase consists of some water and approximately 14% and 86%

pyro- and ortho-phosphoric acid, respectively (Prinsloo 2006, Jameson 1959, Brown & Whitt

1952). When drying a 85% H_3PO_4, the H_3PO_4 does not only concentrate by releasing water but

also forms linear polymers of higher acids, such as pyro- and tripoly- phosphoric acid. Brown

and Whitt proposed the method of estimating the equilibrium data of the hydration of the

phosphoric acid (Brown & Whitt 1952).

Because of easier extraction of heavy oligomers, larger catalyst pore size (larger than 10nm)

is favored showing a longer catalyst life. Due to the sized-selecting function of ZSM-5, products

are limited to methyl branched hydrocarbons (Steynberg & Dry 2004).

Amorphous silica alumina (ASA) has been proposed as a promising oligomerization

catalyst by de Clerk with a high hydrogen transfer propensity, yielding a distillate with density of

810g/L, a cetane value of 28-30, a kinematic viscosity of 2.8-3.6 cSt and good cold flow

properties. The feed used was C_3 - C_6 HTFT condensate and a C_7 - C_{10} fraction from

oligomerized HTFT condensation, operated in the region of 140 ºC - 265 ºC and 3.6 - 6.8 MPa

(de Klerk 2007). Although the cetane index of the distillates was low, it can be improved by

mixing with raw FT diesel which has an above normal cetane value. The catalyst deactivation

occurred at a rate of 0.03 - 0.04mg/h carbon per gram of catalyst, but can be fully restored by

controlled carbon burn-off using oxygen under nitrogen purge conditions. It was concluded that the weaker acid sites in ASA make a better oligomerization catalyst by suppressing the secondary reactions such as cracking. However, when oxygenates are part of the feed, the catalyst life is shortened with reduced product viscosity. Acids will be produced as the products of these oxygenates leading to further removal processing such as aqueous extraction (Steynberg & Dry 2004, de Klerk 2007).

Oligomerization is an exothermic reaction which releases 60 kJ/mol (or 100KJ/mol) of heat. This nature can increase the difficulty of isothermal operation, the possibility of irreversible catalysts' deactivation resulted from clogging and coking from failure to extract heavy oligomers. In this respect, utilization of supercritical fluid as reaction media to improve the heat management and mass transfer is promising to assist the oligomerization process.

1.5.2 Cracking/Isomerization

In the last two decades, a series of environmental factors have led to the promulgation of more stringent automotive emission regulations. The European Union has established and updated (on a regular base) the emission standards for automobile exhaust gases including NO_x, SO_x, CO, HC and particulate emission. FT derived middle distillates are generally accepted as sulfur-free with extremely low content of aromatics. Several investigations have revealed that using FT derived diesel fuel neat or as a blending component can lead to a remarkable reduction in exhaust emissions (Alleman & McCormick 2003, Nakakita *et al.* 2004).

Despite of all kinds of efforts, the enhancement of the intrinsic selectivity of FTS towards the desired fractions (e.g. middle distillates) has only achieved limited success. Researchers have proposed different kinds of post treatment of the FT waxes (Dupain *et al.* 2005, Dancuart *et al.* 2003, de Klerk 2007) and so far the most effective route universally accepted to maximize the

overall middle distillate yield is via FT wax hydrocracking (Sie *et al*. 1991, Leckel & Liwanga-Ehumbu 2006, Steynberg & Dry 2004). There are two primary reactions that occur during the hydroconversion: hydroisomerization and hydrocracking of aliphatic chains. The first reaction route results in a significant enhancement of cold flow properties by generating branched hydrocarbons, while the later is meant to increase the concentration of the middle distillate yields by breaking up the long hydrocarbon chains in waxes (Calemma *et al*. 2010).

By carrying out the reactions under suitable operation conditions and using a viable catalyst, the cold flow properties (cloud point, pour point, cold filter plugging point, etc.) of the FT products can be significantly improved with an enhanced middle distillate yield (80%-85) (Calemma *et al.* 2001). In the wax conversion range of 80% to 90%, the middle distillate yield increases, and with an even higher conversion, the secondary cracking decreases the middle distillate yield. However, larger paraffins are preferentially cracked over small ones, that meaning the wax can be cracked back to diesel range with much less diesel being cracked into gasoline and gases (Abbot & Dunstan 1997). By recycling, the waxes can be cracked into extinction. Normally, a mild catalytic cracking of FT wax can result in a product mixture with 80% diesel, 15% naphtha, and 5% gases (by random beta scission). Compared to petroleum derived feed, cracking of LTFT waxes is much easier due to the high paraffinicity and low aromatics. These features suppress coking and also allow for a lower operation pressure (30 to 70 bar for LTFT wax cracking vs. up to 150 bar for petro-waxes) and lower temperature (300ºC -350ºC for Shell's SMDS vs. higher than 350ºC for petro-waxes) (de Klerk 2008).

Hydrocracking catalysts are bifunctional, having the metal sites for hydrogenation and dehydration and acid sites for isomerization and cracking. They are often composed of active metal and solid acid support. There are two type of active metal, one is Co, Mo, Ni, W and

various form of combination, the other is Pt or Pd and the combination. The solid acid supports which are often used are silica, alumina and their combination, sulphated zirconia, silico-aluminophosphates (SAPO), mesoporous materials (MCM-41), as well as zeolites (Akhmedov & Al-Khowaiter 2007). Supports with strong acidity (such as some zeolites) favor cracking reaction, while moderate acid supports (such as SAPO) show higher selectivity towards isomerization (Deldari 2005, Rossetti *et al.* 2007). Fujimoto's group reported that palladium was superior to platinum and that zeolites impregnated by ion exchange yields a higher isomer selectivity than those using an impregnation method (Liu *et al*. 2006). They also reported for β-zeolite, the optimal Si/Al ratio is 25.6 (Liu *et al*. 2006). Botes and Bohringer concluded that low acidity ZSM-5 with a Si/Al ratio of 280 is superior in activity maintenance than a high acidity ZSM-5 with a Si/Al ratio of 30 (Botes & Bohringer 2004). Calemma *et al.* reported using a Pd/ASA catalyst at 319ºC - 351ºC and pressure in the range of 3.5 - 6.0 MPa for hydrocracking of a C_{10} - C_{70} FT derived wax led to a middle distillate yield up to 85% with enhanced isoparaffin concentration. This resulted in excellent cold flow properties (C_{10} - C_{14} freezing point from -23 ºC to -45 ºC and C_{15} - C_{22} pour point from 13 ºC to -23 ºC). The C_{15} - C_{22} fraction exhibited a cetane number ranging between 75 and 80. NMR and GC detection showed the concentration of branched groups in the middle distillate products follow the order: methyl >> ethyl > propyl (Calemma 2001, Calemma *et al*. 2010).

Arno de Klerk demonstrated that the thermal cracking of FT waxes (C_{20} - C_{120} fraction) presents poor utility for fuel production. At higher temperatures ranging from 460 ºC to 490 ºC and at low (1bar) and high (60 bar) pressure, the process produced a large amount of heavy diesel and light wax with limited levels of branching. In addition, the inorganics plugged the reactor within 18 days (de Klerk 2007).

By using the catalyst, the cracking reaction temperature is reduced considerably. It is due to the improved (compared to thermal cracking) heat transfer because of surface/volume effect (Golombok *et al*. 2000, Lee *et al*. 2004). However, in spite of using catalyst, the high rate of coking and heavy hydrocarbons gasification reactions produce high amount of CO and CO_2 (Mukhopadhyay & Rao 1993, Towfighi *et al.* 2002). Thus, utilization of supercritical fluid as reaction media, offering advanced heat and mass transfer properties, is proposed to benefit the process by slowing down the coking rate and catalyst deactivation rate. There have been investigations on cracking of n-heptane on Y-type zeolites under supercritical and near-supercritical conditions. The researchers concluded that supercritical conditions can offer a much better activity maintenance (Dardas *et al*. 1996).

Chapter 2 Preliminary Catalyst Performance Studies Involving Fischer-Tropsch Synthesis, Oligomerization and Hydrocracking/Isomerization Reactions

2.1 Catalytic Investigations of Fischer-Tropsch Synthesis

2.1.1 Introduction

As described in Chapter 1, Fischer-Tropsch (FT) synthesis yields a wide spectrum of hydrocarbons and oxygenates with carbon numbers ranging from 1 to 120 (de Klerk 2009, Steynberg & Dry 2004). The refining of FT products is different from the refining of crude oil, especially with regards to desired products, heat management and most importantly, the feed composition (de Klerk 2001). However, the same basic technologies and catalysts are applied to FT primary product refining and upgrading (Stell 2001). The desired products are generally split into two types: transportation fuels and chemicals. Traditionally, fuel production is the focus of FT products refining. However, large chemical market profit is drawing attention to FT plants and refineries for the following reasons: 1. ethylene price is twice the price of crude oil per unit weight, 2. wax has more value as itself than as fuels, 3. the price of detergents, which are made from FT alcohols, is six times that of fuels (Dry 1999, Dry 2002, de Klerk 2008).

Fischer Tropsch syncrude (FT products excluding the gaseous portion) is very different from crude oil. The presence of olefins content represents one of the many differences. While their existence is only sparingly present in crude oil, olefins constitute a significant portion in cobalt LTFT syncrude and make up a large part of iron LTFT and HTFT syncrude. Thus the necessity of employment of a well-designed olefin oligomerization process emerges.

FT syncrude properties are largely dependent on the specifics of the Fischer-Tropsch synthesis (FTS) process, such as FT catalyst composition, catalyst deactivation portfolio, reactor

type, operating conditions, etc. (Steynberg & Dry 2004). Since the cobalt-based FT catalysts present a higher hydrogenation activity than iron-based FT catalysts, olefin selectivity and oxygenates selectivity in the Co catalyzed FT syncrude are lower (while H_2O selectivity is higher). Because fixed bed reactors are said to afford higher hydrogenation due to plug-flow behavior compared to slurry bed reactors, they yield less olefins and oxygenates (de Klerk 2009). It has been shown that the syncrude from Shell's Co-LTFT fixed bed reactor exhibits higher paraffin selectivity than the Sasol Co-LTFT slurry bed reactor (de Klerk 2009).

Fe-HTFT syncrude possesses the highest olefinicity, while Co-LTFT produces the highest single pass middle distillate content and Fe-LTFT affords the most balanced syncrude. Other than HTFT syncrude, FT syncrude is predominantly free of aromatics, which is a drawback for FT fuels (Dry 1999). Iron-based FT catalysts present lower hydrogenation activity than cobalt-based FT catalysts, which results in higher olefin selectivity in the LTFT synthesis. Therefore, using a precipitated iron-based LTFT catalyst can offer a more desirable feed (due to higher olefin content) if an oligomerization step is added sequentially downstream to the FTS step. Light olefins can be oligomerized into the gasoline and diesel range fractions to increase the middle distillate selectivity. Additionally, due to the low price of iron and previous experience on the precipitated iron-based FT catalysts in our group, this study was initiated in order to test FTS performance using a precipitated iron catalyst.

2.1.2 Material and Methods

The method of synthesis employed for the precipitated iron-based LTFT catalyst is similar to the method described in Chapter 1. To be specific, deionized ultra-filtered (DIUF) water (Fischer W2-4) was used to dissolve iron nitrate nonahydrate Fe $(NO_3)_3 \cdot$ 9 H_2O (Sigma-Aldrich 216828-500G, CAS# 77-61-8) and zinc nitrate hexahydrate Zn $(NO_3)_2 \cdot$ 6 H_2O (Sigma-Aldrich

228737-100G, CAS # 13778-30-8) to make a 1M solution and 0.1M solution, respectively. The reducing agent used was a saturated ammonium carbonate $(NH_4)_2CO_3$ (Sigma-Aldrich 207861-100G, CAS# 506-87-6) solution. The mixture of iron nitrate solution and zinc nitrate solution was added continuously at a rate of approximately 2ml/min into 30ml DIUF water with vigorous agitation (1000 rotations per hour). The temperature was held constant by a water bath at 80 ºC (± 2 ºC). The pH value was maintained around 7.0 (± 0.5, measured by a Denver Instrument UB-10 pH meter) by the manual addition of saturated ammonium carbonate solution. When the total volume of precipitate and solution was around 1 liter, reagents addition was stopped and the solution temperature was maintained at 80 ºC (± 2 ºC) with continuous stirring to age the precipitate for 1 hour. After aging, the solution and precipitate was allowed to cool to near room temperature. Then, vacuum filtration was applied to the slurry, and the filtered cake was reslurried in DIUF water and stirred to dissolve leftover ions into the water, and then the slurry was vacuum filtered again. This "precipitate washing" process was repeated 3 times. The filter cake was then manually broken up using a glass rod in an evaporation dish and dried overnight at 80 ºC. The dried precipitate was calcined in a tube furnace with flowing air at atmospheric pressure. The furnace temperature was programmed to ramp at 5 ºC/min from room temperature to 400 ºC. It was held for 240 min at 400 ºC, and then cooled to room temperature (RT) at 5 ºC/min. The pore volume of the precursor was measured by addition of DIUF water until it appeared pasty (while measuring the added mass of water). Knowing the water density at the room temperature, the total volume of added water and the pore volume can be determined. The paste was then dried at 80 ºC. The incipient wetness method was used for copper promotion and potassium promotion. The copper promotion was done by addition of copper nitrate trihydrate $Cu (NO_3)_2 \cdot 3 H_2O$ (Sigma-Aldrich 223395-100G, CAS# 3251-23-8) solution. The solution was

prepared based on the total pore volume of a certain amount of the above-mentioned catalyst and a ratio of 0.01 mol Cu per 1 mol Fe. After the addition of this solution by agitation with a stir rod, the catalyst was then dried and calcined as described above. Similarly, based on the total pore volume of a certain amount of the above-mentioned catalyst and a molar ratio of 0.02 mol K per 1 mol Fe, the potassium carbonate (Sigma-Aldrich 209619-100G, CAS# 584-08-7) solution with a proper concentration was prepared. After the copper promotion, potassium was loaded on the catalyst by adding the potassium solution, where the mixture was stirred by a glass rod, and the solution was then dried and calcined following the same procedures as described above.

A diagram of the reactor system for Fischer-Tropsch synthesis in the gas phase is shown in Figure 2.1. Helium gas (Airgas, ultra high purity) is used during the system pressure test, reaction startup and shut down. Synthesis gas (Syngas) (Airgas, vol%: N_2: CO: H_2 = 1.54: 37.2: 61.26) is fed into the reaction system controllably by a mass flow controller (MFC, Porter Instrument Company. Inc., model 221-6KASVBAA, 0 - 500 SCCM, Control box: model CM2). The syngas is initially heated in the pre-heating zone and enters the top of the tubular fixed-bed reactor. From the reactor, the mixture of unreacted syngas and products pass through heated tubing to the back pressure regulator (BPR, Straval Valves Inc. model BPH0502T-N2403) which is employed to control the system pressure, and then through heated tubing to the cold trap (CT, Swagelok Inc. 304L-HDF4-1000). The cold trap is cooled by an ice-water-mixture bath outside its shell. The condensable products are accumulated in the CT and are manually collected and tested periodically by injecting them into a gas chromatograph with a flame ionization detector (GC-FID, Varian GC 3300 with a DB-5 capillary column). The incondensable gas mixture (syngas residue and light products) leaves the CT and is passed through a 10-port injection valve for periodic injection into gas chromatograph with a thermal conductivity detector (GC-TCD,

SRI MultiGas Analyzer #1). After that, the gases are passed through a bubble meter, which allows for the measurement of the real-time gas effluent volumetric flow rates. The gas effluent is then vented into the fume hood.
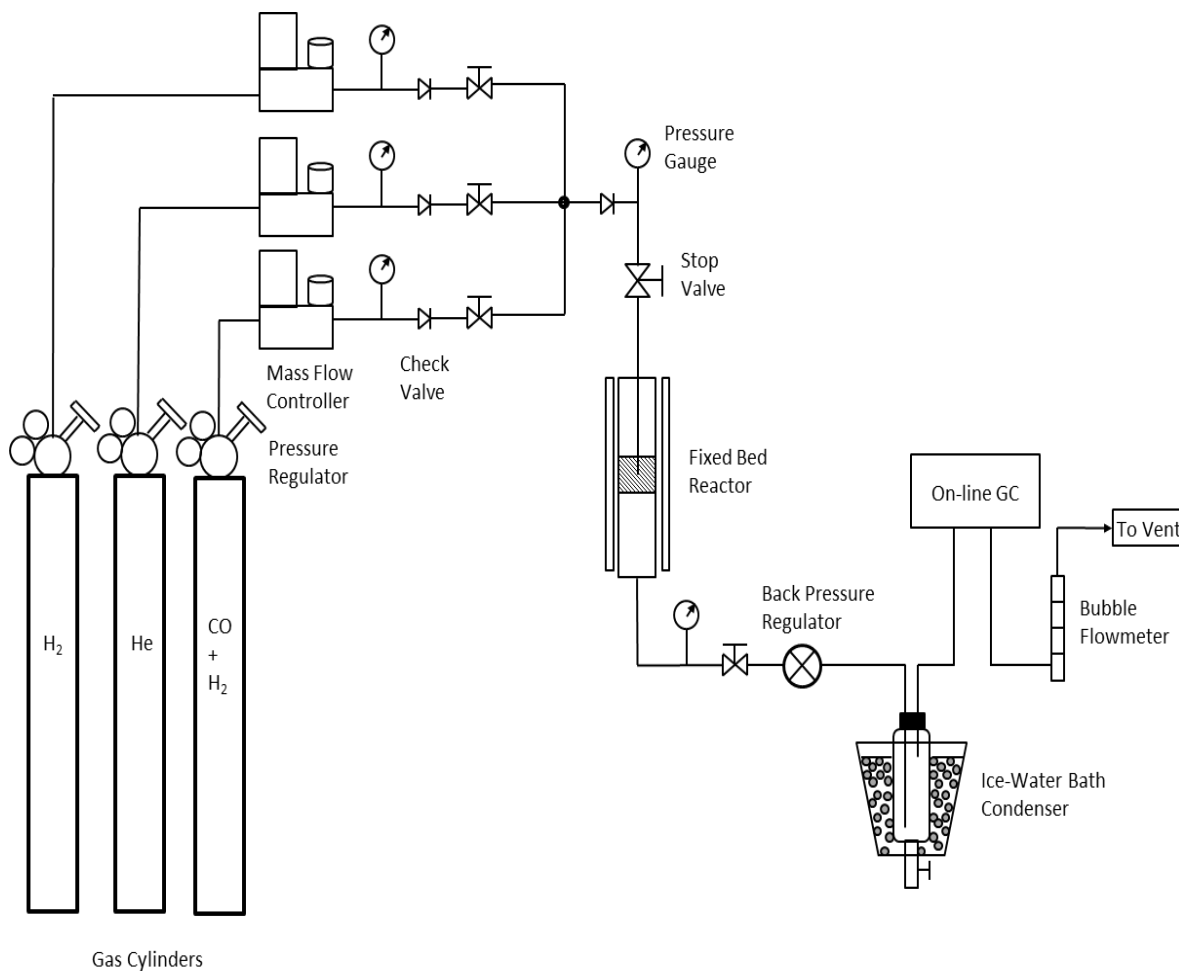
Figure 2.1   Flowchart of the Fischer Tropsch reaction system

The reactor in this system was made from Swagelok stainless tubing (Swagelok SS-T8-S-065) with a length of 6 inches and an O.D. of 1/2 inch. 1 gram of the above mentioned iron-based FT catalyst was diluted with 2 grams of glass beads and then loaded in the middle of the

reactor, kept in place by glass wool (Omega) on the top and the bottom. A thermocouple (Omega, KTSS-116G-12) was placed in the middle of the catalyst material to monitor the temperature at the center of the reaction bed, and this thermocouple is used as the input for a temperature controller (Omega, CSC32) equipped with a tape heater. A stainless steel filter (3B Filters 866-323-4583 P/N S82-2P2P-10) of 100 micrometers was positioned at the bottom of the reactor to prevent catalyst loss into the sequential tubing.

Before an FTS reaction is performed, a catalyst reduction step was performed using a H_2 flow of 50 SCCM at 270 ºC for 10 hours. The bed temperature was controlled to ramp from room temperature to 270 ºC at a rate of 5 ºC/min. After the reduction, the catalyst bed was cooled to room temperature. Hydrogen flow was then switched to helium flow at a rate of 100 SCCM in order to build up the system pressure by adjusting the BPR. When the system pressure was steady at 17.5 bar (254 psi), the reaction bed temperature was increased to 240 ºC at a ramping rate of 5 ºC/min with a stream of Helium at a 50 SCCM flow rate. After the bed temperature was steady at 240 ºC, delivery of syngas (N_2: CO: H_2 = 1.54: 37.2: 61.26, note that a small amount of nitrogen was used as internal standard for gas analysis) was initiated with a flow rate of 50 SCCM. After the reaction pressure was maintained at steady state at 17.5 bar for over 30 hours (254 psi, stage 1), the system pressure was increased to 35 bar (508 psi, stage 2) and held for over 50 hours. 35 bar is a more preferable pressure for upgrading reactions. Then, the system pressure was returned to 17.5 bar (254 psi, stage 3) for comparison of the catalyst activity before, during and after pressure elevation. The reason for running the reaction at elevated pressure (35 bar) was to evaluate the FT performance at a standard upgrading pressure in order to create a basis for further comparison. During the reaction, the system temperature was held steady at 240 ºC. Liquid products were collected from the cold trap every 12 hours after steady state was

reached. The reaction experiment has been performed over three times to confirm the reproducibility

2.1.3 Results and Discussion

The peak areas for the different components in the Cold Trap Outlet Vapor Stream (CTOVS) as resolved at different retention time in the associated gas chromatogram can be readily converted to concentrations using each component's molar response factor, where:

Molar response factor (RF_n) = peak area / moles of this component injected

The response factors for the various components were determined by using the same injection procedure with syngas and other gas standards. While this method helps in determining each of the various components' relative concentration in the CTOVS, the stream concentration relative to initially injected syngas remains unknown. Thus, a small volume of N_2 is added to the syngas as an internal standard, given that it is an inert in the reaction processes. Based on each constituent's relative concentration compared to the N_2 concentration in the outlet vapor, each constituent's concentration variance relative to the original inlet syngas can be determined. Additionally, by combining this with the outlet flow rate, the concentration and flow rate of each component in the CTOVS can be determined.

For the collected cold trap liquid, the mass response factor (RF_m) is used to quantify each component's concentration, where:

Mass response factor (RF_m) = peak area / mass of this component injected

Dietz concluded that the RF_m is approximately identical for nearly all hydrocarbons without heteroatoms (atoms that are not C or H) (Dietz 1967). Thus, the concentration of hydrocarbons with different carbon number can be easily determined. Using external standards, the retention time and the mass response factor of different constituents on the GC-FID can be

62

determined, thus the liquid hydrocarbon components can be determined qualitatively and quantitatively.

In addition to hydrocarbons, FTS also produces oxygenates. Theoretically, the major oxygenates are carbon dioxide (especially when using an iron-based catalyst) and water (especially when using an cobalt-based catalyst). The concentrations of alcohols, aldehydes, ketones, esters, etc. are trivial compared to CO_2 and H_2O for standard gas phase FTS. For easy characterization, one assumption can be utilized in the calculation, which supposes that all the oxygen entering the reactor (brought in by CO) departs the reactor system in the form of CO_2 or H_2O or CO. Thus, via collection and analysis of condensed liquid products and vapor stream from cold trap, the reaction performance can be fully characterized in terms of conversion, selectivity, productivity, etc.

The conversion and selectivity are defined as:

Conversion (H_2) = mole of H_2 consumed/ mole of H_2 injected

Conversion (CO) = mole of CO consumed/ mole of CO injected

Selectivity (CO_2) = mole of CO_2 produced/ mole of CO consumed

Selectivity (CH_4) = mole of CH_4 produced/ mole of CO consumed

Since the FT products are commercially sold on a mass or volume basis, the molar selectivity of the FT process is not as useful as selectivity on a mass basis. As such, for the following study we calculate liquid FT products selectivity based on mass:

Selectivity (C_n hydrocarbon in liquid phase) = mass of C_n hydrocarbon produced/ mass of total liquid hydrocarbons in the sample

The CO conversion as a function of time on stream is presented in Figure 2.2. At standard FT reaction pressure, 17.5 bar, the CO conversion was around 30% at steady state. At elevated

reaction pressure (35 bar), the CO conversion was increased from 30% to c.a. 50%, which is consistent with the generally accepted observation that the conversion is higher at the elevated pressure because the partial pressures of the reactants (i.e. CO and H_2) are effectively doubled (at the inlet of the reaction bed). From the kinetic equation for an iron FT catalyst (Equation 1.1), the reaction rate is only a function of hydrogen partial pressure at low conversion ($P_{H_2O} \approx 0$). At higher partial pressures of the reactants, the conversion increases and the partial pressure of generated water can no longer be regarded as zero. As such, the factor $P_{CO}/(P_{CO} + P_{H_2O})$ from Equation (1.1) is smaller than one, so that the elevated conversion is less than doubled when the hydrogen partial pressure is doubled. Interestingly, it was determined that the use of Swagelok tubing as the FT reactor generated more water than that produced using a similar HIP reactor at the reaction conditions studied here. The surface carbon coverage on the active sites of the FT catalyst decreases at high water partial pressure due to increased surface oxygen coverage, which will further inhibit the surface carbon formation during the dissociation of CO (Steynberg & Dry 2004), thereby negatively affecting the conversion. This may partially explain the lower CO conversion (c.a 30%) obtained in the Swagelok reactor tubing compared to the Hip reactor (c.a. 40%) at similar reaction conditions.
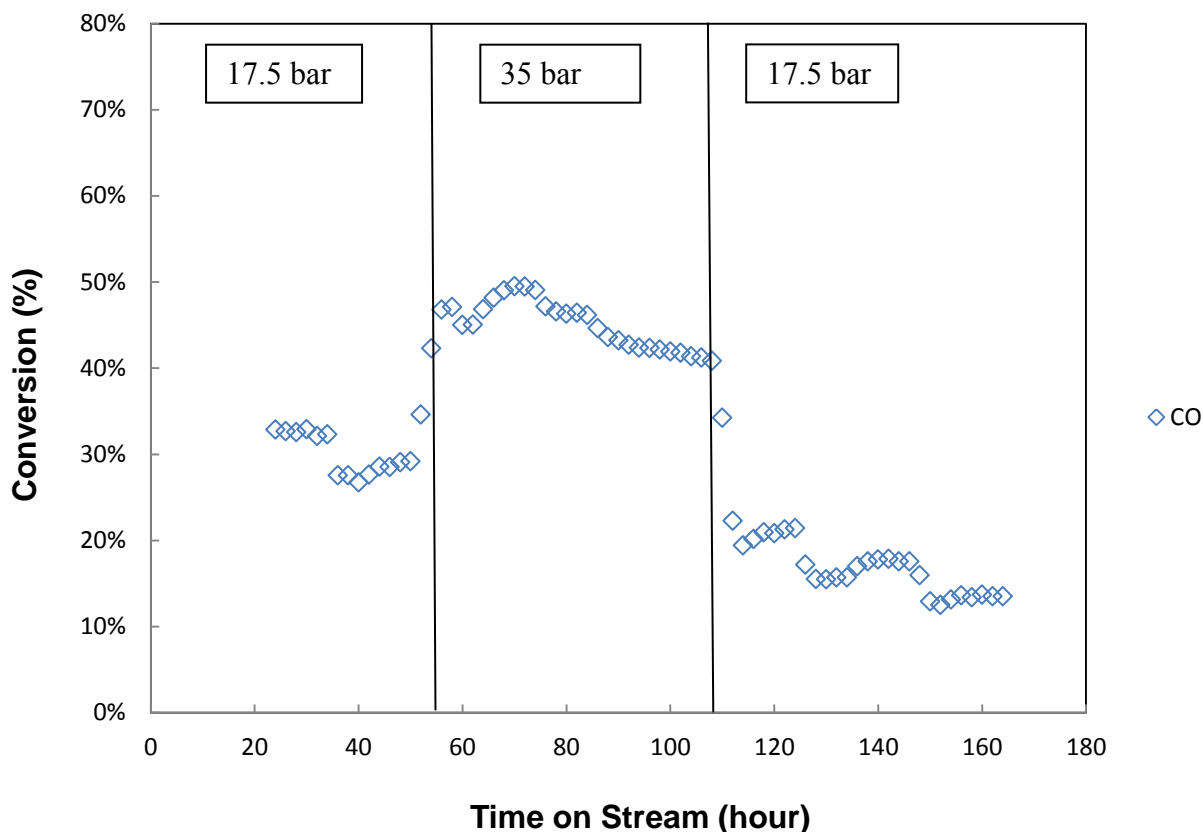
Figure 2.2   CO conversion as a function of time on stream for gas phase Fischer-Tropsch synthesis. (1 gram Fe/Zn/Cu/K FT catalyst in the first reaction bed, T = 240 ºC, synthesis gas flow rate: 50 SCCM, synthesis gas ratio: H_2: CO: N_2 = 62: 36.5: 1.5.)

As shown in Figure 2.2, the CO conversion was initially 33% at 22 hour of time on stream once steady state was reached. The CO conversion then decreased to c.a 28% at 35 hour of time on stream. When the operation pressure was elevated to 35 bar at 50 hour of time on stream, the CO conversion was effectively increased, and reached a value of c.a. 50% at 70 hour of time on stream. Then, the CO conversion slowly diminished to 40% over a time span of 40 hours. After decreasing the system pressure from 35 bar to 17.5 bar at 110 hour of time on stream, the CO conversion was reduced to about 20%, which was nearly half of the CO conversion at the same system pressure (17.5 bar) at the beginning of the reaction. The CO conversion then showed a decreasing trend during the following period of 50 hours (from 110 to 160 hour of time on

stream) and ended up at c.a 14%.

It is well known that the activity of iron FT catalysts declines with time on stream (Steynberg & Dry 2004, Dry 2002). A decrease in CO conversion with time on stream may be an indication of catalyst deactivation, which can result from loss of active sites by reoxidation of active metal/carbide (Bukur *et al*. 1995, Elaison & Bartholomew 1999), coking (Dry 2001, Bukur 2002, Elaison & Bartholomew 1999) and/or fouling among other reasons (Steynber & Dry 2004). For instance, active metal/carbide can be reoxidized by H_2O into inactive oxide (Steynberg & Dry 2004). However, reoxidation should not occur to a significant extent due to the low content of H_2O that is produced in iron-based FTS. Coking results from carbon deposition on a catalyst hot spot where CO (through Boudouard reaction, $2CO \rightarrow CO_2 + C$) or hydrocarbons (i.e. coke precursors) are converted into coke. Consequently, the active sites can be blocked by this coke, resulting in a reversible deactivation. Fouling of the catalyst can also occur by a number of mechanisms including the sintering of active sites due to thermal or leaching by the reaction mixture (Steynberg & Dry 2004). For gas phase FTS using an iron-based catalyst, sintering is the major fouling type. In this case, catalyst particles can be fused at high temperature and the porous structure can be destroyed by the combination of high temperature and high pressure. As a result, the active sites can be diminished. Additionally, mass transfer limitations of products within the catalyst pores and from the catalyst surface to the bulk media can lead to product accumulation in the catalyst pores and on the catalyst external surface, which can contribute to diffusion resistance and thus decreased apparent activity. It is suggested that a combination of these effects results in the negative slope of CO conversion vs. TOS at the different system pressure levels (17.5 bar and 35 bar). These deactivation mechanisms are highly affected by local overheating and accumulation of products. Therefore, enhancement in heat

transfer (to prevent the formation of hot spots and thermal runaway) and mass transfer (to prevent diffusion resistance due to product build-up) are critical for maintaining the FT catalyst performance.

Figure 2.3 shows the methane selectivity and carbon dioxide selectivity as a function of time on stream. At the first pressure level (17.5 bar), the methane selectivity was initially as low as 3.1%, which is nearly the lowest that an iron FT catalyst can achieve. The best FT catalysts can offer a methane selectivity as low as 3% of the carbon in the hydrocarbon products (Steynberg & Dry 2004). Methane selectivity continuously increased with time at the pressure level of 17.5 bar (this can clearly be seen by comparing stage 1 and stage 3), which is consistent with the conclusion by the US Bureau of Mines that over iron catalyst lathe turnings, the selectivity shifted towards lower molecular mass products (Steynberg & Dry 2004). The wax build-up in the catalyst pores can increase the diffusion resistance with time, which can promote methanation (Yan *et al*. 1998). The influence of the pressure change on methane selectivity was insignificant during this reaction study at the pressure range investigated, which is consistent with Mark Dry's conclusion that for an iron-based LTFT catalyst, operation pressure has little effect on the product distribution (Dry 1981).
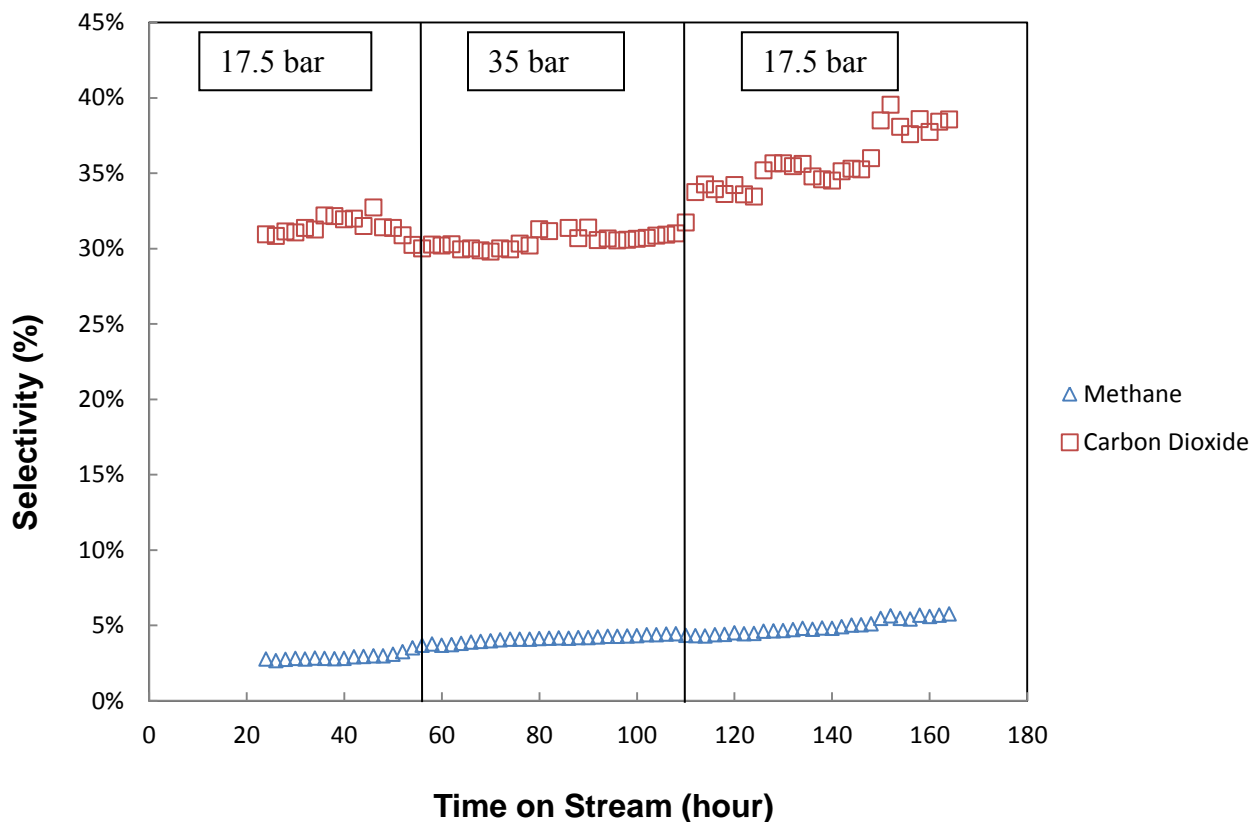
Figure 2.3 CH_4 and CO_2 selectivities as a function of time on stream for gas phase Fischer-Tropsch synthesis. (1 gram Fe/Zn/Cu/K FT catalyst, T = 240 °C, synthesis gas flow rate: 50 SCCM, synthesis gas ratio: H_2: CO: N_2 = 62: 36.5: 1.5.)

As shown in Figure 2.3, the CO_2 selectivity was around 30% which results from the active nature of the iron FT catalyst towards WGS. The CO_2 selectivity increased with time on stream (TOS) at the pressure level of 17.5 bar (by comparing stage 1 and stage 3), indicating the presence of a catalyst deactivation mechanism. The increased degree of oxidation also helps to explain the progressive loss in FT activity, which was suggested by the decrease in CO conversion with TOS, as shown in Figure 2.2. This is also indicated even more by the rapid decrease in the (CO + CO_2) % conversion. The (CO + CO_2) % conversion is often preferred in the commercial FT reactor calculations for several reasons: 1). WGS reaction does not affect this conversion since CO and CO_2 are on both sides of the WGS chemical equation with the same

stoichiometric number for both CO and CO_2 being 1 (water gas shift: $CO + H_2O \rightarrow CO_2 + H_2$).

2). There is excess hydrogen present in commercial FT practices so that it is theoretically impossible to attain a high $(CO + H_2)$ % conversion, but not for $(CO + CO_2)$ % conversion, and

3). Understanding of selectivities towards FT products (including methane) can be made in a more straightforward manner by separating the CO2 formation from the rest of the carbon consumption. For this preliminary study, we simply use the CO% conversion and CO_2 and CH_4 selectivity separately with the aim of clarification of each individual components consumption/accumulation in the FT reaction system. The CO_2 selectivity decreased when the system total pressure increased from 17.5 bar to 35 bar (from stage 1 to stage 2). This observation was in keeping with the generally accepted fact that higher pressure favors long chain alkanes formation (Steynberg & Dry 2004), i.e. the converted CO is directed into long chain hydrocarbons instead of CO_2.

In FTS, the carbon in the carbon monoxide (from the inlet syngas) is converted into hydrocarbons (including oxygenated hydrocarbons) and carbon dioxide. Thus, based on the elemental balance it follows that the reaction rate of CO equals the rate of formation of hydrocarbons (liquid organic compounds, methane, ethane, pentane, etc.) on a carbon basis (units mmol C/gmin) plus the reaction rate of carbon dioxide:

$$R_{CO} = R_{HC} + R_{CO2} \qquad (2.1)$$

Here, HC stands for hydrocarbon. R_i is the algebraic sum of reaction rate for each reaction based on each component i, i.e.

$$R_i = \sum_{j=1}^{m} v_{ij} r_j \qquad (2.2)$$

r_j is the reaction rate for reaction j, multiplied by the stoichiometric number v_{ij} for

component i in reaction j. If in reaction j, component i is a reactant, then v_{ij} is a negative value, if not, then v_{ij} is a positive value. As a result, R_i can be positive or negative. If it is positive, it means that during the FT reactions the amount of this component i is increased, then R_i represents the formation rate. Vice versa, if it is negative, R_i represents the consumption rate or the net conversion rate. As listed in Table 1.4, reactions involving CO includes CO hydrogenation, water gas shift (WGS) and reverse water gas shift, Boudouard reaction and coking. The CO_2 content is affected by the WGS reaction, reverse WGS reaction, and Boudouard reaction.

For the liquid phase FT products (stage 1), Figure 2.4 shows the product distribution as a function of the carbon number, resulting in a carbon chain growth factor of $\alpha = 0.78$. In the C_5 - C_{22} hydrocarbon range, the paraffin selectivity was c.a. 30%, the olefin selectivity was c.a. 50%, the branched compounds selectivity was 8%, and the oxygenates (primarily alcohols) selectivity was 12%. The olefin selectivity was expected to be high since an iron-based LTFT catalyst was used in this gas phase FT investigation. In particular, the product selectivity (on a CO_2 free basis) in the gasoline range (C_5 - C_{12}) was 45%, while the diesel range (C_{12} - C_{22}) selectivity was 25% and the heavy wax (C_{22+}) selectivity was 6%. Though the selectivity towards the fuel range was low, the fuel quality was poor which results from the liquid product functionality, in this case, being primarily linear paraffins and 1-olefins. The olefin content was excessively higher than the general gasoline regulation limit (e.g. Euro-4: the maximum olefin content is 18 vol. %). The selectivity towards light hydrocarbons (C_1 - C_4) was over 20%, suggesting that a follow-up separation-recycle step or a sequential upgrading process is necessary to meet the target fuel regulations.
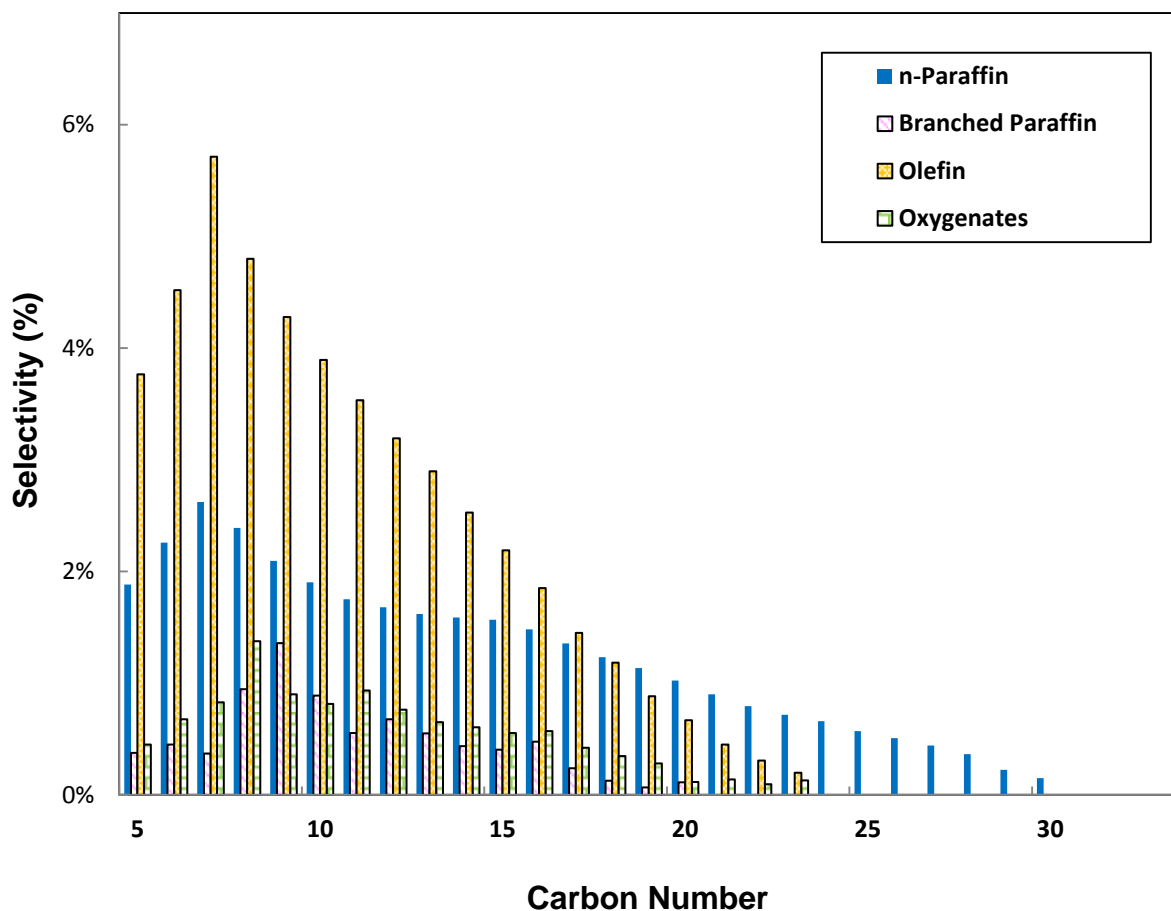
Figure 2.4   Liquid products selectivities from gas phase Fischer-Tropsch synthesis (P= 17.5 bar). (1 gram Fe/Zn/Cu/K FT catalyst, T = 240 ºC, synthesis gas flow rate: 50 SCCM, synthesis gas ratio: H_2: CO: N_2 = 62: 36.5: 1.5.)

In stage 3 (p = 17.5 bar), the product distribution was similar as to stage 1 (p = 17.5 bar). For stage 2 at the elevated operation pressure (p = 35 bar), the product distribution shifted towards the longer chain hydrocarbons with a significantly enhanced chain growth factor α = 0.85. This observation is in keeping with the findings of other researchers (van Berge & Everson 1997) and was consistent with the conclusion that the high pressure promotes long chain hydrocarbon formation (Steynberg & Dry 2004).

2.2 Catalytic Investigation of Oligomerization

2.2.1 Background and Choice of Catalyst for Oligomerization

Distillates are substances in the boiling range from 175 ºC to 370 ºC, corresponding generally to the C_{11} - C_{22} hydrocarbon fraction (de Klerk 2009). In FT syncrude, the distillates concentration can be determined by analysis of the carbon number distribution. The distillate can be simply recovered by separation (usually, distillation). For FT synthesis, the theoretical optimum α value (chain growth probability) for maximum distillate generation is c.a. 0.88 (de Klerk 2009). Thus LTFT syncrude has been proven to be superior to HTFT syncrude in the light of straight run distillate production due to operating at a higher α value. However, it is possible to manipulate the α value in order to change the carbon number distribution, i.e. to maximize the distillate production (Steynberg & Dry 2004). In addition, sequential refining and upgrading processes can be implemented accordingly in order to achieve the desired products, such as diesel or jet fuels.

Diesel fuels are distillates that fulfill the requirement of certain fuel legislations. Although fuel regulations are different from country to country, migration towards Euro-4 specifications was claimed to be likely (de Klerk 2009). Octane number indicates the tendency of fuels to self-ignite during compression prior to the desired position of the piston as appropriate for valve and ignition timing. Compared to previous fuel regulations, heavy metal additives are not acceptable to enhance octane number for gasoline and the acceptable level of research octane number (RON ≥ 95) and motor octane number (MON > 85) was increased. Aromatic content is limited (< 35% by volume), which places a higher barrier for crude oil refineries (due to high aromatic content) (de Klerk 2009). The highest sulphur content was limited to 10 parts per million (ppm). The olefin content was limited to 18% by volume, thus placed pressure on HTFT refineries (de Klerk

2009, Steynberg & Dry 2004). While the choice of FTS process does have certain effect on the syncrude produced, the subsequent upgrading steps in the refinery have the most impact on the ultimate fuel properties and composition (Bisio & Atkinson 2002, de Klerk 2009). FT-derived fuels possess some superior properties compared to petro-derived fuels. Taking FT diesel as an example, the advantages include: 1). It can be produced from sources other than petroleum. 2). It has lower sulfur content (5 ppm) than the "Ultra Low Sulfur Diesel" (15ppm) (Calemma *et al.* 2001, Leckel 2007). 3). It can promote motor oil durability (de Klerk 2008), and 4). It is reported to offer cleaner burning (Terblanche 1997). The issues of FT diesel include problematic cold-flow properties (due to lack of branched compounds) and low density (due to nearly complete absence of aromatics) (Steynberg & Dry 2004, de Klerk 2009). The FT diesel density is reported to be 770 g/L for iron-based LTFT, 776 g/L for cobalt-based LTFT and 796 g/L for iron-based HTFT, while the required density ranges from 800 - 845 g/L according to the European regulations (de Klerk 2009). Addition of biodiesel represents one potential solution to enhance the mass density. However, for energy density, aromatics addition is the most viable choice, since it can improve the lubricity, too (Steynberg & Dry 2004, Wadumesthrige *et al.* 2009).

The non-paraffin content of C_3-C_{10} gaseous and oil range products increases in the order of: Co-LTFT (45%) < Fe-LTFT (75%) < Fe-HTFT (85%) (de Klerk 2009). And C_3-C_{10} products can be converted into distillate range materials by suitable technologies such as alkylation and oligomerization. To maximize the distillate range materials selectivity, in addition to choosing the Fe-LTFT process (with a higher olefin selectivity at low temperature FT conditions), we also choose to employ an oligomerization process to manipulate the carbon chain length because it is easier to convert the short chain olefins into the middle distillate range compared to the short chain paraffins. For gaseous C_2 hydrocarbons, industrial recovery requires cryogenic separation,

which is not acknowledged as part of a basic Fischer-Tropsch gas loop design (de Klerk 2009).

Thus, addition of a sequential oligomerization step can also afford a better utilization of the C_2

hydrocarbons.

As discussed in chapter 1.5.1, solid phosphoric acid (SPA) and ZSM-5 are used commercially in the FT refineries for different target product fractions, gasoline and diesel, respectively. Amorphous silica alumina (ASA) was proposed by de Klerk (de Klerk 2006) to offer a promising oligomerization performance, affording a high hydrogen transfer propensity. By addition of 1- 4 wt. % oxygenate content (carbonyls, carboxylic acids and esters, alcohols and water) in the feed (a Sasol HTFT stabilized light oil), de Klerk investigated the oxygenates addition on the performance of the ASA catalyst for oligomerization and found it is not necessarily negative (de Klerk 2007). Considering the viability of ASA, we decided to start our oligomerization investigation with ASA.

2.2.2 Materials and Methods

A diagram of the reactor system for oligomerization in a fixed bed reactor system is shown in Figure 2.5. Helium gas (Airgas, ultra high purity) was used during the system pressure test, reaction startup and shut down, and in addition, as an inert carrier gas. Helium was fed into the reaction system by a mass flow controller (MFC: Porter Instrument Company. Inc., model 221-6KASVBAA, 0 - 500 SCCM, Control box: model CM2) and was heated in the pre-heating zone prior to the reactor. Then, the stream of helium was mixed with the preheated simulated FT products (1% pentene: 99% hexane by mole) and this mixture entered the top of the tubular fixed-bed reactor. From the outlet of the reactor, the mixture of reactant residues and products passed through heated tubing to the back pressure regulator (BPR, Straval Valves Inc. model BPH0502T-N2403) which was employed to control the system pressure, and then through heated

tubing to a cold trap (CT, Swagelok Inc. 304L-HDF4-1000). The cold trap was cooled by an ice-water-mixture bath. The condensable products were accumulated in the CT and were manually collected and tested periodically by injecting them into a gas chromatograph with a flame ionization detector (GC-FID, Varian GC 3300 equipped with a DB-5 capillary column, Agilent 125-5032). The incondensable gases exited the CT and were passed through a 6-port injection valve for periodic injection into a gas chromatograph with a thermal conductivity detector (GC-TCD, Varian 3380). The column in the GC-TCD was a Haysep DB 100/120 (Alltech part number 2836PC). After that, the gases were passed through a bubble meter, which allows for measurement of the real-time gas effluent volumetric flow rates. The gas effluent was then vented into the fume hood.
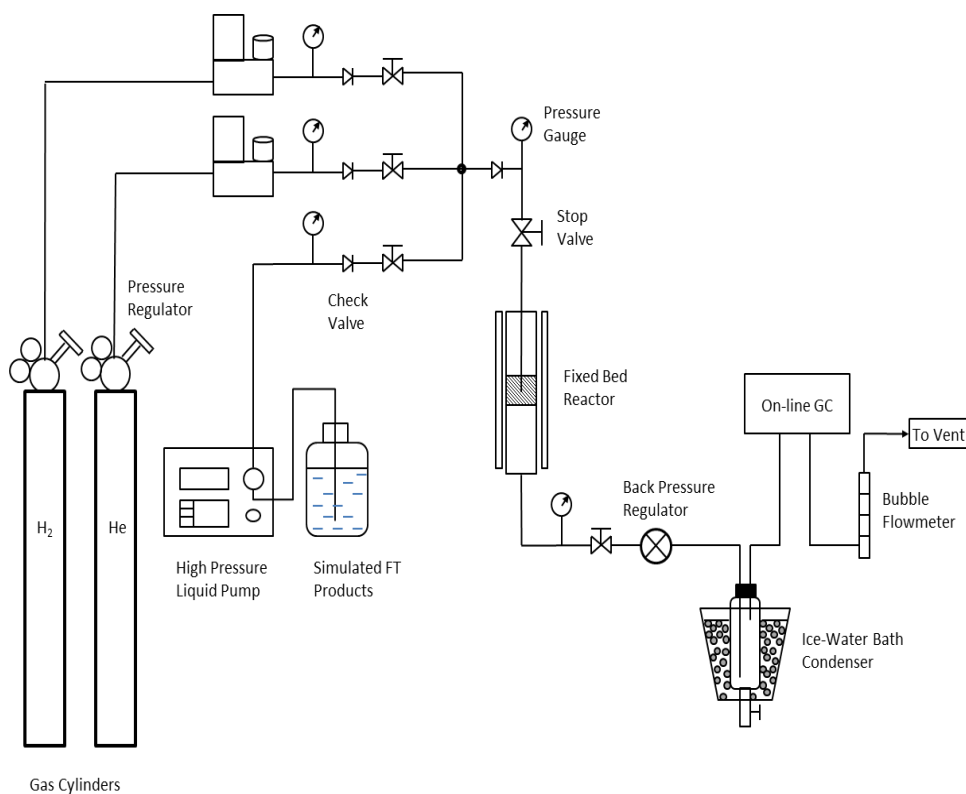
Figure 2.5 Flowchart of the oligomerization (hydrocracking/isomerization) reaction system

The reactor in this system was obtained from High Pressure Equipment Company (20-LM9-6). 2 grams of ASA (Sigma-Aldrich 343358-1KG, grade 135) were diluted with 2 grams of glass beads and this mixture was then loaded into the middle of the reactor and was kept in place by glass wool (Omega) inserted from both the top and the bottom. A thermocouple (Omega, KTSS-116G-12) was placed in the middle of the catalyst material in order to monitor the temperature at the center of the reaction bed, and this thermocouple was used as the input for a temperature controller (Omega, CSC32) equipped with a furnace in which the reactor was placed. A filter disc (0.5 µm, HIP# B01450) was positioned at the bottom of the reactor to prevent catalyst loss into the sequential tubing.

Before the oligomerization reaction, a catalyst pretreatment step was performed using a H_2 flow at a flow rate of 50 SCCM, and the temperature was kept at 420 ºC and held for 10 hour. Then, the H_2 was switched to helium with a flow rate of 50 SCCM, and the bed temperature was decreased from 420 ºC to 370 ºC and held at 370 ºC for another 5 hour, after which the temperature is returned to room temperature. For this reduction process, the bed temperature was initially ramped from room temperature at a rate of 5 ºC/min. To prepare for a reaction, helium was used to build up the system pressure to 17.5 bar at a flow rate of 100 SCCM. When the system pressure was steady at 17.5 bar (254 psi), the reaction bed temperature was increased to 240 ºC at a ramping rate of 5 ºC/min with a 25 SCCM stream of helium. After the bed temperature was steady at 240 ºC, injection of the simulated FT product (1% 1-pentene: 99% hexane by mole) was started with a flow rate of 1ml/min using a high pressure liquid pump (Acuflow Series III pump). 1-pentene was used as a short chain olefin and hexane was used as the supercritical solvent medium. It is also noted that hexane is a typical FT paraffin. The helium stream continued to be delivered into the system as a carrier gas at 25 SCCM (MFC range of 0-

500 SCCM, 5% open). During the reaction, the system pressure and temperature were held steady at 17.5 bar and 240 ºC, respectively. The liquid products were collected from the cold trap every 12 hours once steady state was reached. The experiment has been performed over three times to confirm the reproducibility.

The pore volume of the ASA (Sigma-Aldrich 343358-1KG, grade 135) was 0.75ml/g, as determined by the supplier and the apparent bulk density of this ASA was c.a. 0.45g/ml with a surface area of 475 m^2/g. This ASA contains 13% Al_2O_3 and 75% SiO_2 on a mass basis while the SiO_2/Al_2O_3 molar ratio is 9.8 to 1.

2.2.3 Results and Discussion

This investigation involves the catalytic oligomerization of 1-pentene (as the monomer) and hexane as the reaction medium (1-pentene: hexane = 1: 99, molar ratio) at 240°C and 17.5 bar using amorphous silica alumina (ASA) as the catalyst. We found that the oligomerization product was primarily 5-decene. The 1-pentene conversion was c.a. 20% and the reaction was primarily dimerization. This result illustrated that this ASA catalyst has a certain degree of oligomerization activity while being limited by the inlet monomer species and reaction conditions.

The typical oligomerization pressure using an ASA catalyst ranges from 36 bar to 60 bar. A. de Klerk reported that at 60 bar the oligomerization reaction using ASA showed higher activity and a much better activity maintenance while irreversible deactivation was observed at 40 bar (de Klerk 2006). The deactivation could result from the fouling and coking due to low diffusivity and solubility of long chain hydrocarbon products (coke precursor) from catalyst surface into the bulk media. With regards to this point, supercritical hexane is an excellent reaction medium that offers high solubility and mass transfer properties at these reaction

conditions (as mentioned in chapter 1) and can also serve as a convenient heat sink for the reaction heat.

As helium was used as the only carrier gas (i.e. no CO or H_2 was present), no carbon insertion was observed and no branched hydrocarbons with carbon number between 5 and 10 were produced. Hydrogen can be used as the carrier gas as well which will likely lead to hydrogenated products (decane). The acidity of the active sites on the ASA may be another potential contributor to the low product versatility (Brouwer 1962). It has been shown that a shift in the double bond (isomerization) can result from variation of the acidity of the catalyst (Brouwer 1962). This preliminary result illustrates potential for further investigations involving of this ASA catalyst.

2.3   Catalytic Investigation of Hydrocracking and Isomerization

2.3.1   Background and Choice of the Catalyst

A significant number of regulation changes with respect to gasoline, jet fuel, diesel and lubricating oil have been made due to concerns about negative environmental effects of fuel and oil usage during the past three decades. To meet the challenges proposed by the requirements for high quality fuels, technological breakthroughs and improvements are required. For example, methyl tertiary butyl ether, i.e. MTBE, plays a key role in the development of regulations controlling the vehicle emissions (Gary & Handwerk 2001). As a gasoline blend component to prevent engine knocking and to increase octane value, MTBE has been reported to contribute to environmental issues such as contaminating surface and groundwater (Kaufmann *et al*. 2000). However, elimination of MTBE from gasoline has resulted in operational cost change and further capital investment for refineries and petrochemical producers to replace the volume and octane loss that its removal generated. In addition, more regulations for sulfur, aromatic compounds and

olefins have been discussed (Kaufmann *et al*. 2000, Akhmedov *et al*. 2007). This prompts the needs for environmentally clean octane number enhancers and also other gasoline additives. Refineries have been looking for more environmentally safe gasoline blending component alternatives (Kaufmann *et al*. 2000). FT derived fuels can offer potential provided that appropriate product upgradings can be performed to improve the fuel yield and structural properties. Hydrocracking and isomerization are important steps in this regard.

Due to the fact that LTFT is operated at a higher carbon chain growth probability (α value), the primary product that is made by LTFT is wax. The wax color, penetrability, congealing point and carbon number distribution are the major factors for evaluation of the wax (Espinoza *et al*. 1999). Through hydrocracking, the long chain hydrocarbons, especially heavy wax, can be broken up into shorter chain hydrocarbons, as such, the amount of fuel range products and the middle distillate range products can be enhanced. As described in chapter 1.5.2, hydrocracking is always accompanied with isomerization. Thus by shifting the FT hydrocarbons from the wax range back to distillate range and enhancing branching, catalytic hydrocracking/isomerization plays an important role in providing an alternative for distillate and/or high quality fuels manufacturing compared to traditional crude oil refining. In addition, associated hydrogenation in this process will stabilize (hydrogenate) the olefins, which can result in distillate/wax deterioration when in storage (de Klerk 2009).

Isomerization, which induces the conversion of linear paraffins into branched isomers, is one of the important processes in crude oil refining (Steynberg and Dry 2003, Rossini 2003). Highly branched paraffins with 7-10 carbon atoms is considered a proper additive to fulfill the more and more stringent gasoline regulations (Rossini 2003). Additionally, long chain normal paraffin and heavy wax which usually crystallize below 100 ºC can deteriorate the fuel (and

lubricating oil) viscosity (Rossini 2003, de Klerk 2009). Their removal is essential for production of fuels with good cold flow properties (Steynberg and Dry 2004, de Klerk 2009). Industrially, these compounds are removed by physical processes such as extraction or by catalytic dewaxing using shape selective catalysts. Due to the fact that the FT products are also rich in linear paraffins, integration of isomerization in FTS or subsequent to FTS can be utilized to produce high quality fuels that possess good anti-knocking properties and cold flow properties.

It is well acknowledged that isomerization of n-paraffins is the first reaction step in this process while cracking is a consecutive reaction. Mono-branched paraffins show a lower tendency to cracking than multi-branched paraffins (Martens *et al*. 1986). The bifunctional catalysts used for hydrocracking/ isomerization often contain metallic sites (for hydrogenation/ dehydrogenation) and acid sites (for skeletal isomerization via carbenium ions) (Weitkamp 1982, Alvarez *et al*. 1996, Walendziewski and Pniak 2003, Liu *et al*. 2004). Park and Ihm (Park and Ihm 2000) proposed a pathway for the isomerization and cracking, as shown in Figure 2.6. Paraffins are firstly activated and dehydrogenate on the metal sites, then the generated olefin intermediates protonate to corresponding carbenium ions (usually cyclic) on the acid sites. Through intramolecular reactions and intermolecular reactions, the carbenium irons are hydrogenated or dehydrogenated to produce branched paraffins with corresponding carbon number (Park and Ihm 2000). The intramolecular reactions include type A rearrangements: hydride shift and alkyl shift, and type B rearrangements: PCP (protonated cyclopropane) branching and cracking by β - scission. The intermolecular reactions consist primarily of hydrogen transfer. The stability of carbenium ions (R+) increases in the order of $CH_3^+ \ll RCH_2^+ \ll R_2CH^+ \ll R_3C^+$ (Weitkamp 1982, Park and Ihm 2000).

n - alkane

± 2H
De-/hydrogenation

+ H⁺
Addition of proton

n - alkene ⟷ n – alkylcarbenium ion (Cyclic) ⟵ n – alkylcarbenium ion

± H⁺
De-/protonation

- 2H
Dehydrogenation

Competitive | ad-/de- sorption on acid sites

Rearrangement

Mono-branched alkane ⟵ Mono-branched carbenium ion ⟶ n-1 - alkane
Hydrogenation   β - scission

Dibranched alkane ⟵ Dibranched carbenium ion ⟶ Cracked products
Hydrogenation   β - scission

Tri-branched alkane ⟵ Tri-branched carbenium ion ⟶ Cracked products
Hydrogenation   β - scission

Figure 2.6   Reaction pathway of hydrocracking/isomerization (Park and Ihm, 2000)

Baltanas *et al.* concluded that it is not easy for linear and mono-branched isomers to crack directly; dibranched isomers are formed by isomerization of mono-branched isomers and can be further isomerized into tri-branched isomers or can undergo cracking while tetra-branched isomers have never been observed; in addition, the occurrence of secondary cracking is insignificant (Baltanas *et al.* 1989). This statement is consistent with the mechanism shown in Figure 2.6.

The catalyst should possess appropriate compositional and structural characteristics to show high activity and shape-selectivity (with n-paraffins), such as appropriate pore size, high dispersion of metal on the catalyst surface, and proper acid strength distribution on the catalyst surface (Deldari 2005). The metals that are typically employed are palladium, platinum and

bimetallic systems such as Ni/Co, Ni/W, W/Mo in the sulfided form (Calemma *et al*. 2000). There have been 4 types of acid supports which are commonly used: 1. Oxides: such as $SiO_2 - Al_2O_3$; 2. Zeolites: such as ZSM-5, ZSM-22, β-zeolite; 3. Silicoaluminophosphates (SAPO): such as SAPO-11, SAPO-41; 4. Mesoporous materials such as MCM-41 (Calemma *et al*. 2000). The balance between hydrogenation activity of the metal sites and the acidity of the acid supports affects the hydroisomerization activity versus hydrocracking activity (Deldari 2005). It has been concluded that high degree of hydrogenation activity and low degree of the supports acidity results in high isomerization rather than hydrocracking (Deldari 2005). In addition, the pore size of the acid supports can also spatially influence these catalysts' selectivities. When the pore opening is small enough to restrict the iso-paraffins (presenting a larger size) from accessing to the acidic sites therefore to prevent iso-paraffins from being converted, the catalyst shows a better selectivity towards conversion of n-paraffins (presenting a smaller size) (Taylor & Perry 1994).

Amorphous silica alumina (ASA) has been selected as the support material in the following hydrocracking/isomerization investigations due to its high hydroisomerization performance (de Klerk 2006, Deldari 2005). There are three major factors that contribute to its performance: high surface area, mild acidity (n_{Si} / n_{Al} ratio), and narrow distribution of pores (Deldari 2005). Palladium has been chosen as the active metal for hydrogenation/ dehydrogenation since it is a strong hydrogenation/dehydrogenation noble metal compared to the other active metals (Deldari 2005). Palladium shows a weaker hydrogenation-dehydrogenation activity compared to platinum (Carter *et al*. 1971), thus it can afford a higher cracking activity than platinum (Deldari 2005). Additionally, Liu *et al*. reported that palladium based catalysts showed a better catalytic performance maintenance than platinum based catalysts (Liu *et al*.

2005). As such, palladium has been chosen over platinum as the active metal in initiating these investigations.

2.3.2　Material and Methods

A 1.0 wt. % palladium on amorphous silica alumina (ASA, Sigma-Aldrich 343358-1KG) (Pd/ASA) catalyst was prepared by the wetness impregnation method. The palladium doping was done by addition of palladium nitrate dihydrate Pd $(NO_3)_2 \cdot$ 2 H_2O (Sigma-Aldrich Fluka 76070-1G, CAS# 10102-05-3) solution (0.1g Pd in 30ml solution). After addition of this solution to ASA on a mass ratio of 1 g Pd per 99 g ASA at an agitation rate of 200 rpm, the catalyst paste was aged at room temperature for 24 h. The catalyst was then dried at 100 ºC for 12 h under air flow. Subsequently, the catalyst was calcined at 500 ºC for 5 h. The oven temperature was programmed to ramp at 5 ºC/min to 500 ºC and held for 5 hour, then the oven was cooled to room temperature (RT) at 5 ºC/min.

A diagram of the fixed bed hydrocracking/isomerization reactor system, as shown in Figure 2.5, was arranged consecutively in the vertical direction. Helium gas (Airgas, ultra high purity) was used to test the system for leaks under pressure, and was also employed during reaction startup and shut down. Hydrogen gas (Airgas, ultra high purity) was fed into the reaction system by a mass flow controller (MFC: Brooks Instrument Company. Inc., model 5850 TR, 0 - 500 SCCM, Control box: 0154E) and was heated in the pre-heating zone prior to the reactor. This stream of H_2 was mixed with preheated simulated heavy FT products: 1 mol. % eicosane (Acros 204370020-2G, CAS# 112-95-8): 99 mol. % hexanes (Fischer Scientific H304-4-4L, HPLC grade, CAS# 101-54-3) through a static mixer. The mixture entered the top of the tubular fixed-bed reactor. The reactor effluent, the mixture of reactant residues and products, was passed through heated tubing to the back pressure regulator (BPR, Straval Valves Inc. model

BPH0502T-N2403) which was employed to control the system pressure. This stream was then passed through heated tubing to the cold trap (CT, Swagelok Inc. 304L-HDF4-1000). The cold trap was cooled using 5ºC cooling water which was circulated by a chiller unit (Thermo Electron Corporation, Neslab RTE 7). The condensable products were accumulated in the CT and were manually collected and tested periodically by injecting them into a gas chromatograph with a flame ionization detector (GC-FID, Varian GC 3380). The column in the GC-FID is a DB-5 column (Agilent 125-5032). The incondensable gases left the CT and were passed through a 6-port injection valve for periodic injection into a gas chromatograph with a thermal conductivity detector (GC-TCD, Varian 3380). The column in the GC-TCD was a Haysep DB 100/120 (Alltech part number 2836PC). Then, the gases were passed through a bubble meter, which allows for measurement of the real-time gas effluent volumetric flow rates. The gas effluent was then vented into the fume hood.

The reactor in this system was obtained from High Pressure Equipment Company (20-LM9-6). 0.4 gram of the Pd/ASA (1 wt.%) catalyst was diluted with 2 grams of glass beads and then loaded into the middle of the reactor and was kept in place by inserting into glass wool (Omega) on both the top and the bottom of the reactor. A thermocouple (Omega, KTSS-116G-12) was placed in the middle of the catalyst material to monitor the temperature of the center of the reaction bed. This thermocouple was used as the input for a temperature controller (Omega, CSC32) equipped with a furnace in which the reactor was placed. A filter disc (0.5 μm, Hip #B01450) was positioned at the bottom of the reactor to prevent catalyst loss into the sequential tubing.

Then, the H_2 was switched to helium with a flow rate of 50 SCCM, and the bed temperature was decreased from 420 ºC to 370 ºC and held at 370 ºC for another 5 hour, after

which the temperature is returned to room temperature. For this reduction process, the bed temperature was initially ramped from room temperature at a rate of 5 ºC/min.

Before the hydrocracking/isomerization reaction was performed, a catalyst pretreatment step was performed using a H_2 flow at a flow rate of 22 SCCM, and the reaction bed temperature was ramped from room temperature to 400 ºC at a rate of 5 ºC/min and was held at 400 ºC for 16 hours. A stream of helium was used to build up the system pressure to 35 bar at a flow rate of 100 SCCM. When the system pressure was steady at 35 bar (508 psi), reaction bed temperature was increased to 330 ºC at a ramping rate of 5 ºC/min with a 50 SCCM stream of helium flow. After the bed temperature was steady, injection of simulated FT product (1 mol % eicosane: 99 mol % hexane, eicosane was used as a long chain wax simulant and hexane was used as the supercritical media) was initiated with a flow rate of 0.5ml/min using a high pressure liquid pump (Acuflow Series III pump). Hydrogen was delivered into the system at a flow rate of 22 SCCM. During the reaction the system pressure and temperature were maintained at 35 bar and 330 ºC. Liquid products were collected from the cold trap every 12 hours once steady state was reached. The experiment has been performed over three times to confirm the reproducibility.

2.3.3   Results and Discussion

The purpose of these experiments with a small amount of Pd/ASA (1 wt. %) catalyst is to preliminarily test this catalyst's ability to crack wax compounds under supercritical phase conditions. In this case, traditional FT wax was modeled as eicosane (C_{20}). We fed only hydrogen into the reactor to promote hydrogenation and to eliminate the possibility of oligomerization of light molecules and other reactions such as CO insertion.

Gross conversion of C_{20} was calculated based on the outlet concentration of C_{20}, divided by the inlet C_{20} concentration. Under the studied conditions, the gross C_{20} conversion over this

Pd/ASA catalyst was approximately 75% and the yield of products in the range of C_5 - C_{19} (excluding C_6 solvent) was c.a. 37%. Selectivity of hydrocracking was around 50%. The yield of the C_5 - C_{19} range products (excluding C_6) was calculated with following formula:

$$Yield = \frac{\sum_{i=5,7,8,9,...18,19} Area\ of\ peaks\ of\ Ci \times response\ factor\ of\ Ci \times (i/20)}{Initial\ concentration\ of\ C_{20}}$$

Figure 2.7 shows the distribution of hydrocracking/isomerization products as a function of carbon number. Because the different hydrocarbon isomers have similar response factors, peak areas for products with the same carbon number were summed as one component with an average response factor for ease of calculation. As shown in Figure 2.7, the concentration of products generally decreased with an increase in carbon number. The concentration for hydrocarbons with 19 carbons was significantly higher because C_{19} is the primary hydrocracking product being only one carbon less than the reactant, eicosane. This observation is in keeping with the general observed cracking behavior that the carbon chain is broken apart stepwise as indicated in Figure 2.6. Not as prevalent as C_{19}, C_{18} and other long chain hydrocarbons were not the primary product, showing a much lower concentration. This result indicates a continuous secondary hydrocracking. The concentration decreases with increasing carbon number, which is in consistent with the observation that heavier hydrocarbons are more likely to be involved in cracking (Martens et al. 1986).
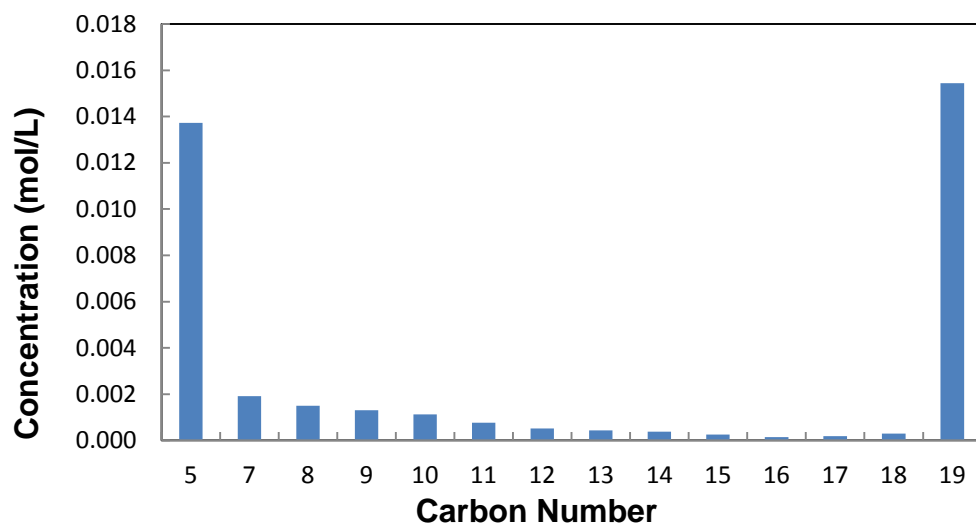
Figure 2.7 Hydrocracking/isomerization of eicosane in hexane (C20: C6 = 1: 99, molar) products distribution. (0.4 gram of Pd/ASA 1.0 wt.% catalyst, T = 330 ºC, p = 35 bar, hydrogen gas flow rate: 22 SCCM, liquid injection rate: 0.5 ml/min.)

Multiple products with the same carbon number were obtained as shown in Figure 2.8. Peak groups obtained at distinct time intervals in the gas chromatography showed that in addition to hydrocracking, this Pd/ASA catlayst showed distinguishable isomerization activity. Isomerization of the reactant (n-eicosane) took place with a conversion of 20% where most isomers were mono-branched eicosane.
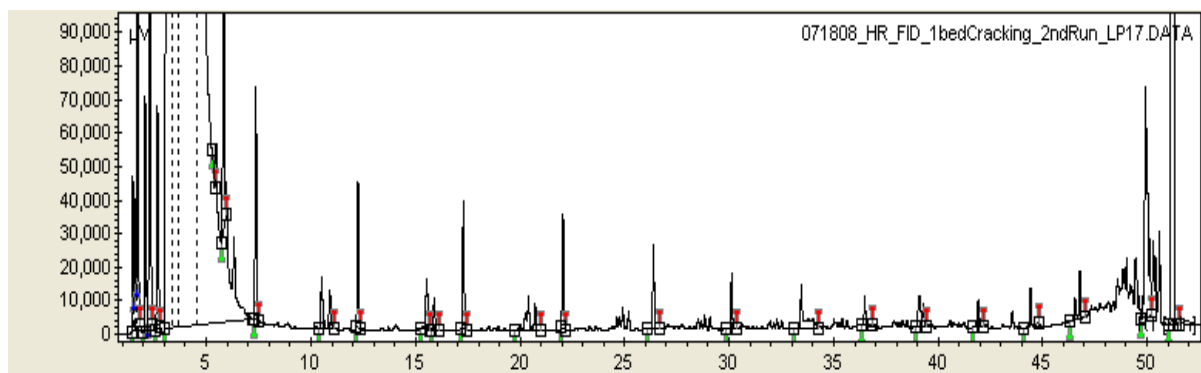
Figure 2.8 GC-FID results from the hydrocracking/isomerization of eicosane in hexane (C_{20}:C_6 = 1: 99, molar) products distribution. (0.4 gram of Pd/ASA 1.0 wt.% catalyst, T = 330 ºC, p = 35 bar, hydrogen gas flow rate: 22 SCCM, liquid injection rate: 0.5 ml/min.)

To illustrate that the hexane solvent media does not significantly participate in the hydrocracking reactions, a blank study was performed at the same reaction conditions without addition of eicosane (as a model wax compound). Figure 2.9 demonstrates that no products above C_6 were produced in this control study. While the C_6 conversion was negligible, there were some C_5 products that were produced from the cracking of C_6, as shown in Figure 2.9. This result is consistent with the general observation that the longer the hydrocarbon is the more it tends to be hydrocracked (Martens *et al*. 1986).
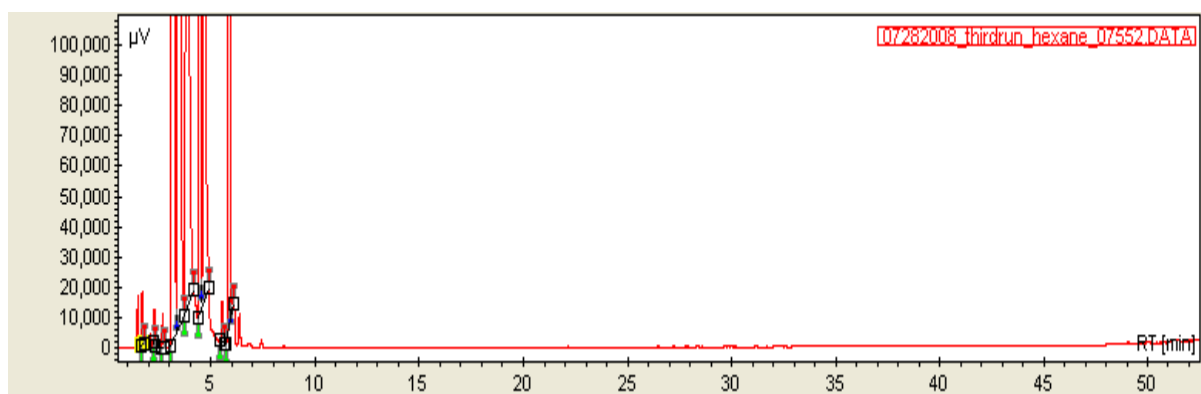
Figure 2.9   GC-FID results from blank test with only hexane in liquid inlet (0.4 gram of Pd/ASA 1 wt.% catalyst, T = 330 ºC, *p* = 35 bar, hydrogen gas flow rate: 22 SCCM, liquid injection rate: 0.5 ml/min.)

2.4   Conclusion

Using a precipitated iron-based low temperature FTS catalyst in a single fixed bed under traditional gas phase conditions demonstrated this iron-based FTS catalyst possesses good catalytic FTS activity, showing a ~ 30% CO conversion (at 17.5bar) and a typical FTS product distribution, such as in the C_5 - C_{22} hydrocarbon range, the paraffin selectivity was c.a. 30%, the olefin selectivity was c.a. 50%, the branched compounds selectivity was 8%, and the oxygenates (primarily alcohols) selectivity was 12%. The experiment using ASA for the oligomerization

reaction using pentene as a feed monomer exhibited this ASA catalyst possesses certain oligomerization activity and can be used for the following FTS product upgrading research. 1.0 wt.% Pd/ASA catalysts has been examined and validated for its activity of effective hydrocracking towards C_{20} paraffin with negligible hydrocracking towards C_6 paraffin (which is used as the supercritical fluid solvent in the following investigations).

Chapter 3   Production of Middle Distillate Range Hydrocarbons via Iron-based Fischer-Tropsch Synthesis with Integrated Product Upgrading under Supercritical Phase Conditions

3.1   Introduction

There has been a great deal of contemporary interest in the utilization of a variety of carbonaceous feedstocks to produce readily usable transportation fuels via synthesis gas (syngas, a mixture of H_2 and CO) (Lynd et al 2009, Elbashir et al 2010, Van Der Laan and Beenackers 1999, Larson et al 2005, Dry 1989, Dry 1999, Dry 2002). Specifically, Fischer-Tropsch synthesis (FTS) can be used to convert synthesis gas into hydrocarbon products and oxygenated hydrocarbons (Dry 2002, Jacobs et al 2002, Schulz 1999, Davis 2003, Iglesia 1997, Bukur and Sivaraj 2002, Khodakov 2009, Steynberg et al 1999, Espinoza 1999, Schulz et al 2005). Fischer-Tropsch synthesis is a surface-catalyzed polymerization process that converts in situ generated C_1 species monomers into hydrocarbons with a broad range of carbon chain lengths and functionalities (Elbashir et al 2010, Van Der Laan and Beenackers 1999, Schultz et al 2005, Martinez et al 2007, Li et al 2008, de Smit and Weckhysen 2008, Subramaniam 2001, Ngamcharussrivichai et al 2007, Durham et al 2010, Aufray et al 2007, Huang and Roberts 2003). With appropriate separation, upgrading and hydro-processing, these products can be further converted into high quality fuels and value-added chemicals (Elbashir et al 2010, Guo et al 2011, de Klerk 2005, Eilers 1990, Hamelinck et al 2004, Liu et al 2011, Leckel 2007, Calemma et al 2010). FTS has been commercially employed by Sasol and Shell in the production of fuels and chemicals as part of their gas-to-liquid (GTL) technology (Van Der Laan and Beenackers 1999, Dry 2002, Schulz 1999, Steynberg et al 1999, Duvenhage and Shingles 2002, Steynberg and Dry 2004, Sakuneka et al 2008, Leckel 2007, Wilhelm et al 2001). Compared to crude-oil-derived

transportation fuels, FT-derived fuels have distinct features, that can be considered advantageous or disadvantageous depending on the ultimate fuel application, and these features includes the absence of sulphur and nitrogen, low aromatic concentration, etc. (Steynberg and Dry 2004, Morales and Weckhuysen 2006)(A. Steynberg & Dry 2004; Morales & Weckhuysen 2006). FTS with conventional supported metal catalysts yields a wide spectrum of hydrocarbons since the product distribution is governed by the Anderson–Schulz–Flory (ASF) polymerization kinetics. As such, the FTS process is unselective towards individual products or product fractions (Subramaniam 2001, Calemma et al 2010, Steynberg and Dry 2004, Zhang et al 2010, Khodakov et al 2007). This imposes a limitation on the maximum selectivity for a given hydrocarbon product. To improve the selectivity of the FTS process towards middle distillate range products (C_8-C_{22}), additional upgrading reactions are required. A significant number of studies have focused on two major topics related to improving selectivities towards the middle distillates: 1) modification of the reaction catalysts through the use of bi-/multi- functional catalysts (Zhang 2010, Li et al 2005, He et al 2005) and 2) modification of the reaction system by adding further upgrading processes downstream of FTS (Xiaohong Li et al. 2005; Cho et al. 2008; Z.-W. Liu et al. 2005a). The studies involving catalyst modifications primarily employ hybrid catalyst systems. The hybrid catalyst systems are typically composed of an FTS catalyst (the catalyst support may or may not be modified) and an acid catalyst with/without noble metal doping (Z.-W. Liu et al. 2006; Ngamcharussrivichai et al. 2007; Z.-W. Liu et al. 2005b; Xiaohong Li et al. 2003; Q. Zhang et al. 2010; Ge et al. 2007; Martinez et al. 2007; Xiaohong Li et al. 2005; Xiaohong Li et al. 2008; Tsubaki et al. 2003). Supports, such as HZSM-5, ZSM-11, ZSM-12 and ZSM-34, have been intensively studied (Bessel 1995; Deldari 2005; Ngamcharussrivichai et al. 2007; Martinez et al. 2007; Morales & Weckhuysen 2006). Fujimoto's group has investigated

serial catalyst bed arrangements using hybrid catalyst systems that are composed of a Co/SiO_2 catalyst and a Pd/β-zeolite catalyst with various compositions (Z.-W. Liu et al. 2005b; Z.-W. Liu et al. 2006; Li et al. 2003; Li et al. 2008). Investigations on upgrading Fischer-Tropsch synthesis by modification of the reaction system typically involve the use of a dual bed reactor system that includes the integration of an FT wax hydrocracking stage in the second bed (Cho et al. 2008; Li et al. 2005; Z.-W. Liu et al. 2005a; Z.-W. Liu et al. 2006). Li *et al.* tested a two stage reactor system (fixed bed) by using a Co/SiO_2 catalyst (1g) in the first FT reaction bed and a Pd/ β-zeolite catalyst (3g) in the second hydrocracking/isomerization bed (Li et al. 2005). Liu and coworkers investigated C_4 - C_{11} iso-paraffin production from syngas using a consecutive dual fixed-bed reactor system, where a physical mixture of Co/SiO_2 FT catlayst and Pd/β-catalyst was used in the first bed, while a Pd/β-zeolite was installed for promoting the iso-paraffin selectivity in the second bed (Z.-W. Liu et al. 2006). Cho et al. used a Co/TiO_2 catalyst in the first FT bed, which yielded more than 35 wt.% middle distillates and more than 20 wt.% waxes, and a Pd loaded solid acid catalyst in the second reaction bed to enhance the middle distillates selectivity by hydrocracking the upstream FT wax (Cho et al. 2008).

There have been few investigations that have incorporated oligomerization into the FT process since most of the studies involving modification of the FT products are focused primarily on the conversion of heavy hydrocarbons into the middle distillate range. However, implementation of oligomerization into the FT process could potentially allow the conversion of light olefins into longer fuel range hydrocarbons.

To improve the selectivity of the process to middle distillates requires additional upgrading reactions. To carry this out, a three bed reactor system (consisting of three sequential fixed bed reactors) has been designed and constructed in this work in order to promote the direct

production of middle distillate range hydrocarbons from syngas in a single pass arrangement. FT is performed in the first catalyst bed, generating a variety of hydrocarbon lengths and types. The second bed is used for oligomerization to convert light olefins into gasoline and diesel range products (to promote branching and to enhance octane rating and cold-flow properties or aromatization to enhance density). The third bed is used for cracking and isomerization reactions to convert the heavy product into the middle distillate range and to increase branching.

To achieve the optimum performance within each catalyst bed, this three bed reactor was arranged consecutively so that the operation parameters of each reactor can be adjusted and maintained individually. A precipitated iron-based FTS catalyst was used in the first FTS bed. Iron-based FTS catalysts offer lower hydrogenation activity than cobalt-based FTS catalysts, which therefore results in higher olefin selectivity in low temperature FT synthesis (Van Der Laan and Beenackers 1999). Therefore, using a low-cost precipitated iron-based low temperature FTS catalyst can offer a more desirable feed (due to higher olefin content) when an oligomerization step is implemented sequentially downstream of the FTS step. Light olefins can therefore be oligomerized into the gasoline (C_5-C_{12}) and diesel (C_{12}-C_{22}) range fractions so as to increase the middle distillates selectivity in a single pass. Solid phosphoric acid (SPA) and ZSM-5 are used commercially in FTS refineries to convert raw FTS products via oligomerization and isomerization into different target product fractions including gasoline and diesel (De Klerk 2006). Amorphous silica alumina (ASA) has been less studied and has been proposed by de Klerk to offer promising oligomerization performance (De Klerk 2006). Researchers have shown that ASA offers higher distillate density and viscosity in the production of middle distillates by oligomerization compared to SPA and ZSM-5 (de Klerk 2006; de Klerk 2007a). In addition, de Klerk reported that oxygenates (in the range of 1-4 mass %) had little effect on the productivity

of the ASA catalyst or the quality of the oligomerization product (de Klerk 2007a). Given the prospects that ASA offers as a potential oligomerization catalyst, we have decided to utilize ASA to initiate these oligomerization investigations in the second bed of this sequential reactor system.

The third bed of this sequential reactor system is intended to convert long chain FTS hydrocarbons into middle distillate range products through catalytic hydrocracking and isomerization. Common hydrocracking catalysts include Pd and Pt based solid acid catalysts (Ancheyta et al. 2005; Calemma et al. 2000; Archibald et al. 1960). Pd exhibits a weaker hydrogenation-dehydrogenation activity compared to Pt (Carter et al. 1971), thus it can offer a higher cracking activity than Pt (Deldari 2005). Additionally, Liu et al. reported that Pd based catalysts showed better catalytic performance maintenance than Pt based catalysts (Z.-W. Liu et al. 2005a). As such, Pd has been chosen over Pt as the active metal in initiating these investigations. ASA has been selected as the support material in the following hydrocracking/isomerization investigations due to its high hydroisomerization performance (Deldari 2005; de Klerk 2006; de Klerk 2007b).

There have been a very large number of research studies that have utilized supercritical fluids (SCF) in reactions (Subramaniam & McHugh 1986; Elbashir et al. 2010), extraction (Chester et al. 1998) and material processing studies (MCCLAIN n.d.), to name a few. Compared to traditional FTS, the advantages of FTS under supercritical phase conditions (SC-FT) using a supercritical fluid as the reaction medium have been studied and reported by several researchers (Wensheng Linghu et al. 2004; Wensheng Linghu et al. 2007; Elbashir et al. 2010; Huang & C. B. Roberts 2003; Elmalik et al. 2011; Xiaohong Li et al. 2005; Durham et al. 2010; Jacobs et al. 2003; Abbaslou et al. 2009; Biquiza et al. 2010; Fujimoto & Yokota 1991; Elbashir & C. B. Roberts 2004; Bukur et al. 1997; Subramaniam 2001; X Liu et al. 2006; Joyce et al.

1999). The advantages of the utilization of supercritical solvents in FTS include: 1). The elimination of interphase transport limitations can lead to enhanced reactivity towards the desired products (Bochniak & Subramaniam 1998); 2). The heavy hydrocarbons can be extracted in situ from the catalyst surface resulting from the high solubility in the supercritical phase (Jacobs et al. 2003; Bochniak & Subramaniam 1998; Yokota et al. 1990; Elbashir et al. 2010); 3). The desorption of primary products can be enhanced prior to being converted though secondary reactions, as an example a higher α-olefin selectivity is observed (Jacobs et al. 2003; Bukur et al. 1997; Fujimoto & Yokota 1991; Huang & C. B. Roberts 2003) compared to gas phase FTS; and 4). Supercritical solvents can provide superior heat transfer compared to gas phase FTS (the FTS presents a highly exothermic nature) thus bringing about more long chain compounds (Jacobs et al. 2003; Huang & C. B. Roberts 2003; Yokota et al. 1990). It has been consistently shown that SC-FT can afford the opportunity to suppress methane formation (Jacobs et al. 2003; Huang & C. B. Roberts 2003; Yokota & Fujimoto 1989; Elbashir & C. B. Roberts 2005; Yan et al. 1998) due to reduced hot spots (which can lead to elevated methane selectivity (Van der Laan & Beenackers 1999) in SC-FT (Huang & C. B. Roberts 2003; Fujimoto & Yokota 1991; Fan & Fujimoto 1999). Suppressed CO_2 selectivity was reported in SC-FT by Davis' group (Jacobs et al. 2003) and Roberts' group (Durham et al. 2010) using a cobalt-based FT catalyst and an iron-based FTS catalyst, respectively. In SC-FT, olefin selectivity at the lower carbon numbers has been reported to decrease (Lang et al. 1995; Fujimoto & Yokota 1991) or was not affected (Huang & C. B. Roberts 2003), while olefin selectivity at the higher carbon numbers showed an increasing trend (Jacobs et al. 2003; Bukur et al. 1997; Lang et al. 1995; Yokota et al. 1991). In this study, supercritical fluid as reaction media is also utilized to allow for better heat management, improved product solubility in the bulk reaction media and enhanced catalyst

maintenance. Hexanes were chosen as the supercritical solvent based on the three criteria which were proposed by Fujimoto (Fan & Fujimoto 1999).

3.2   Material and Methods

In this three bed reactor system, the first reaction bed has been used for FTS thereby generating a variety of hydrocarbon lengths and types. The second reaction bed has been used for catalytic oligomerization to convert the light olefins from the FTS bed into gasoline and diesel range products (with potential branching). The third reaction bed has been used for cracking and isomerization reactions to convert the heavy product into the middle distillate range and to increase branching. A traditional precipitated Fe-based catalyst has been selected as the FTS catalyst in the first-bed of this reactor due to its low cost (compared to cobalt-based FTS catalyst) and its ability to yield olefinic products which can be used as feed for the following oligomerization step. In the second reactor, ASA catalysts have been examined for the oligomerization reaction due to the above-mentioned reasons. Pd-loaded ASA (1.0 wt.% prepared by wetness impregnation method) has been selected as the catalyst in the third reactor bed in order to investigate the subsequent hydrocracking/isomerization step. The hydrocracking and isomerization bed with Pd/ASA catalyst is intentionally placed last in this sequence of reaction steps. The Pd/ASA is also a functional hydrogenation and hydroconversion catalyst, and as such, this catalyst can convert olefins into their hydrogen-saturated state (i.e. paraffin). Therefore, if this hydrocracking and isomerization step was placed before the oligomerization bed, no potential oligomerization would occur because of the feed having been already hydrogenated. The reactor system has also been designed to allow the beds to operate at different temperatures so as to optimize each reaction stage, although, isobaric operation is required. A diagram of the three bed reactor system for Fischer-Tropsch synthesis with product upgrading

under the supercritical phase conditions is shown in Figure 1.
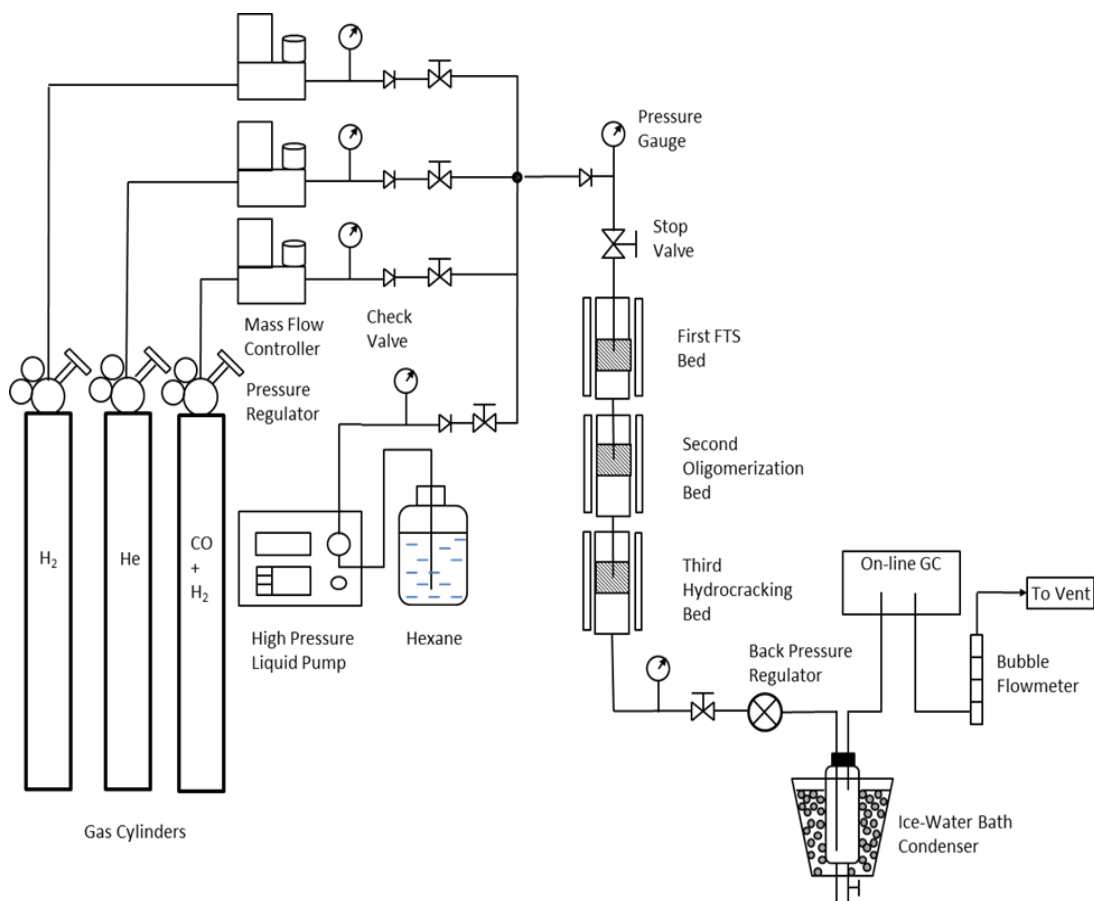
Figure 3.1 Schematic diagram of the three-bed catalytic reactor system for Fischer-Tropsch synthesis with subsequent oligomerization and hydrocracking/isomerization stages.

Helium gas (Airgas, ultra high purity) was used during the system pressure test, reaction startup and shut down. Synthesis gas (Syngas) (Airgas, vol%: N_2: CO: H_2 = 1.5: 37: 61.5) was fed into the reaction system by a mass flow controller. Hexanes (Fischer, HPLC grade, CAS# 110-54-3) were used as the supercritical fluid reaction media in this investigation, and were delivered into the reaction system using an HPLC pump at a flow rate of 1ml/min in the case of supercritical phase operation. The syngas and hexanes were mixed in a static mixer and the

97

mixture was initially heated in the pre-heating zone. The reactant (and the supercritical fluid medium in the case of supercritical phase operation) entered the top of the tubular fixed-bed reactor and then was passed through each reaction bed sequentially. The reactor effluent was passed through heated tubing to the back pressure regulator (BPR, Straval Valves Inc. model BPH0502T) which was employed to control the system pressure. The effluent was then passed through heated tubing to a cold trap (CT, Swagelok Inc. 304L-HDF4-1000). The cold trap was cooled by an ice-water-mixture. The condensable products were accumulated in the CT and were manually collected and tested periodically by injecting them into a gas chromatograph with a flame ionization detector (GC-FID, Varian GC 3300 with a DB-5 capillary column) and a GC-MS (Waters. Inc.). The incondensable gas mixture (syngas residue and light products) left the CT and was passed through a 10-port injection valve for periodic injection into a gas chromatograph with a thermal conductivity detector (GC-TCD, SRI Multi-Gas Analyzer #1). The gases were then passed through a bubble meter, which allowed for the measurement of the real-time gas effluent volumetric flow rates. The gas effluent was then vented into the fume hood.

Figure 3.2 shows the catalyst loading for each bed during each different operation. The experiments were performed in four modes of operation: gas phase Fischer-Tropsch synthesis (GP-FT), supercritical phase Fischer-Tropsch synthesis (SC-FT), gas phase Fischer-Tropsch synthesis with product upgrading (GP-FTOC) and supercritical phase Fischer-Tropsch synthesis with product upgrading (SC-FTOC). 1 g of precipitated Fe/Zn/K/Cu (molar ratio, Fe : Zn : Cu : K = 1: 0.1 : 0.01 : 0.02) FTS catalyst in the first FTS bed, 1 g of ASA (Sigma-Aldrich, 343358-1KG) catalyst in the second bed, and 1 g of Pd/ASA (1.0 wt.%) hydrocracking/isomerization catalyst in the third bed were used for the corresponding experiments. Before the reactions were performed, a catalyst reduction step was performed using a H_2 flow of 50 SCCM at the desired

reduction temperature for each reaction bed. The reduction temperature was ramped from room temperature to 270 ℃ (the first FTS bed), 400 ℃ (the second oligomerization bed), and 400 ℃ (the third hydrocracking/isomerization bed) at a rate of 5 ℃/min, respectively. The bed temperature was held at the desired temperature value for 10 hours. After the reduction, all the catalyst beds were cooled to room temperature. Hydrogen flow was then switched to helium flow at a rate of 100 SCCM in order to build up the system pressure by adjusting the BPR. The reaction temperature for each bed was: FTS at 240 ℃, oligomerization at 200℃ and hydrocracking/isomerization at 330℃ and syngas flow rate for all cases was 50 SCCM with a H_2: CO ratio of 1.75:1 (vol). The system pressure was uniform for all three reaction beds during each operation. The system pressure for GP-FT was 17.2 bar, for GP-FTS was 35 bar (the pressure preferred by the upgrading reactions) and 76 bar for all supercritical phase operations (with a hexanes flow rate of 1ml/min while maintaining the partial pressure of syngas at 17.2 bar by ensuring a constant flow rate of syngas). Table 3.1 shows the catalyst loading and reaction conditions for each operation. The carbon chain propagation probability (α) of the products was defined by the Anderson-Schulz-Flory (ASF) plot, in which the carbon number extended from C_5 to C_{32}. Each experiments set has been performed over three times to confirm the reproducibility.
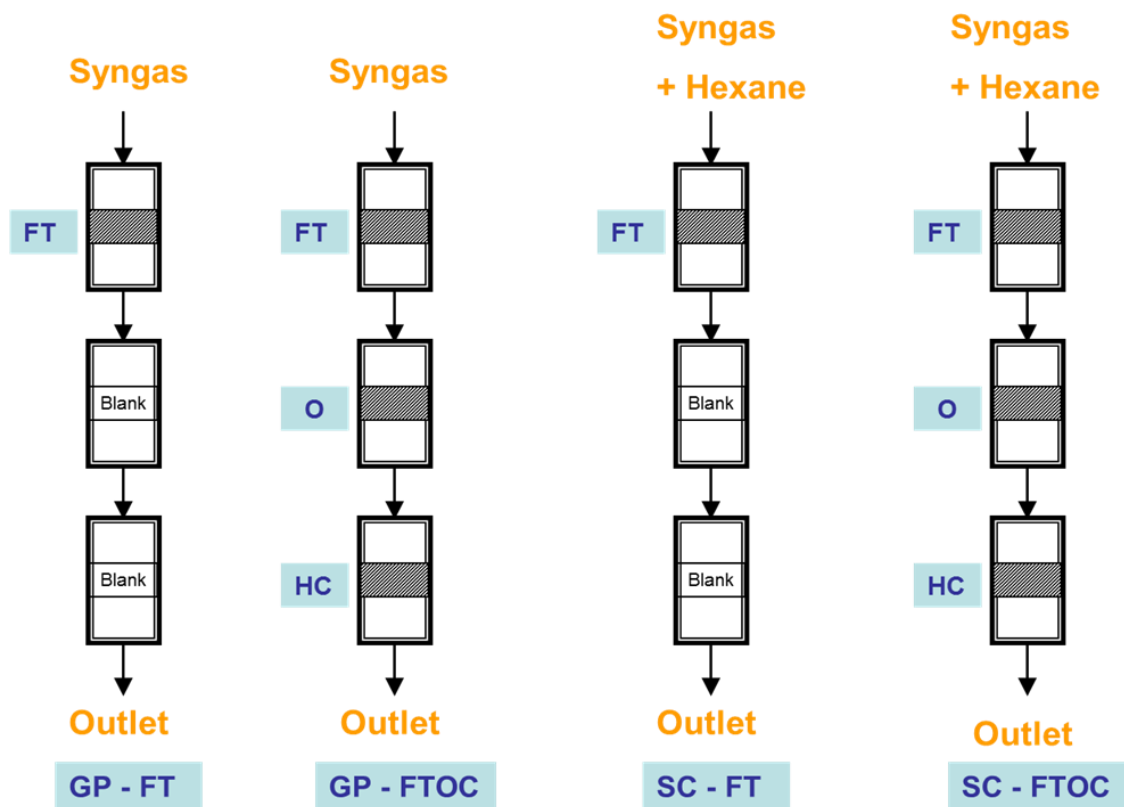
Figure 3.2 Catalyst loading configurations and reactant/solvent feed schemes for gas phase and supercritical phase Fischer-Tropsch synthesis with and without subsequent oligomerization and hydrocracking/isomerization stages.

Table 3.1   Reaction conditions and catalysts employed in the Fischer-Tropsch synthesis with and without subsequent oligomerization and hydrocracking/isomerization stages under gas phase and supercritical phase conditions.

Reaction Conditions		T (°C) (FT/O/C)	P (Bar)	Synthesis Gas Flow Rate (SCCM)[a]	Catalysts loading (FT/O/C)
Operation Phase	Reaction Stages				
Gas Phase	FT[b]	240/240/240	17.2	50	1g Fe[d] / - / -
Gas Phase	FTOC[c]	240/200/330	35.0	50	1g Fe[d] / 1g ASA / 1g Pd-ASA
Supercritical Phase[e]	FT[b]	240/240/240	76	50	1g Fe[d] / - / -
Supercritical Phase[e]	FTOC[c]	240/200/330	76	50	1g Fe[d]/ 1g ASA / 1g Pd-ASA

a: Syngas H_2: CO: N_2 ratio = 62.0: 36.5: 1.5, SCCM stands for standard cubic centimeter per minute
b: FT stands for Fischer-Tropsch synthesis
c: FTOC stands for Fischer-Tropsch synthesis with subsequent oligomerization and hydrocracking/isomerization
d: Fe -based FT catalyst, with a molar ratio of Fe: Zn: K: Cu = 1: 0.1: 0.02: 0.01
e: Supercritical media is Hexane with a media to syngas ratio of 3.5: 1, supercritical media flow rate is 1ml/min

3.3   Results and Discussion

As shown in Figure 3.3, under supercritical phase conditions, the carbon monoxide (CO) conversion dropped slowly as a function of time on stream (over a 100+ hour period). The CO conversion under these SC conditions was distinguishably higher (ca. 75%) than that obtained in the gas phase studies (ca. 35%) while the syngas flow rate (50 SCCM) and the syngas composition (H_2: CO = 1.75:1) were held at consistent values in each of the GP-FT, SC-FT, GP-FTOC and SC-FTOC cases. The syngas partial pressure in the GP-FT, SC-FT and the SC-FTOC experiments were held constant at 17.2 bar, while the syngas partial pressure in the GP-FTOC was maintained at 35 bar. There are several possible reasons for the high CO conversion during the supercritical phase experiments compared to the gas phase experiments. One potential reason is that the supercritical phase affords the ability to perform in-situ product extraction from the FT

catalyst's surface, thereby improving the availability of catalytic active sites thus enhancing the reaction rate (which is proportional to the availability of catalytic active sites (Iglesia 1997; Soled et al. 2003; Iglesia et al. 1993)). As such, more CO (as well as hydrogen) would react on the catalyst's surface, thereby enhancing the CO conversion with all other conditions being held constant. Another possibility is that during the startup period of the FTS reaction, a tremendous amount of reaction heat is released once the FTS reaction conditions (temperature and pressure) are achieved since the FTS reactions are so highly exothermic. In gas phase operation, the local heat removal rate may not be sufficient such that catalytic hot spots can be generated which would inherently lead to catalyst sintering (Dry 1990; D. J. Duvenhage et al. 1994; D. Duvenhage & N. Coville 2006) and fouling (deposition of inactive carbonaceous compounds such as amorphous carbon, graphitic carbon, coke) (Saib et al. 2010; Nlemantsverdrlet & Kraan 1980; Bukur, Koranne, et al. 1995; Bukur & Lang 1999; Bukur, Okabe, et al. 1995) and thus loss of surface area and active catalyst sites (Dry 2002; Fan & Fujimoto 1999; de Smit & Weckhuysen 2008). As a result, catalyst deactivation may have occurred due to a loss of catalyst active sites before steady state operation was achieved in GP-FT and GP-FTOC. However, in the supercritical phase operation, a large amount of reaction heat can be efficiently removed due to the presence of the bulk supercritical reaction media which basically serves as a thermal sink. As a result, the catalyst would not deactivate in the very initial period of the reaction as drastically under SC-FT conditions and SC-FTOC conditions as in the GP-FT and GP-FTOC.

Figure 3.3   CO conversion as a function of time on stream for gas phase Fischer-Tropsch synthesis (GP-FT), gas phase Fischer-Tropsch synthesis with oligomerization and hydrocracking/isomerization (GP-FTOC), supercritical phase Fischer-Tropsch synthesis (SC-FT) and supercritical phase Fischer-Tropsch synthesis with oligomerization and hydrocracking/isomerization (SC-FTOC).

(For all tests: syngas flow rate was 50 SCCM with a ratio of H_2: CO: N_2 = 62: 36.5: 1.5. For all supercritical phase operation, hexanes flow rate was 1.0 ml/min. GP-FT: system pressure = 17.2 bar, 1 gram of Fe/Zn/Cu/K catalyst in the 1st FT stage at 240ºC. GP-FTOC: system pressure = 35 bar, 1 gram of Fe/Zn/Cu/K catalyst in the 1st FT stage at 240ºC, 1 gram of ASA catalyst in the 2nd oligomerization stage at 200 ºC, 1 gram of 1.0 wt. % Pd/ASA catalyst in the 3rd hydrocracking/isomerization stage at 330 ºC. SC-FT: system pressure = 76 bar, 1 gram of Fe/Zn/Cu/K catalyst in the 1st FT stage at 240ºC. SC-FTOC: system pressure = 76 bar, 1 gram of Fe/Zn/Cu/K catalyst in the 1st FT stage at 240ºC, 1 gram of ASA catalyst in the 2nd oligomerization stage at 200 ºC, 1 gram of 1.0 wt. % Pd/ASA catalyst in the 3rd hydrocracking/isomerization stage at 330 ºC.)

The carbon dioxide (CO_2) selectivity obtained during SC-FT (ca. 17%) and SC-FTOC (ca. 13%) operation was lower than in the GP-FT (ca. 23%) and GP-FTOC (ca. 30%) operation (note that the CO conversion was also different), as shown in Figure 3.4. This result is consistent with our group's previous investigations of SC-FT in that the CO_2 selectivity is decreased relative to GP-FT (Durham et al 2010). Again, this can be attributed to the better heat management in the supercritical phase operation (Huang & Roberts 2003, Fujimoto and Yokota 1991, Fan &

Fujimoto 1999) thereby suppressing side reactions that affect CO_2 generation. In addition, the CO_2 selectivity did not show an increasing trend as a function of time on stream (over a 100+ hour period) in the supercritical operations, which is different than that observed in the gas phase operations where there is a modest increase in CO_2 selectivity with time on stream. This observation indicates that the catalyst deactivation rate may be lower in the supercritical phase operations than in the gas phase operations. This may be due to better heat transfer (so as to prevent the formation of the hot spots) and better mass transport (so as to inhibit loss of catalytic active sites by removing heavy products and coke precursors). The methane selectivity was low in both of the supercritical phase operations, below 4%, as shown in Figure 3.5. Methanation and cracking reactions are promoted by high temperature operation, and as such, temperature uniformity within the catalytic reaction beds is important in suppressing methane formation (Huang & Roberts 2003, Jacobs et al 2003, Fujimoto & Yokota 1991, Yokota & Fujimoto1989, Elbashir & Roberts 2005). The results in Figure 3.5 indicate that better heat management is obtained in supercritical phase operations as a result of the integration of the superior properties of the supercritical fluid medium into the FTS and FTOC processes.
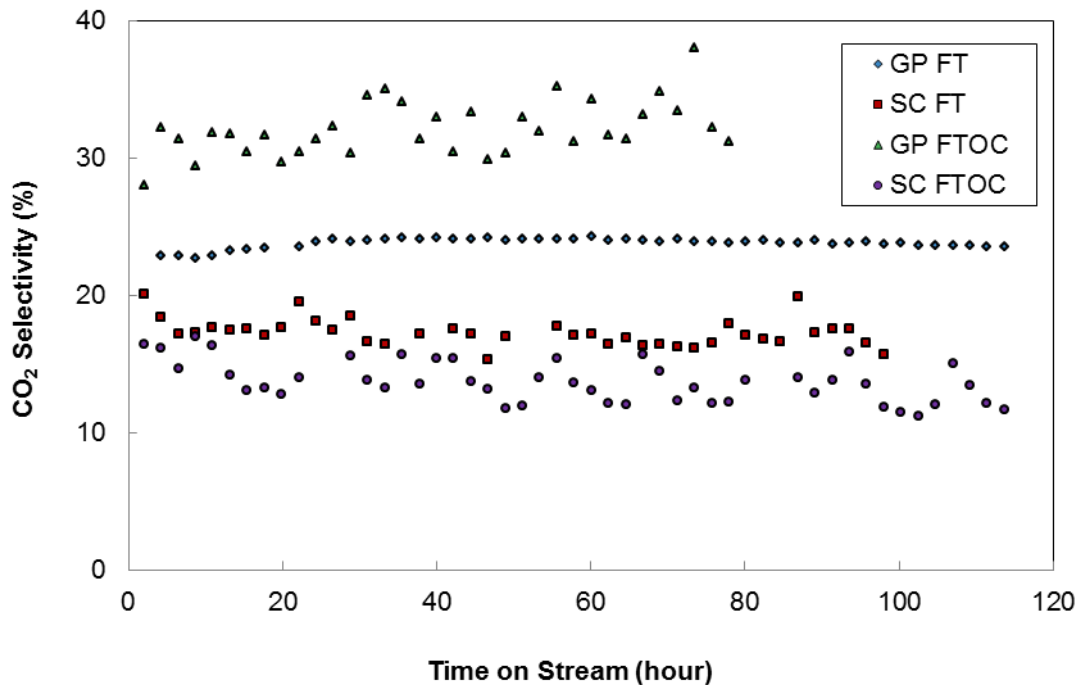
Figure 3.4 CO_2 selectivity as a function of time on stream for gas phase Fischer-Tropsch synthesis (GP-FT), gas phase Fischer-Tropsch synthesis with oligomerization and hydrocracking/isomerization (GP-FTOC), supercritical phase Fischer-Tropsch synthesis (SC-FT) and supercritical phase Fischer-Tropsch synthesis with oligomerization and hydrocracking/isomerization (SC-FTOC).

(For all tests: syngas flow rate was 50 SCCM with a ratio of H_2: CO: N_2 = 62: 36.5: 1.5. For all supercritical phase operation, hexanes flow rate was 1.0 ml/min. GP-FT: system pressure = 17.2 bar, 1 gram of Fe/Zn/Cu/K catalyst in the 1st FT stage at 240°C. GP-FTOC: system pressure = 35 bar, 1 gram of Fe/Zn/Cu/K catalyst in the 1st FT stage at 240°C, 1 gram of ASA catalyst in the 2nd oligomerization stage at 200 °C, 1 gram of 1.0 wt. % Pd/ASA catalyst in the 3rd hydrocracking/isomerization stage at 330 °C. SC-FT: system pressure = 76 bar, 1 gram of Fe/Zn/Cu/K catalyst in the 1st FT stage at 240°C. SC-FTOC: system pressure = 76 bar, 1 gram of Fe/Zn/Cu/K catalyst in the 1st FT stage at 240°C, 1 gram of ASA catalyst in the 2nd oligomerization stage at 200 °C, 1 gram of 1.0 wt. % Pd/ASA catalyst in the 3rd hydrocracking/isomerization stage at 330 °C.)
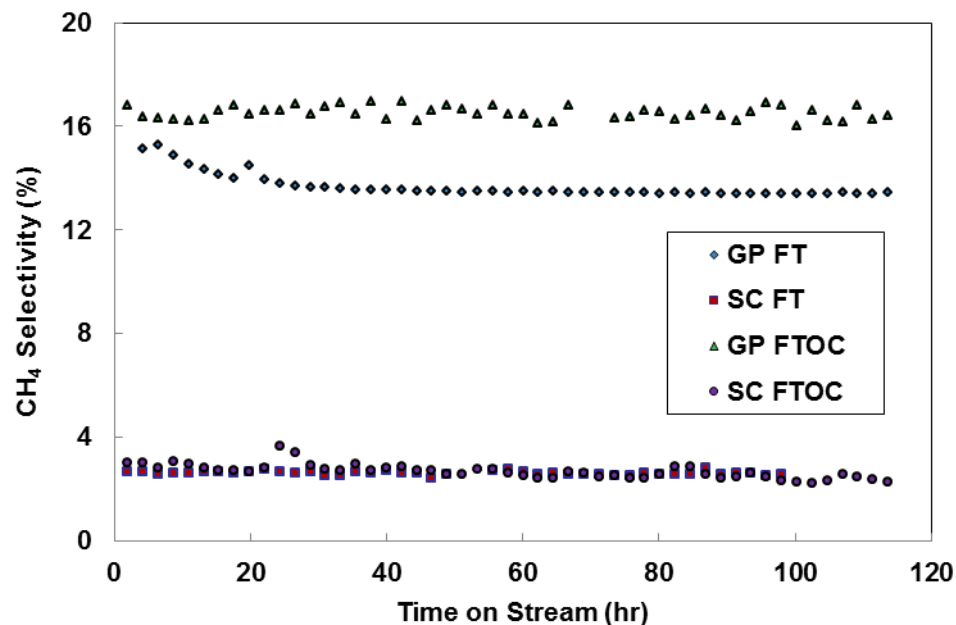
**Figure 3.5** CH$_4$ selectivity as a function of time on stream for gas phase Fischer-Tropsch synthesis (GP-FT), gas phase Fischer-Tropsch synthesis with oligomerization and hydrocracking/isomerization (GP-FTOC), supercritical phase Fischer-Tropsch synthesis (SC-FT) and supercritical phase Fischer-Tropsch synthesis with oligomerization and hydrocracking/isomerization (SC-FTOC).

For all tests: syngas flow rate was 50 SCCM with a ratio of H$_2$: CO: N$_2$ = 62: 36.5: 1.5. For all supercritical phase operation, hexanes flow rate was 1.0 ml/min. GP-FT: system pressure = 17.2 bar, 1 gram of Fe/Zn/Cu/K catalyst in the 1st FT stage at 240ºC. GP-FTOC: system pressure = 35 bar, 1 gram of Fe/Zn/Cu/K catalyst in the 1st FT stage at 240ºC, 1 gram of ASA catalyst in the 2nd oligomerization stage at 200 ºC, 1 gram of 1.0 wt. % Pd/ASA catalyst in the 3rd hydrocracking/isomerization stage at 330 ºC. SC-FT: system pressure = 76 bar, 1 gram of Fe/Zn/Cu/K catalyst in the 1st FT stage at 240ºC. SC-FTOC: system pressure = 76 bar, 1 gram of Fe/Zn/Cu/K catalyst in the 1st FT stage at 240ºC, 1 gram of ASA catalyst in the 2nd oligomerization stage at 200 ºC, 1 gram of 1.0 wt. % Pd/ASA catalyst in the 3rd hydrocracking/isomerization stage at 330 ºC.

In both of the supercritical phase operations, CH$_4$ and CO$_2$ selectivity were reduced compared to GP-FT and GP-FTOC indicating that more carbon from CO was converted into heavier hydrocarbons, particularly in light of the higher CO conversion. Table 3.2 provides a summary of the experimental results of the GP-FT, GP-FTOC, SC-FT and SC-FTOC studies. It is noted that the CO conversion, CH$_4$ and CO$_2$ selectivity listed in table 2 are average values over the whole operation period.

Table 3.2   CO conversion and product selectivities from Fischer-Tropsch synthesis with and without subsequent oligomerization and hydrocracking/isomerization stages under gas phase and supercritical phase conditions.

Operation Phase	GasPhase	Gas Phase	Supercritical Phase	SupercriticalPhase
Reaction Stages	FT[c]	FTOC[d]	FT[c]	FTOC[d]
X CO (%)[a]	31.5	33	75	84
S CO_2 (%)[b]	23	32	17	13
S CH_4 (%)	14	17	3	3
S C_2-C_4 (%)	13.5	9.5	2.1	3.7
S C_5-C_{11} (%)	27.5	12.2	23.8	27.5
S C_{12}-C_{22} (%)	21.3	26.8	40.5	42.7
S C_{22}+ (%)	0.6	2.3	13.6	10.1
S Normal Paraffin (% of C_{5+} products)	24.0	47.9	57.6	53.8
S Olefin (% of C_{5+} products)	45.6	10.5	18.6	30.5
S Branched Paraffin (% of C_{5+} products)	16.3	31.2	-	5.3
S Alcohol (% of C_{5+} products)	14.8	-	-	-
S Aldehyde (% of C_{5+} products)	-	-	23.6	-
S Aromatics (% of C_{5+} products)	-	10.4	-	-
S cyclo Paraffin (% of C_{5+} products)	-	-	-	10.3

a: X stands for conversion
b: S stands for selectivity
c: FT stands for Fischer-Tropsch synthesis
d: FTOC stands for Fischer-Tropsch synthesis with subsequent oligomerization and hydrocracking/isomerization

A high propagation probability (α value of 0.94) was observed in SC-FT, as determined by the analysis of the liquid products using GC-FID and GC-MS. This α value is higher than that obtained in the GP-FT (α value of 0.78). This result is in keeping with literature that indicates

that the liquid products shift towards the heavy hydrocarbon range under supercritical phase

conditions (Huang & Roberts 2004, Jacobs et al 2003, Yokota et al 1990). Figures 3.6 and 3.7

present product selectivities as a function of carbon number for GP-FT and SC-FT, respectively.

These results indicate that using the supercritical fluid as the reaction medium can promote the

carbon chain growth during the FT synthesis (Huang & Roberts 2004, Jacobs et al 2003, Yokota

et al 1990).
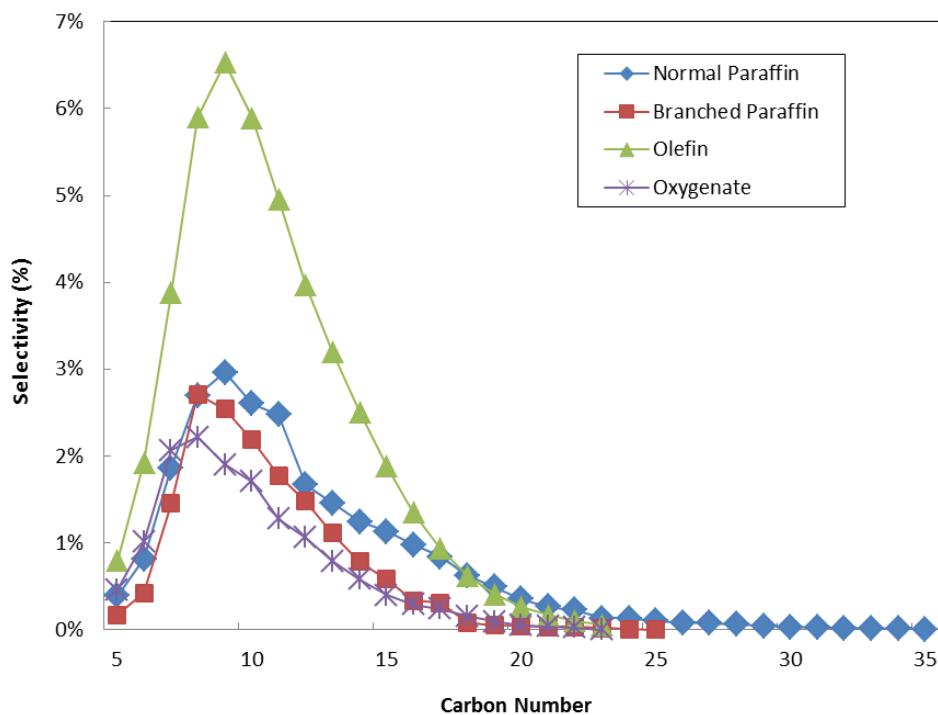
Figure 3.6   Liquid products selectivities from gas phase Fischer-Tropsch synthesis (GP-FT). GP-FT: 1 gram Fe/Zn/Cu/K catalyst in the 1st FT stage, T = 240 °C, p = 17.2 bar, synthesis gas flow rate: 50 SCCM, synthesis gas ratio: H_2: CO: N_2 = 62: 36.5: 1.5.
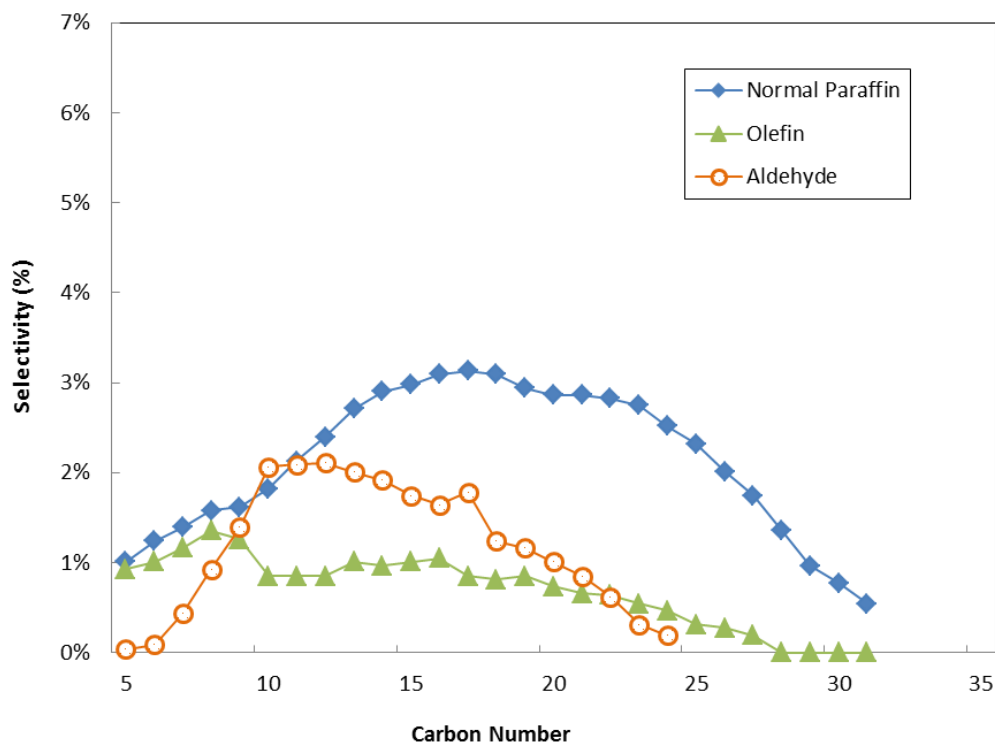
Figure 3.7 Liquid products selectivities from supercritical phase Fischer-Tropsch synthesis (SC-FT). SC-FT: 1 gram Fe/Zn/Cu/K catalyst in the 1st FT stage, T = 240 ℃, p = 76 bar. synthesis gas flow rate: 50 SCCM, synthesis gas ratio: H_2: CO: N_2 = 62: 36.5: 1.5, hexanes flow rate: 1.0 ml/min.

Consistent with our previous experience in operating SC-FT using an iron-based catalyst, a significant concentration of aldehyde (23.6%) was detected in the liquid products (rather than other oxygenates typically obtained from GP-FT such as alcohols) (Durham et al 2010). Our previous results show that these aldehydes are actually intermediates that are generated in the FTS reactions, which can be further converted to other oxygenates or olefins depending on various factors including residence time, catalyst acidity, and operating conditions (Durham et al. 2010). We have found that the enhanced solubility afforded by the use of the supercritical fluid as the reaction medium allows these aldehydes intermediates to be efficiently solvated by the

supercritical hexanes and extracted from the catalyst active sites and carried out of the catalyst bed as one of the reaction products. Durham et al. illustrated that aldehydes are primary products on an Fe-based catalyst under these SC-FT conditions which are then converted to other oxygenates and olefins which can then remain as olefins or can be subsequently transformed into paraffins through secondary reactions (Durham et al 2010). The mechanisms that underpin this aldehyde formation are a continuing focus of investigations in our lab.

Hydrocarbon product selectivity (expressed as mole percentage of a given compound or a group of compounds), and CO conversion obtained in these four tests are shown in Table 3.2. The synthesis gas flow rate for each of these four tests was kept constant at 50 SCCM in order to maintain the same apparent residence time.

After introducing the catalytic oligomerization and hydrogenation reaction beds, the olefin selectivity was greatly reduced in GP-FTOC (Figure 3.8) compared to GP-FT (Figure 3.6). As shown in Table 3.2, the olefin selectivity for the C_{5+} liquid products decreased from 45.6% in GP-FT to 10.5% in GP-FTOC. In GP-FT, terminal olefins are predominant, while in GP-FTOC, internal olefins (middle olefin, etc) are also observed. The introduction of the oligomerization bed and the hydrocracking bed effectively modified the total olefin yield, thus, the olefin concentration is greatly reduced in the GP-FTOC products in which case the olefin concentration can better meet the olefin content limit in certain fuel regulations (webpage references from EPA website).
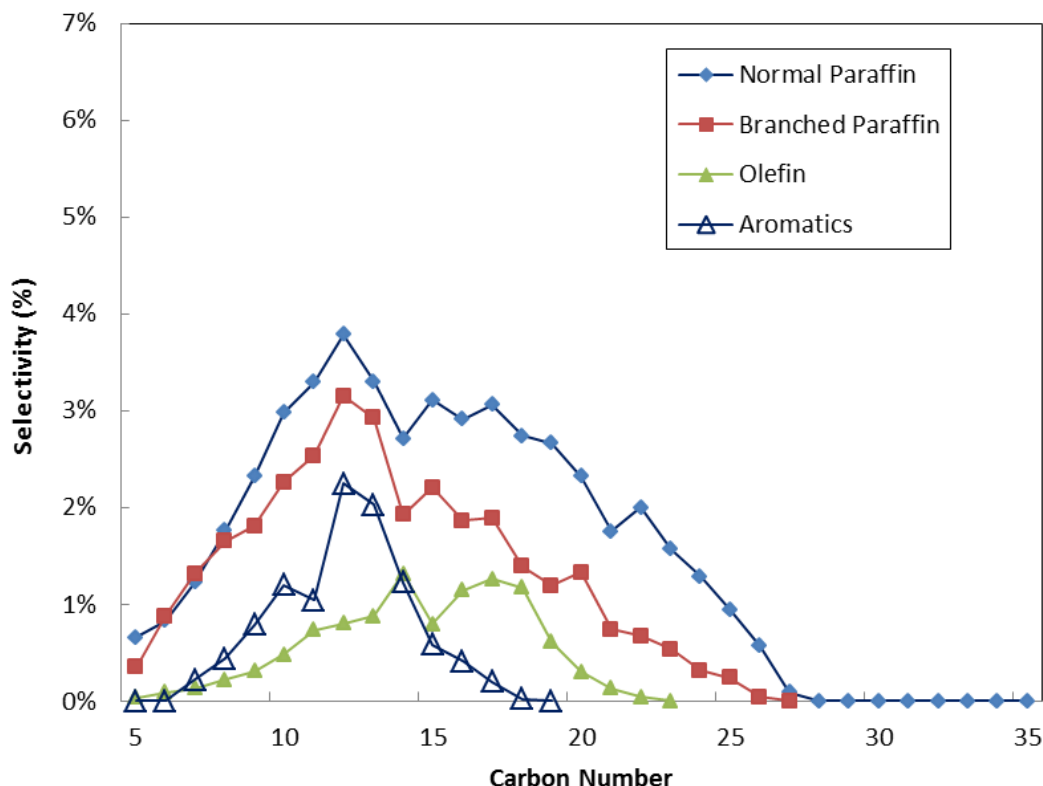
Figure 3.8   Liquid products selectivities from gas phase Fischer-Tropsch synthesis with subsequent oligomerization and hydrocracking/isomerization stages (GP-FTOC). GP-FTOC: 1 gram Fe/Zn/Cu/K catalyst in the 1st FT stage at T = 240 ºC, 1 gram ASA catalyst in the 2nd oligomerization stage at T = 200 ºC, 1 gram 1.0 wt. % Pd/ASA catalyst in the 3rd hydrocracking/isomerization stage at T = 330 ºC, p = 35 bar, synthesis gas flow rate: 50 SCCM, synthesis gas ratio: H_2: CO: N_2 = 62: 36.5: 1.5.

As shown in Table 3.2, the olefin selectivity in SC-FT was around 18.6%, which was significantly less than that in GP-FT (45.6%). However, recall that the aldehyde selectivity was 23.6% under these conditions, and, in light of the work of Durham et al. (Durham et al 2010), there appear to be aldehydes (which are produced as the primary product) that have not been converted to olefins under these SC-FT conditions. We note that the sum of the olefin selectivity and the oxygenate selectivity in this SC-FT experiment ($S_{olefin} + S_{aldehyde}$ = 42.2%) was about 18% less than the value from the GP-FT experiment ($S_{olefin} + S_{alcohol}$ = 60.4%). In addition, the paraffin selectivity (either normal paraffin or the sum of the normal paraffin and the branched

111

paraffin) in the SC-FT experiment is higher than that in the GP-FT experiment, as shown in Table 3.2. All together, the data show that hydrogenation is enhanced under these SC-FT conditions when compared to GP-FT. This observation is consistent with the fact that supercritical reaction solvents have be exploited for elimination interphase gas-liquid mass transport resistances so that it is possible to perform solid catalyzed hydrogenation with enhanced productivity (Subramaniam 2001). It is also in keeping with the suggestion that the enhanced readsorption of 1-olefins on the active sites can enhance the secondary reactions such as hydrogenation compared to gas phase operations (Li et al. 2005; Fan & Fujimoto 1999). It is worth noting that both enhanced products extractability (desorption) and products readsorption can result from utilization of supercritical fluid solvent, though there should be a balance which is dependent on the reaction conditions. Moreover, due to the enhanced solubility and mass transport that can occur under supercritical phase conditions (compared to gas phase operation), the reaction intermediates can more readily readsorb on catalytic active sites therefore bringing about further carbon chain growth, and thus higher α-value in SC-FT compared to GP-FT (Elbashir & Roberts 2005). The bigger the carbon number of the reaction intermediates, the longer residence time (as a result of slower diffusion rate) they will have within the catalysts thereby resulting in a higher probability of being hydrogenated (Fan & Fujimoto 1999). Overall, the product distribution shifts to longer chain hydrocarbons in SC-FT compared to that in GP-FT, which is consistent with general observations that have been made in supercritical phase Fischer-Tropsch synthesis by several research groups (Elbashir et al 2010, Jacobs et al 2003, Bochniak & Subramaniam 1998, Yokota et al 1990).

de Klerk tested an ASA catalyst for oligomerization under pressure ranging from 35 bar to 60 bar (De Klerk 2006). He reported that at 60 bar the oligomerization reaction using an ASA

catalyst showed higher activity and better activity maintenance than that at 40 bar (De Klerk 2006). Based on this, the oligomerization conversion would be expected to be higher in supercritical phase operation than that in gas phase since the system total pressure is higher. However, the results from SC-FTOC in Table 3.2 show that the use of the supercritical phase reaction media resulted in a higher selectivity towards C_{5+} olefins (30.5%) compared to GP-FTOC conditions (10.5%), noting that the CO conversions were different with values of 75% and 31.5%, respectively. This higher olefin selectivity in SC-FTOC (as shown in Figure 3.9) could result from either olefinic products being generated from the cracking/isomerization reactions (as reaction intermediates as discussed below), or due to a suppression of the oligomerization function because of the presence of the supercritical medium (however, the later is not consistent with the positive effect of pressure on ASA catalyzed oligomerization as observed by de Clerk (de Klerk 2006)). But it should be noted that the tests done by de Clerk were performed using a fluidized bed reactor under gas phase feed conditions).
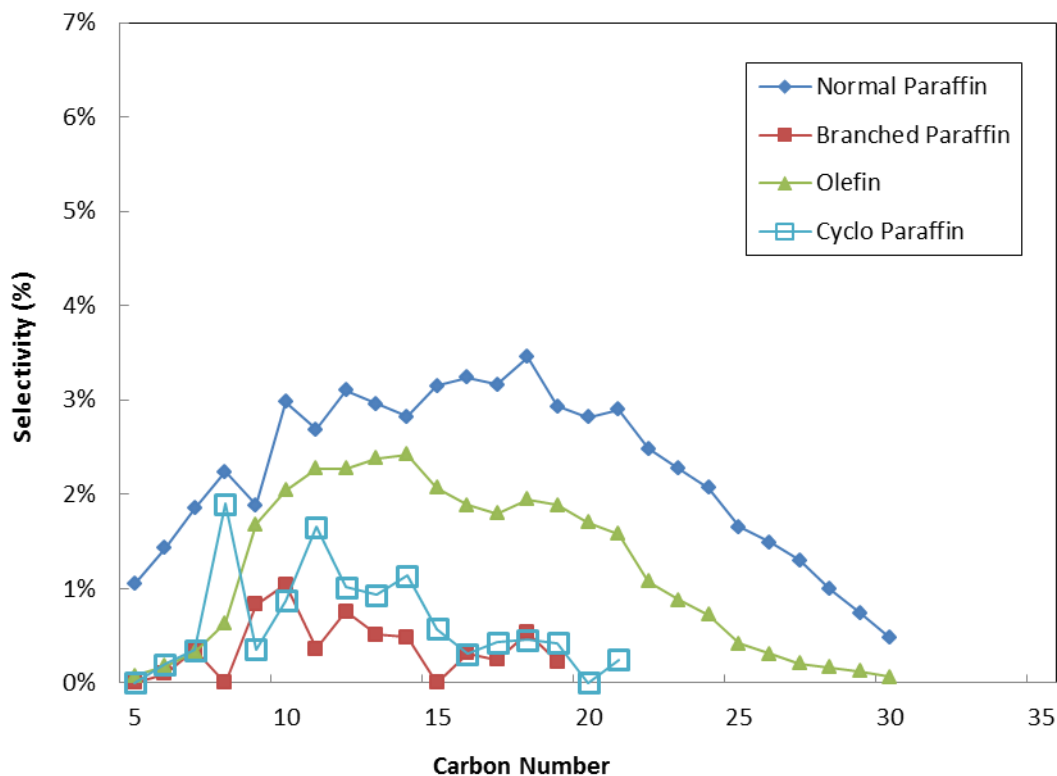
Figure 3.9   Liquid products selectivities from supercritical phase Fischer-Tropsch synthesis with subsequent oligomerization and hydrocracking/isomerization stages (SC-FTOC). SC-FTOC: 1 gram Fe/Zn/Cu/K catalyst in the 1st FT stage at T = 240 ºC, 1 gram ASA catalyst in the 2nd oligomerization stage at T = 200 ºC, 1 gram 1.0 wt. % Pd/ASA catalyst in the 3rd hydrocracking/isomerization stage at T = 330 ºC, p = 76 bar, synthesis gas flow rate = 50 SCCM, synthesis gas ratio: H$_2$: CO: N$_2$ = 62: 36.5: 1.5, hexanes flow rate: 1.0 ml/min.

The normal paraffin selectivity was increased from 24.0% in GP-FT to 47.9% in GP-FTOC due to the introduction of the hydrocracking reaction bed (on the 1 wt. % Pd/ASA catalyst) which brings about hydrogenation of olefinic products and hydrogen-unsaturated hydrocarbons. The noble metal, in this case palladium, mainly contributes to hydrogenation as it is active towards electron transfer (Deldari 2005). The difference in the normal paraffin selectivities between the SC-FT (57. 6%) and the GP-FT (24.0%), and between the SC-FTOC (53.8%) and the GP-FTOC (47.9%) indicate that the supercritical phase operations exhibit higher

hydrogenation activity. As widely discussed in other supercritical phase Fischer-Tropsch synthesis literature, reduced interphase gas-liquid mass transport resistance and enhanced hydrogen diffusivity can be contributing factors (Bochniak & Subramaniam 1998).

Due to the polymerization nature of FT synthesis, it is not particularly selective towards fuel range hydrocarbons. Additionally, the FT fuel that is produced possesses certain quality issues for use as both gasoline and diesel fuel, including poor cold-flow properties (cloud point, pour point, cold filter plugging point, etc.), low lubricity and low density, etc. (Bochniak & Subramaniam 1998; Van der Laan & Beenackers 1999; A. Steynberg & Dry 2004). Increasing the content of branched hydrocarbons in FT fuels can improve these cold-flow properties. Branched hydrocarbons, especially asymmetrical isomers, are more difficult to crystallize than linear paraffins of the same molecular weight, and therefore possess a lower melting point and congealing point than linear paraffins. In addition, asymmetric branched hydrocarbons and most substituted cyclic hydrocarbons contribute to the lubricating capacity of fuels (Trimm et al 1989). Yet, the paraffinic hydrocarbons generated from FT synthesis are highly linear. As a result, typically derived FT hydrocarbon fuels that contain low content of branched compounds offer poor cold-flow properties and low lubricity (Leckel 2007, Calemma et al 2010, Steynberg & Dry *Eds.* 2004). Various fuel additives can be added into the FT fuel blends to improve the cold-flow properties and lubricity, such as methyl ester (Huang & Roberts 2003, Steynberg & Dry *Eds*. 2004). Aromatics can be used to increase the fuel density and octane number along with the other fuel additives (de Klerk 2007, Dancuart et al 2010 chap 6).

In GP-FTOC, a significant amount of branched paraffin was generated. The branched paraffin selectivity in the GP-FTOC experiment increased from 16.3% in GP-FT up to 31.2% by adding the hydrocracking/isomerization stage. The branched paraffin types that were collected in

GP-FTOC include 2-methyl-, 3-methyl-, 4-methyl-, 2-dimethyl-, 2,3-dimethyl, 4-ethyl-, etc. For the fuel range (in the carbon number range from 5-22) the branched paraffin selectivity was significantly promoted. In SC-FTOC (Figure 3.9), the presence of the supercritical solvent allows for efficient extraction of reaction intermediates and products (as was also the case in SC-FT), such that cyclo-paraffins (1-R, 2-R, cyclopropanes) and more olefins were collected as reaction intermediates from the cracking/isomerization reactor bed. This observation is consistent with the mechanisms described by Park and Ihm (Park & Ihm 2000). It is well recognized that isomerization of n-paraffins is the first reaction step in this process while cracking is a subsequent reaction. Mono-branched paraffins show a lower tendency towards cracking than multi-branched paraffins (Calemma et al 2010). The bifunctional catalysts commonly used for hydrocracking/isomerization often contain metallic sites (for hydrogenation/ dehydrogenation) and acid sites (for skeletal isomerization via carbenium ions) (Calemma et al 2010, Liu et al 2005, Deldari 2005, Park & Ihm 2000, Alvarez et al 1996). in this case, Pd and ASA, respectively. In the cracking/isomerization pathway proposed by Park and Ihm (Park & Ihm 2000), paraffins are first activated and dehydrogenated on the metal sites, then the generated olefin intermediates protonate to corresponding carbenium ions (usually cyclic) on the acid sites. Through intramolecular reactions and intermolecular reactions, the carbenium ions are hydrogenated or dehydrogenated to produce branched paraffins with corresponding carbon number. The intramolecular reactions include type A rearrangements: hydride shift and alkyl shift, and type B rearrangements: PCP (protonated cyclopropane) branching and cracking by β - scission (Park & Ihm 2000). In this study, the SC-FTOC results are consistent with this mechanism by having exhibited the presence of cyclo-paraffins (1-R, 2-R, cyclopropanes) and the enhanced olefin selectivity. Note that there were negligible amounts of these cyclo-paraffins

116

observed in GP-FT and GP-FTOC.

Though the isomer selectivity (isomerization activity) was substantial, the cracking of long chain hydrocarbons (C_{22+}) was insignificant when comparing GP-FTOC with GP-FT. Yet, the C_{22+} product selectivity was higher in GP-FTOC than that in GP-FT, which suggests that the oligomerization activity was high for middle range compounds that were converted into C_{22+} products to an extent greater than the cracking of the C_{22+} compounds. However, the GP-FTOC C_{26+} product selectivity (0.1%, not listed in Table 2) was lower than that in GP-FT(0.3%, not listed in Table 2), which means that hydrocracking using this Pd/ASA catalyst under these gas phase conditions favors the cracking of the heavier hydrocarbons (C_{26+}). This result is consistent with the observation that the heavier hydrocarbons are more likely to be involved in cracking (Calemma et al 2010). Under supercritical phase conditions, the selectivity of C_{22+} compounds in SC-FTOC was 10.1% compared to 13.6% in SC-FT, thereby illustrating the impact of having introduced the hydrocracking stage. It is important to note that the production of C_{22+} hydrocarbons was significantly greater in SC-FT than in GP-FT, as described above, yet the activity of the hydrocracking stage under supercritical conditions was sufficient to lower the overall C_{22+} hydrocarbon selectivity. The balance between cracking and isomerization can be modified to further affect the product distribution by adjusting the catalyst for hydrogenation/dehydrogenation activity (noble metal) vs. the isomerization activity (acid sites) (Deldari 2005, Calemma et al 2000, Park & Ihm 2000, Alvarez et al 1996).

There were some aromatics produced in the gasoline and jet fuel range in the GP-FTOC experiment, which can enhance the density of the derived FT fuels. Identified aromatics ranged from C_7-C_{12}, including toluene, ethyl-benzene, p-xylene, o-xylene, 1-ethyl, 3-methyl-benzene, 1,3,5-trimethyl-benzene, 1,3-diethyl-benzene, 1-methyl,4-propyl-benzene, 1-methyl, 4-(1-

methylethyl)-benzene, pentamethyl-benzene, etc. Quantitatively, the aromatics concentration (as identified by GC-MS) was approximately 35% of the C_7-C_{12} hydrocarbons. However, the generation of aromatics was only observed in the GP-FTOC operation. Potential contributing factors are that the aromatization process was suppressed thermodynamically or that the concentrations of reactants for aromatization were too low such that there were no distinguishable aromatics generated under supercritical phase conditions.

In examining the liquid products as a function of carbon number, it can be seen that gasoline range (C_5-C_{11}) products was dominate in GP-FT while diesel range (C_{12}-C_{22}) was more prominent in GP-FTOC. In both SC-FT and SC-FTOC, the selectivity towards liquid products was greatly enhanced due to lower production of gas phase products. This is especially true for SC-FTOC where the fuel range products were further intensified through higher selectivity towards gasoline range and diesel range products and less heavy hydrocarbon (C_{22+}) production compared to SC-FT.

3.4 Conclusions

This study demonstrates that Fischer-Tropsch synthesis with subsequent oligomerization and hydrocracking/isomerization stages (FTOC) can be effectively performed using a newly designed three-bed catalytic reactor system. This three-bed reactor system consists of three sequential fixed bed reactors (arranged vertically), using 1g Fe-based FT catalyst in the first FT stage, 1g ASA catalyst in the second oligomerization stage and 1g of 1.0 wt.% Pd/ASA catalyst in the hydrocracking/isomerization stage. This integrated FTOC process provides opportunities to effectively modify the Fischer-Tropsch synthesis product. For instance, the liquid product C_{5+} olefin selectivity was observed to be greatly reduced to 10.5% in gas phase FTOC (GP-FTOC) compared to 45.6% in gas phase Fischer-Tropsch synthesis (GP-FT). The selectivity towards

branched paraffins, which can help to improve the fuel's cold flow properties and lubricity, was significantly promoted to ca. 31.2% through the implementation of the hydrocracking and isomerization stages in the GP-FTOC experiment compared to 16.3% in the GP-FT experiment. In addition, appreciable amounts of aromatics, which can enhance the fuel density, were produced in the gasoline and jet fuel range (C_5-C_{15}) in the GP-FTOC experiment. The selectivity towards long chain hydrocarbons (C_{26+}) that are typically produced in GP-FT was diminished due to the introduction the hydrocracking stage. Overall, this work demonstrates that the resulting product distribution can be distinguishably modified towards fuel range products in GP-FTOC through the integration of the oligomerization and hydrocracking/isomerization stages immediately subsequent to FTS.

Consistent with related work in the literature, the utilization of supercritical fluid (SC) media (in this case supercritical hexanes) in Fischer-Tropsch synthesis (SC-FT) was shown to reduce the selectivity towards CH_4 and CO_2 compared to gas phase Fischer-Tropsch synthesis (GP-FT). Moreover, SC-FT resulted in a shift in the product distribution towards longer chain hydrocarbons along with an enhanced normal paraffin selectivity compared to GP-FT. These results indicate improved carbon chain propagation probability and elevated hydrogenation under supercritical phase conditions. Additionally, in accordance with our previous experience in operating SC-FT on an iron catalyst, a significant concentration of aldehyde (23.6%) was detected in the SC-FT liquid products (rather than the other oxygenates typically obtained from GP-FT such as alcohols). In the case of SC-FTOC, higher concentrations of cyclo-paraffins (1-R, 2-R, cyclopropane) and olefins were observed in the liquid effluent from the cracking and isomerization stage, when compared to the liquid obtained from the GP-FTOC. The selectivity towards C_{22+} hydrocarbons was distinguishably less under SC-FTOC conditions compared to

119

SC-FT. Overall, this work illustrates that the selectivity towards fuel rage hydrocarbons (C_5-C_{22}) can be enhanced in SC-FTOC while simultaneously reducing the selectivity towards the undesired products of CH_4 and CO_2.

Chapter 4   Advancement of Iron-based Fischer-Tropsch Synthesis with Integrated Product Upgrading under Supercritical Phase Conditions

4.1   Introduction

In Fischer-Tropsch synthesis (FTS), a set of surface-catalyzed polymerization reactions take place, which convert syngas (a mixture of CO and H_2) into hydrocarbons and oxygenated hydrocarbons with a broad range of carbon chain lengths and type (Lynd et al 2009, Elbashir et al 2010, Van Der Laan and Beenackers 1999, Larson et al 2005, Dry 1989, Dry 1999, Dry 2002, Jacobs et al 2002, Schulz, 1999, Davis 2003, Iglesia 1997, Bukur and Sivaraj 2002, Khodakov 2009, Steynberg et al. 1999). With appropriate subsequent product separation and upgrading procedures, these FTS products can be further processed and converted into high quality fuels and value-added chemicals (Lynd et al 2009, Elbashir et al 2010, Van Der Laan and Beenackers 1999, Larson et al 2005, Dry 2002, Khodakov 2009, Steynberg et al. 1999, Espinoza et al 1999, Schulz et al 2005, Martinez et al 2007, Li et al 2008). Specifically, FTS can be performed at low temperature (LTFT) for the production of diesel and wax using iron or cobalt catalysts (Lynd et al 2009, Van Der Laan and Beenackers 1999, Khodakov 2009, de Smit and Weckhuysen 2008, Subramaniam 2001, Ngamcharussrivicha et al. 2007, Durham et al 2010, Anfray et al 2007, Huang and Roberts 2003, Guo et al 2011, de Klerk 2005), or can be performed at high temperature (HTFT) for the production of gasoline and light alkenes using fused iron catalysts (Lynd et al 2009, Van Der Laan and Beenackers 1999, Khodakov 2009, Steynberg et al 1999, Eilers et al 1990).

As such, FTS provides an alternative pathway to the production of contaminant (sulfur, nitrogen) free liquid fuels and value-added chemicals (e.g. polymers, detergents) from

carbonaceous feedstocks other than crude oil, namely coal, biomass and natural gas. The related technology is referred as coal-to-liquid (CTL), biomass-to-liquid (BTL) and gas-to-liquid (GTL), respectively. These technologies have been commercialized by Sasol (Mossel Bay, Sasolburg, Secunda, Ras Laffan), Shell (Bintulu), Qatar petroleum (Ras Laffan), and others (Lynd et al 2009, Khodakov 2009, Eilers et al 1990, Hamelinck et al 2004).

Iron-based FT catalysts are less expensive (Lynd et al 2009, Khodakov 2009) though less active (Khodakov 2009, Liu et al 2011) than cobalt-based FT catalysts. Iron-based FT catalysts offers lower CH_4 selectivity but higher olefin content than cobalt-based FT catalysts (Leckel 2007, Calemma et al 2010). Due to good catalytic activity towards the water-gas-shift (WGS) reaction, iron based FT catalysts allow for a wider range of the syngas H_2/CO ratio than cobalt-base FT catalysts, which is especially advantageous when using coal-derived or biomass-derived syngas (since the H_2/CO ratio derived from these feedstocks is typically lower than that of the natural-gas-derived syngas) (Leckel 2007, Duvenhage and Shingles 2002). One more attractive feature of iron-based FT catalysts is that the product functionality can be tuned over a wide range since the product distribution (such as olefins and alcohols) is different from that obtained when using a cobalt-based FT catalyst (Iglesia 1997). This provides more diversity in the production of chemicals for the CTL or BTL plants (Iglesia 1997). However, the iron-based FT catalyst suffers from fast deactivation due to surface carbon deposition and oxide sintering, which results from the combination of insufficient reaction heat removal (since FTS is highly exothermic) and poor products mass transport in gas phase operations (Elbashir et al 2010).

Supercritical phase FTS (SC-FTS) operations have been reported to provide better catalytic activity maintenance, in addition to many other advantages (Elbashir et al 2010, Subramaniam 2001, Durham et al 2010, Huang and Roberts 2003, Li et al 2005). A supercritical fluid (SCF) is

any material that has been heated and compressed over its critical temperature and pressure. SCFs possess properties that are intermediate between that of a vapor and that of a liquid, such as vapor-like diffusivity and liquid-like density. Compared to traditional gas phase FTS (GP-FTS), the use of a supercritical fluid as the reaction media in FTS has been shown to offer certain benefits, including: 1) Greater heat transfer as compared to GP-FTS (Huang and Roberts 2003, Jacobs et al2003, Yokota et al 1990,); 2) Enhanced removal of interphase transport limitations (Bochiniak and Subramaniam 1998); 3) Elevated reactant and product (and reaction intermediate) solubilities in the bulk media (Jacobs, et al 2003, Bochniak and Subramaniam 1998, Yokota et al 1990). In this study, hexanes were chosen as the supercritical solvent based on the three criteria which were proposed by Fujimoto (Yokota and Fujimoto 1989, Yokota et al 1990), so as to allow for enhanced catalyst maintenance, better heat management, and improved product solubility in the bulk reaction media.

FTS follows the Anderson–Schulz–Flory (ASF) polymerization kinetics, and as such, the FTS process is unselective towards specific products or product fractions (Calemma et al 2010, Steynberg and Dry 2004, Zhang et al 2010, Khodakov et al 2007), where the compounds produced typically range from C_1 to C_{50+} in carbon number. To intensify the selectivity of the FTS process towards middle distillate range products (C_8-C_{22}), additional upgrading reactions are required. A considerable number of studies have been performed to improve selectivities towards the middle distillates by: 1) modification of the reaction catalyst systems, such as noble metal doping or integration of advanced support materials (Zhang et al 2010, Li et al 2005, Li et al 2003, He et al 2005) and 2) modification of the reaction system by adding upgrading processes subsequent to FTS (Li et al 2005, Cho et al 2008, Liu et al 2005) . Modification of the FTS reaction system to intensify the FTS process typically involves the use of a FT wax

hydrocracking stage subsequent to the FTS catalytic reaction bed (FTC) (Li et al 2005, Cho et al 2008, Liu et al 2005, Liu et al 2006). For this two stage operation, a cobalt-based FT catalyst is often used (Liu et al 2006, Liu et al 2005) in the first FT bed to generate long chain hydrocarbons since cobalt-based FT catalysts yield heavier hydrocarbons compared to iron-based FT catalysts (de Smit and Weckhysen 2008, Khodakov 2009, Steynber and Dry 2004). The consecutive reactor bed apparatus allows for the products that are produced in the first bed to be used as the feed to the second cracking/isomerization stage. This synthesis plus upgrading arrangement allows for the production of more desired hydrocarbons with proper carbon chain length and functionality. Since most of the investigations are focusing on the conversion of heavy hydrocarbons into the middle distillates, studies on the feasibility of using iron-based FT catalyst in the first FT bed are insufficient. Additionally, there are considerable advantages for the use of iron-based FT catalysts, as discussed above. As such, an iron-based FT catalyst has been chosen in this study as an active FTS catalyst in the first reaction bed.

Investigations involving incorporation of oligomerization into the FT process (FTO) can potentially allow the conversion of light olefins produced from FTS to be converted into longer fuel range hydrocarbons (with potential branching). In particular, considering that iron-based FTS yields more olefinic products than cobalt-based FTS (Van Der Laan & Beenackers 1999), a sequential catalytic oligomerization in the reaction bed following FTS can intensify the process by upgrading the light products. In addition to the FTS plus hydrocracking/isomerization arrangement (FTC), the dual bed reactor system can be used to examine the implementation of an oligomerization reaction bed subsequent to the first FTS stage (FTO). Moreover, this study also examines the use of a supercritical reaction solvent which can be expected to enhance the heat management in the oligomerization reaction (also highly exothermic) similarly to the way it

does in SC-FTS.

A dual bed reactor system is investigated in this study in order to improve the direct production of middle distillates from syngas in a single pass arrangement. The reactor system consists of two vertically arranged sequential fixed bed reactors. Low temperature FTS is performed in the first catalyst bed using a precipitated iron-based FTS catalyst, generating a variety of hydrocarbon types and lengths. The second bed is employed to evaluate each of the upgrading reactions, oligomerization or hydrocracking/isomerization, separately. The operation temperature can be adjusted individually for each reaction bed to achieve the optimum catalytic performance within each reactor.

Solid phosphoric acid (SPA) and ZSM-5 are used commercially in FTS refineries in the oligomerization and isomerization steps to yield diverse target product fractions such as gasoline and diesel (De Klerk 2006). Amorphous silica alumina (ASA) has been suggested by de Klerk as a promising oligomerization catalyst while not having been sufficiently studied (Martinez et al 2007). Advantages of using ASA in oligomerization has been previously reported, such as good oxygenates resistance (Tsubaki et al 2003). In this study, ASA is employed as the catalyst in the second oligomerization bed for the study of the FTO dual bed process.

Pd and Pt based solid acid catalysts are regularly used in hydrocracking/isomerization processes (Ancheyta et al. 2005; Calemma et al. 2000; Archibald et al. 1960). In this study, Pd has been chosen as the active metal for the hydrocracking/isomerization stage for the following reasons: 1) it offers higher cracking activity than Pt (Deldari 2005); and 2) it exhibits better activity maintenance than Pt (Liu et al 2005). ASA has been selected as the support material for this study due to its high hydroisomerization performance (Deldari 2005; de Klerk 2006; de Klerk 2007b). Thus, Pd/ASA has been used as the catalyst in the FTC experiments

125

4.2 Material and Methods

In this study, two sets of investigations have been performed: FTS plus oligomerization (FTO) and FTS plus hydrocracking/isomerization (FTC). A diagram of the dual bed reactor system for Fischer-Tropsch synthesis with product upgrading under the supercritical phase conditions is shown in Figure 4.1. Helium gas (Airgas, ultra high purity) was used during the system pressure test, reaction startup and shut down. Synthesis gas (Syngas) (Airgas, vol%: N_2: CO: H_2 = 1.5: 37: 61.5) was fed into the reaction system by a mass flow controller. Hexanes (Fischer, HPLC grade, CAS# 110-54-3) were used as the supercritical fluid reaction media in this investigation, and were delivered into the reaction system using an HPLC pump at a flow rate of 1ml/min in the case of supercritical phase operation. The syngas and hexanes were mixed in a static mixer and the mixture was initially heated in the pre-heating zone. The reactant (and the supercritical fluid medium in the case of supercritical phase operation) entered the top of the tubular fixed-bed reactor and then was passed through each reaction bed sequentially. The reactor effluent was passed through heated tubing to the back pressure regulator (BPR, Straval Valves Inc. model BPH0502T) which was employed to control the system pressure. The effluent was then passed through heated tubing to a cold trap (CT, Swagelok Inc. 304L-HDF4-1000).
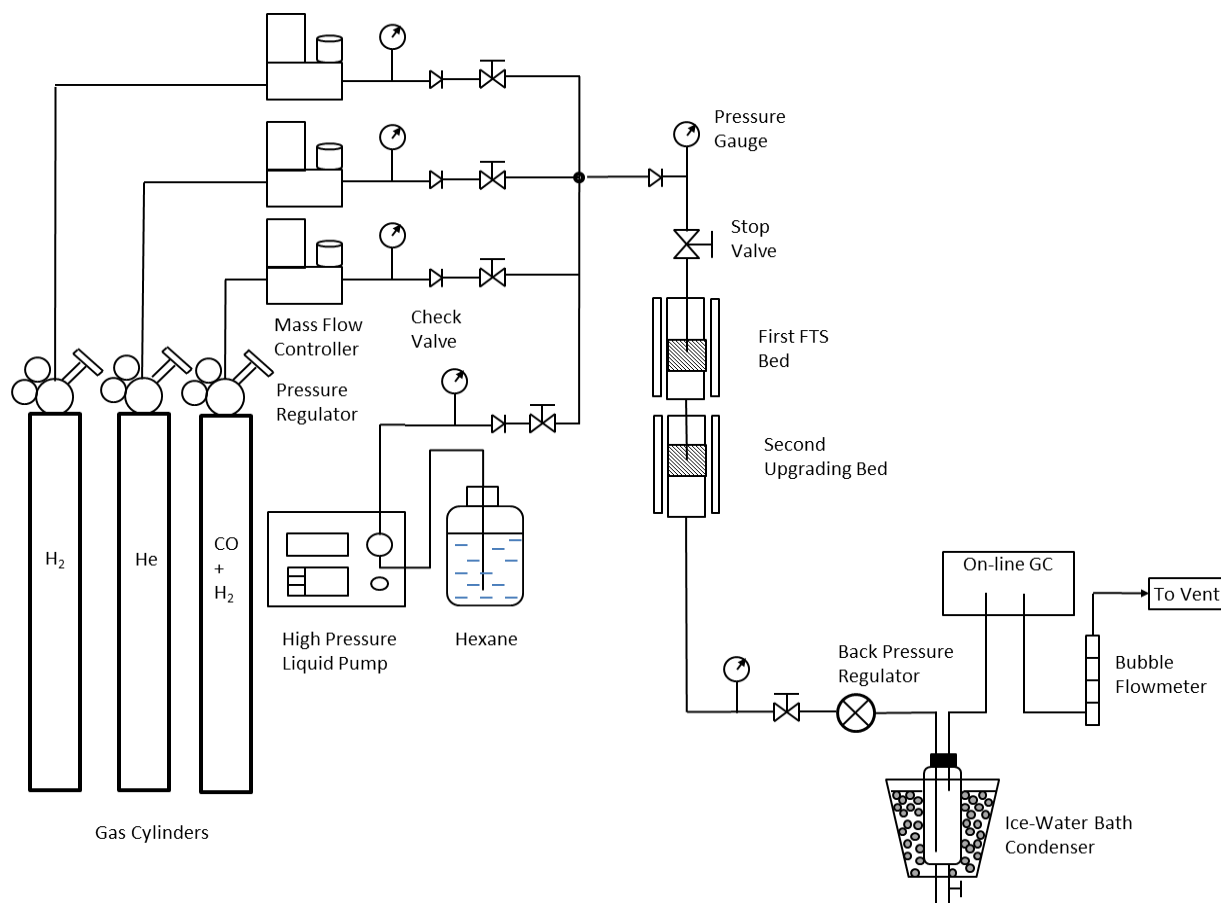
Figure 4.1   Schematic diagram of the three-bed catalytic reactor system for Fischer-Tropsch synthesis with subsequent oligomerization or hydrocracking/isomerization stages

The cold trap was cooled by an ice-water-mixture. The condensable products were accumulated in the CT and were manually collected and tested periodically by injecting them into a gas chromatograph with a flame ionization detector (GC-FID, Varian GC 3300 with a DB-5 capillary column) and a GC-MS (Waters. Inc.). The incondensable gas mixture (syngas residue and light products) left the CT and was passed through a 10-port injection valve for periodic injection into a gas chromatograph with a thermal conductivity detector (GC-TCD, SRI Multi-Gas Analyzer #1). The gases were then passed through a bubble meter, which allowed for the measurement of the real-time gas effluent volumetric flow rates. The gas effluent was then vented into the fume

127

hood.

Figure 4.2 shows the catalyst loading for each bed during each different operation. The experiments were performed in four modes of operation: gas phase Fischer-Tropsch synthesis plus oligomerization (GP-FTO), supercritical phase Fischer-Tropsch synthesis plus oligomerization (SC-FTO), gas phase Fischer-Tropsch synthesis plus hydrocracking/isomerization (GP-FTC) and supercritical phase Fischer-Tropsch synthesis plus hydrocracking/isomerization (SC-FTC). For FTO experiments, 1 g of precipitated Fe/Zn/K/Cu (molar ratio, Fe: Zn: Cu: K = 1: 0.1: 0.01: 0.02) FTS catalyst in the first FTS bed, 1 g of ASA (Sigma-Aldrich, 343358-1KG) catalyst in the second bed were used. For FTC experiments, 1 g of precipitated Fe/Zn/K/Cu (molar ratio, Fe: Zn: Cu: K = 1: 0.1: 0.01: 0.02) FTS catalyst in the first FTS bed and 1 g of Pd/ASA (1.0 wt.%) hydrocracking/isomerization catalyst in the third bed were loaded. Before the reactions were performed, a catalyst reduction step was performed using a H_2 flow of 50 SCCM at the desired reduction temperature for each reaction bed. The reduction temperature was ramped from room temperature to 270 ℃ (the first FTS bed), 400 ℃ (the oligomerization bed), and 400 ℃ (the hydrocracking/isomerization bed) at a rate of 5 ℃/min, respectively. The bed temperature was held at the desired temperature value for 10 hours. After the reduction, all the catalyst beds were cooled to room temperature. Hydrogen was then switched to helium at a rate of 100 SCCM in order to build up the system pressure by adjusting the BPR. The reaction temperature for each bed was: FTS at 240 ℃, oligomerization at 200℃ and hydrocracking/isomerization at 330℃ and syngas flow rate for all cases was 50 SCCM with a H_2: CO ratio of 1.75:1 (vol). The system pressure was uniform for both reaction beds during each operation. The system pressure for gas phase was 17.2 bar (a conventional FTS pressure) and 35 bar (the pressure preferred by the upgrading reactions) and 76 bar for all supercritical

phase operations (with a hexanes flow rate of 1ml/min and a constant 50 SCCM flow rate of syngas). Each experiments set has been performed over twice to confirm the reproducibility.
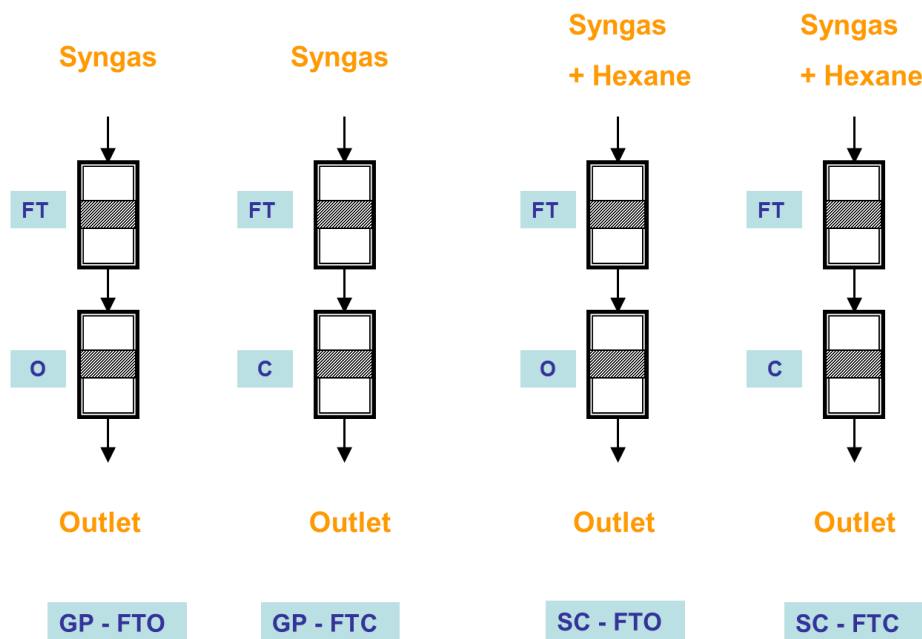
Figure 4.2   Catalyst loading configurations and reactant/solvent feed schemes for gas phase and supercritical phase Fischer-Tropsch synthesis with and without subsequent oligomerization or hydrocracking/isomerization stages

4.3   Results and Discussions

The CO conversion for the investigations of FTS plus hydrocracking/isomerization in this dual bed configuration under both gas phase and supercritical phase (GP-FTC and SC-FTC) conditions is shown in Figure 4.3 as a function of time on stream. The CO conversion under gas phase conditions (GP-FTC) at steady state remained at a value around 44% over the 80 hours of operation. This activity performance was similar to the previously observed gas phase FTS CO conversion that was described in chapter 2 (operated at 35 bar with a CO conversion of c.a. 45%). In SC-FTC, the CO conversion dropped slowly from 80% to 70% once steady state was achieved and persisted at this level over the 100 hour period of time. The CO conversion in the

gas phase was distinguishably lower than that in the supercritical phase, which is consistent with the results in chapter 2 and chapter 3. A possible reason for this may be that the iron-based FTS catalyst was overheated and deactivated in the gas phase operation during the reaction start-up period due to the extreme exothermic nature of the FTS and related reactions. However, due to the significantly greater heat capacity of the supercritical phase medium, this large amount of reaction heat can be more efficiently removed from the catalytic reaction sites. This issue is further addressed later in this chapter. It is noted that the partial pressure of syngas, and as such the pressure of CO, was different in these two experiments. To be specific, the partial pressure of syngas was 35 bar in GP-FTC and 17.5 bar in SC-FTC, respectively.
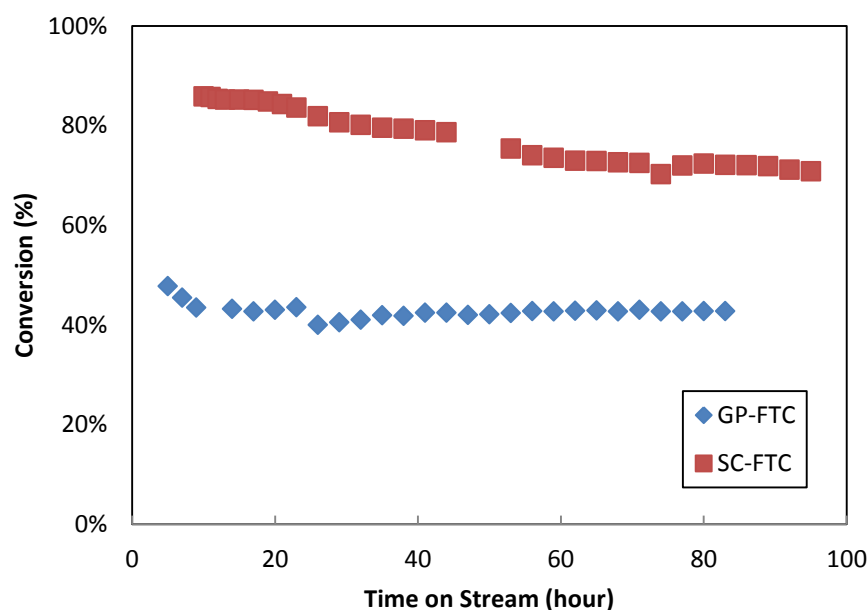
Figure 4.3   CO conversion as a function of time on stream for Fischer-Tropsch synthesis plus hydrocracking/isomerization under gas phase and supercritical phase (GP-FTC and SC-FTC).

(For all tests: syngas flow rate was 50 SCCM with a ratio of H_2: CO: N_2 = 62: 36.5: 1.5, 1 gram of Fe/Zn/Cu/K catalyst in the 1st FT stage at 240ºC, 1 gram of 1.0 wt. % Pd/ASA catalyst in the 2nd hydrocracking/isomerization stage at 330 ºC. For GP-FTC: system pressure = 35 bar. For SC-FTC, hexanes flow rate was 1.0 ml/min, system pressure = 76 bar.)

In the SC-FTC operations, the methane and CO_2 selectivity were 2% and ca. 15%,

respectively, as shown in Figure 4.4. These values are lower than those obtained from the gas

phase operation, where the methane selectivity was 4% and the CO_2 selectivity was ca. 30%.

This result is consistent with previously reported observations that the better heat management

provided by the supercritical solvent can significantly suppress the methane and carbon dioxide
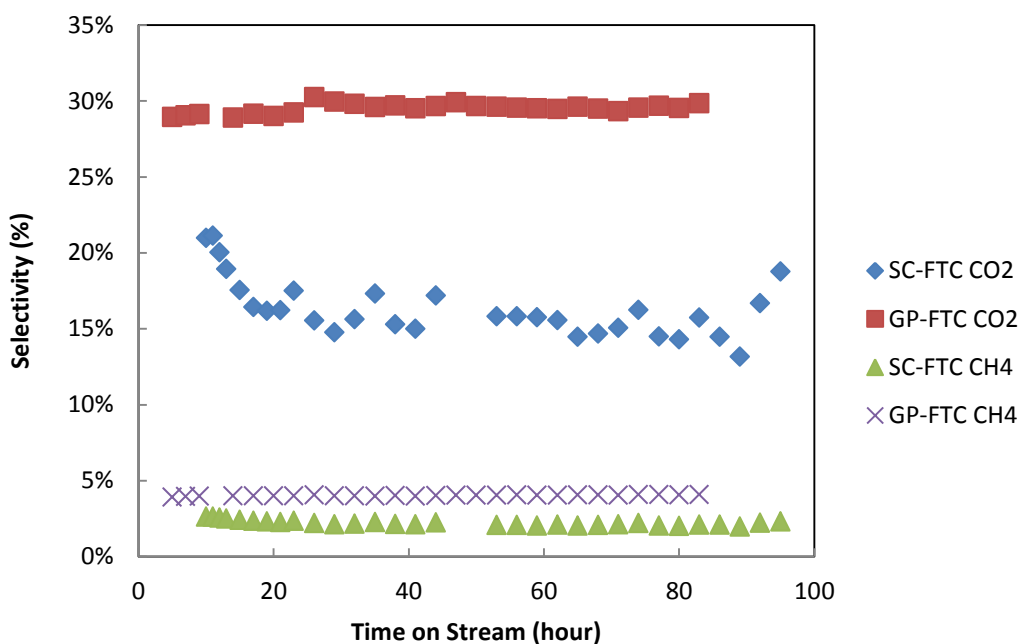
selectivity.

Figure 4.4 CO_2 and CH_4 selectivity as a function of time on stream for Fischer-Tropsch synthesis plus hydrocracking/isomerization under gas phase and supercritical phase (GP-FTC and SC-FTC) operation.

(For all tests: syngas flow rate was 50 SCCM with a ratio of H_2: CO: N_2 = 62: 36.5: 1.5, 1 gram of Fe/Zn/Cu/K catalyst in the 1st FT stage at 240ºC, 1 gram of 1.0 wt. % Pd/ASA catalyst in the 2nd hydrocracking/isomerization stage at 330 ºC. For GP-FTC: system pressure = 35 bar. For SC-FTC, hexanes flow rate was 1.0 ml/min, system pressure = 76 bar.)

To further study the effect of the presence of the supercritical solvent on the initial activity

of the catalyst, a step-wise process with a switch between the supercritical phase FTS (SC-FT)

and gas phase FTS (GP-FT) was conducted. All the operational parameters were intentionally maintained to be comparable to each of the previously reported FTS reactions. The reaction was started with the injection of supercritical solvents for 24 hours of time on stream, which allowed for the observation of the catalyst activity under supercritical phase conditions during the initial period of the reaction. The system pressure was then adjusted to using the back pressure regulator (BPR) to achieve gas phase operation at 17 bar (standard FTS pressure). Then, after c.a. 200 hours of operation, the system pressure was further adjusted to 38 bar (this elevated pressure is closer to the value that is preferred by the upgrading reactions) in order to examine the effect of pressure on the FTS reaction performance in the gas phase. In this FTS-only investigation (without the inclusion of the upgrading reactions), the first bed (240°C) of the multi bed reactor system was loaded with one gram of a Fe/Zn/Cu/K (molar ratio: 100/10/1/2) FT catalyst (this is the same FTS catalyst that was used in chapter 2 and chapter 3), while no catalysts were loaded into the subsequent upgrading reaction beds. The upgrading bed temperatures were maintained at 240°C. The system total pressure was initially kept at 77.5 bar. Hexanes were used as the supercritical solvent with a constant inlet flow rate of 1ml/min during the supercritical operation. The hexane to syngas molar ratio was 3.5:1. The syngas (H_2: CO = 1.65:1) flow rate was constant at 50 SCCM during the whole process of operation. After 24 hours of supercritical phase operation, the injection of hexanes was stopped. The system pressure was then adjusted to 17 bar using only syngas as the inlet feed, and this pressure was later adjusted to 38 bar by tuning the BPR. Before the reaction was initiated, the Fe catalyst was activated in situ for 10 h in a 50 SCCM H_2 gas stream at 270 °C. Helium was used to test the reactor system pressure and was also used as the inert gas blanket during the reaction start up and shut down periods.

As shown in Figure 4.3, the CO conversion was approximately 90% in the SC-FT stage

(which is consistent with results presented in chapter 2 and chapter 3). The CO conversion under gas phase conditions (17 bar) decreased to c.a 40% after discontinuing injection of hexane into the system. The CO conversion level in this SC-FT operation (see Figure 4.5) is comparable to the CO conversion level in SC-FTC (as shown in figure 4.3). It is noted that the CO conversion was ca. 90% in the SC-FT period (with a syngas partial pressure of 17 bar) of operation which is significantly higher than the CO conversion of ca. 40% that was obtained in the GP-FT period at the syngas pressure of 17 bar, as well as the CO conversion of ca. 60% that was obtained in the GP-FT period of operation at the elevated pressure of 38 bar. This result further illustrates an enhanced catalytic activity in the supercritical phase compared to that in gas phase FT. As discussed above, the reaction heat can be more efficiently removed by the supercritical medium thereby allowing it to serve as an effective heat sink. This improved heat management capability can help to prevent the formation of catalytic "hot spots" (i.e. local overheating of the catalyst active sites) that lead to catalyst deactivation. Another contributing factor to the elevated CO conversion under supercritical phase operation is that the supercritical solvent affords enhanced reactant and product solubility (compared to gas phase operation). This elevated solubility can prevent catalyst deactivation by alleviating heavy hydrocarbon (e.g. waxy products) build-up on the catalyst active sites. The CO conversion in SC-FT (~90%) is higher than that obtained in the SC-FTC (~75%), illustrated that the hydrocracking/isomerization stage affects the CO generation/consumption to some extent. Moreover, the CO conversion in the GP-FT (~60%) is higher than that obtained in the GP-FTC (~44%), further illustrating this point.
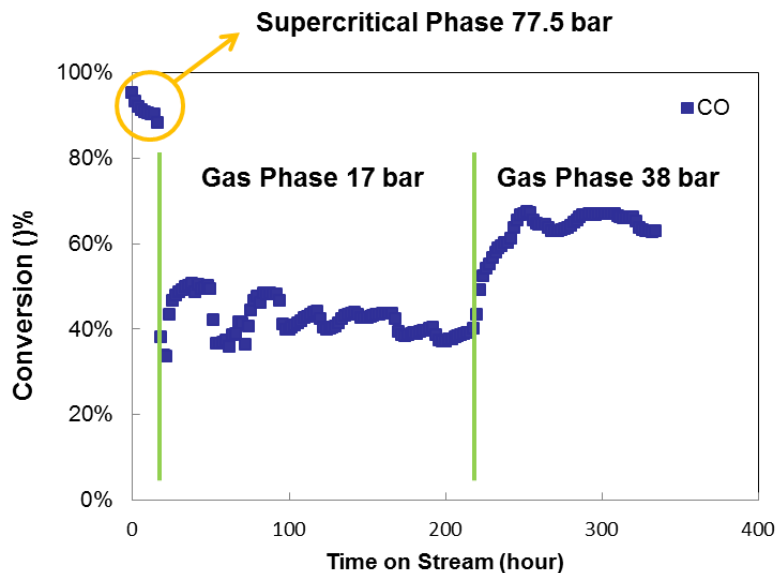
Figure 4.5   CO conversion for SC-FT and GP-FT

(For all tests: syngas flow rate was 50 SCCM with a ratio of H_2: CO: N_2 = 62: 36.5: 1.5, 1 gram of Fe/Zn/Cu/K catalyst in the 1st FT stage at 240ºC. For GP-FT: system pressure = 17 bar and 38 bar. For SC-FT, hexanes flow rate was 1.0 ml/min, system pressure = 77.5 bar.)

Figure 4.6 presents that the CO_2 selectivity was ca. 15% in SC-FT, and the CO_2 selectivity increased to 30% and 28% in GP-FT at the pressures of 17 bar and 38 bar, respectively. This result is also consistent with the general observation that by better heat management in the supercritical phase, the selectivity towards carbon dioxide can be reduced.
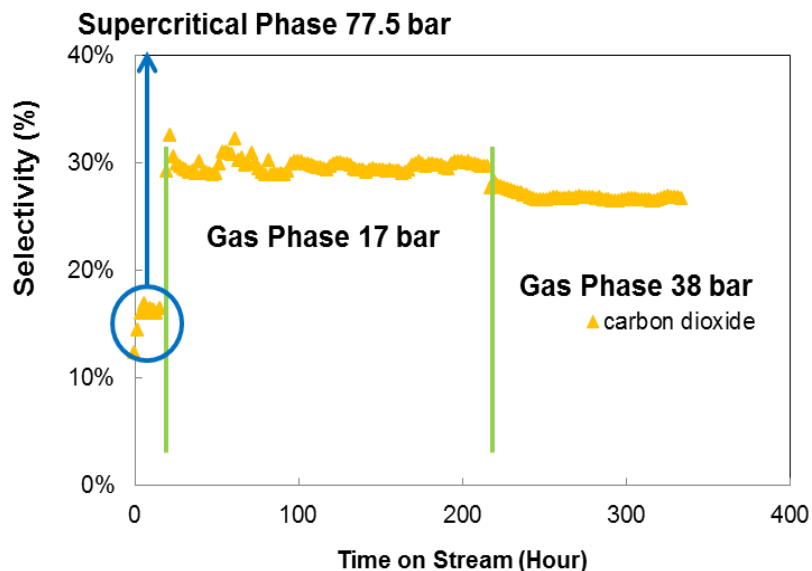
Figure 4.6 CO_2 selectivity for SC-FT and GP-FT

(For all tests: syngas flow rate was 50 SCCM with a ratio of H_2: CO: N_2 = 62: 36.5: 1.5, 1 gram of Fe/Zn/Cu/K catalyst in the 1st FT stage at 240ºC. For GP-FT: system pressure = 17 bar and 38 bar. For SC-FT, hexanes flow rate was 1.0 ml/min, system pressure = 77.5 bar.)

The CO conversion for the investigations of FTS plus oligomerization in this dual bed configuration under both gas phase and supercritical phase (GP-FTO and SC-FTO) conditions is shown in Figure 4.7 as a function of time on stream. In GP-FTO, a slight decrease in the CO conversion was observed as a function of time on stream, from an initial value of 40% to a value of c.a. 32% at the end of the experiment. In SC-FTO, the CO conversion was fairly stable at a level of c.a. 70% once steady state was achieved and the CO conversion level persisted over the 50 hour period of time. The CO conversion in the gas phase was distinguishably lower than that in the supercritical phase, which is consistent with the results that have been discussed previously. Again, it should be noted that the partial pressure of syngas, and as such the partial pressure of CO, was different in these two experiments. To be specific, the partial pressure of syngas was 35 bar in GP-FTO and 17.5 bar in SC-FTO, respectively.

135
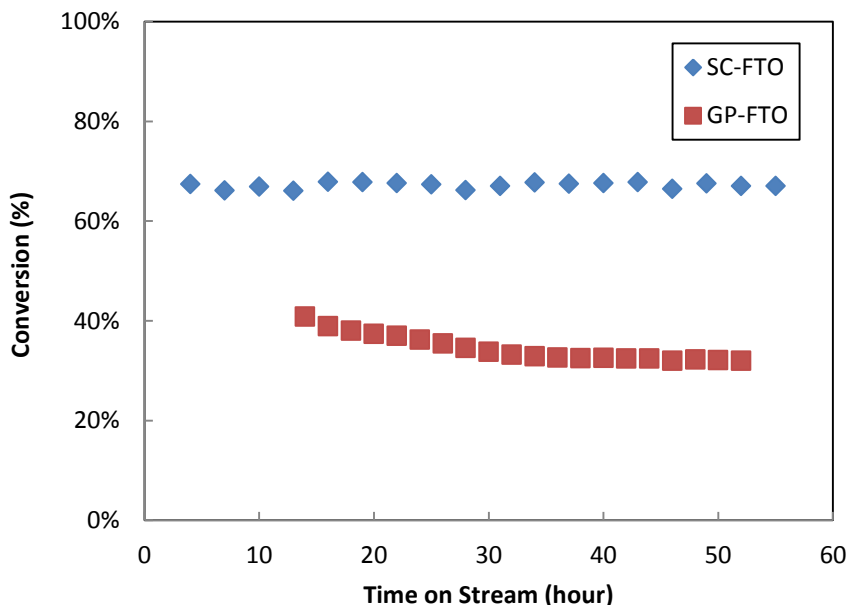
Figure 4.7   CO conversion as a function of time on stream for Fischer-Tropsch synthesis plus oligomerization under gas phase and supercritical phase (GP-FTO and SC-FTO) operation.

(For all tests: syngas flow rate was 50 SCCM with a ratio of H_2: CO: N_2 = 62: 36.5: 1.5, 1 gram of Fe/Zn/Cu/K catalyst in the 1st FT stage at 240ºC, 1 gram of ASA catalyst in the oligomerization stage at 200 ºC. For GP-FTO: system pressure = 35 bar. For SC-FTO, hexanes flow rate was 1.0 ml/min, system pressure = 76 bar.)

In the SC-FTO operations, the CH_4 and CO_2 selectivity were 1.6% and ca. 13%, respectively, as shown in Figure 4.8. These values are lower than those obtained from the gas phase operation, where the CH_4 selectivity was 3% and the CO_2 selectivity was ca. 25%. This result is again consistent with previously reported observations that the better heat management provided by the supercritical solvent can significantly suppress the methane and carbon dioxide selectivity in highly exothermic reactions.
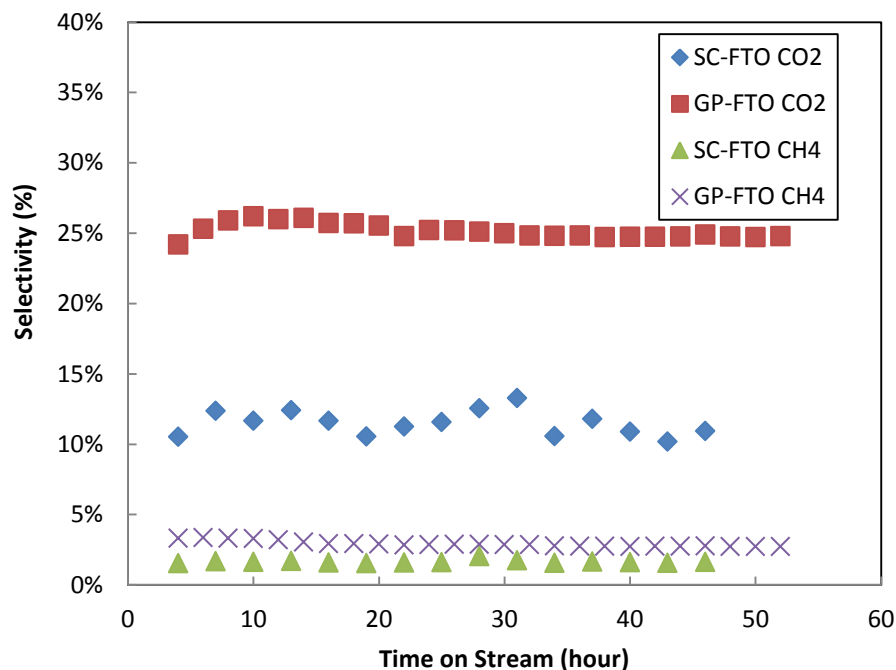
Figure 4.8 CO_2 and CH_4 selectivity as a function of time on stream for Fischer-Tropsch synthesis plus oligomerization under gas phase and supercritical phase (GP-FTO and SC-FTO) operation.

(For all tests: syngas flow rate was 50 SCCM with a ratio of H_2: CO: N_2 = 62: 36.5: 1.5, 1 gram of Fe/Zn/Cu/K catalyst in the 1st FT stage at 240ºC, 1 gram of ASA catalyst in the oligomerization stage at 200 ºC. For GP-FTO: system pressure = 35 bar. For SC-FTO, hexanes flow rate was 1.0 ml/min, system pressure = 76 bar.)

From the GP-FTC, GP-FTO, SC-FTC and SC-FTO experiment, the CO conversion and selectivity towards CH_4 and CO_2 are comparable with the results reported in chapter 3 (as shown in Figure 3.3 and Figure 3.4). The values of the CO conversion are approximately at the same level in all of the supercritical operations. In addition, the values of the CO conversion are nearly at the same level for all of the gas phase operations as well. This general trend is also true for the selectivities toward CH_4 and CO_2. However, this does not necessarily mean that the oligomerization reaction or the hydrocracking/isomerization reaction does not impact the generation/consumption of CO or CH_4 or CO_2. More likely, the CO, CH_4 and CO_2 participate actively in the upgrading reactions, but there is a balance of their consumption and production

rate so that in the observation of the outlet gas, the CO conversion and selectivities towards CH_4 and CO_2 remain at comparable level to those observed in the FTS only processes. Further investigations should be performed to study this issue in more detail.

The liquid products obtained from the FTC and FTO experiments were also analyzed in detail in terms of their chemical composition. The liquid products that were obtained from GP-FTC exhibited negligible (lower than 3%) olefin and oxygenate content compared to the amount of paraffins that were produced. Figure 4.9 shows the weight percentage of normal paraffin and branched paraffin on a basis of total paraffin production. The selectivity towards branched paraffin is significant in GP-FTC when compared to GP-FTS, as shown in Figure 3.6. The selectivity towards $C_8 - C_{22}$ branched paraffins is 35% in GP-FTC. As such, this GP-FTC offers a promising pathway for the production of branched-paraffin rich fuels. This result demonstrates that the hydrocracking/isomerization stage functionally enhances the branching of the FTS products that originate from the first stage. In addition, the normal paraffin content from GP-FTC is significantly larger than that obtained in GP-FTS. This increase in normal paraffin content results from the fact that hydrogenation of the FTS olefinic products occurs to a significant extent in the downstream hydrocracking stage. The selectivity towards C_{20+} hydrocarbons in GP-FTC is quite low compared to GP-FT, which is demonstrated in the ASF plot provided in Figure 4.10. The discontinuity of the ln(Wn/n)- n (carbon number) curve for the C_{25+} hydrocarbons suggests that the chain growth factor above C_{25+} is negligible or even negative. This difference in the chain growth probability at high carbon number, compared to the more typical chain grown probability for the lower carbon number products, results from the implementation of the hydrocracking reactions that preferentially convert longer chain hydrocarbons (heavy wax) into shorter chain species, as discussed in chapter 3. It is well known that the activity towards

catalytic cracking of longer chain hydrocarbon species is higher than each successively smaller

hydrocarbon molecule (Calemma *et al*. 2010).
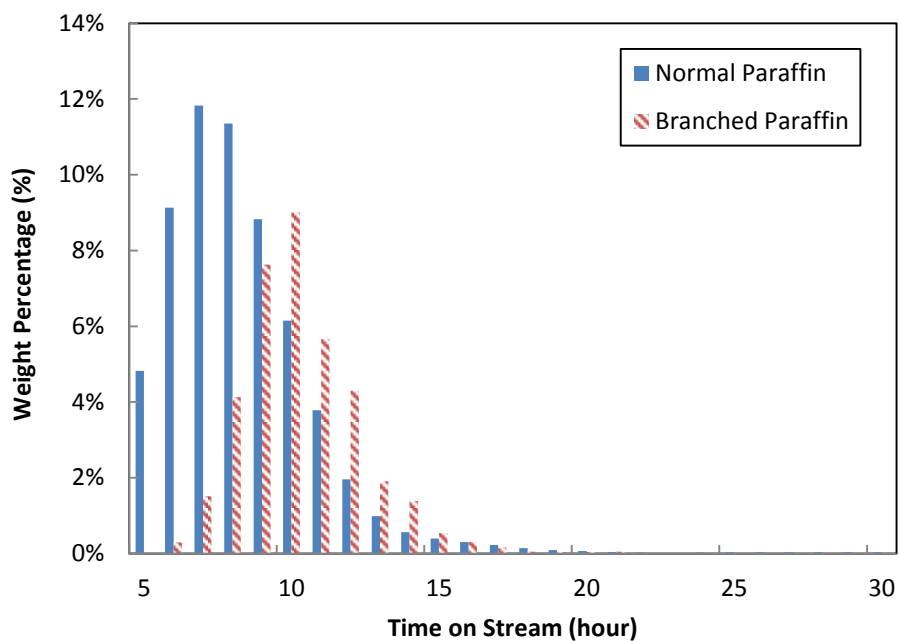
Figure 4.9 Paraffin distribution from gas phase FTS plus hydrocracking/isomerization (GP-FTC). Syngas flow rate was 50 SCCM with a ratio of H_2: CO: N_2 = 62: 36.5: 1.5, 1 gram of Fe/Zn/Cu/K catalyst in the 1st FT stage at 240ºC, 1 gram of 1.0 wt. % Pd/ASA catalyst in the 2nd hydrocracking/isomerization stage at 330 ºC, system pressure = 35 bar.)
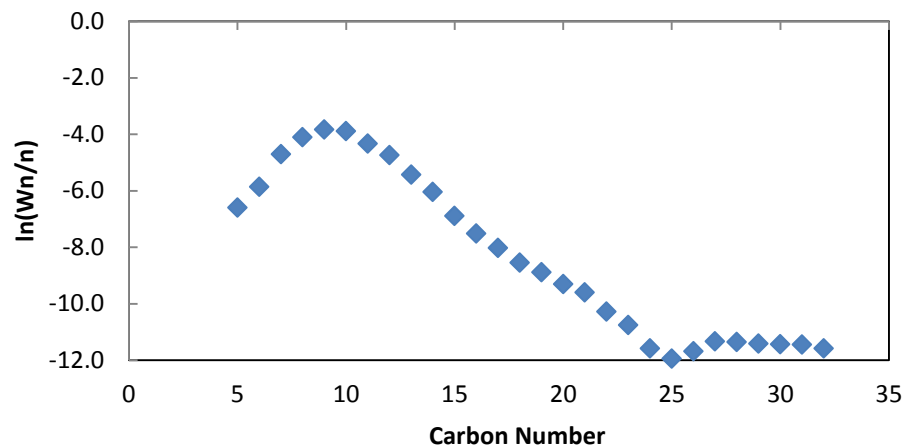
Figure 4.10   ASF plot of the liquid products obtained from gas phase FTS plus hydrocracking/ isomerization (GP-FTC). Syngas flow rate was 50 SCCM with a ratio of H_2: CO: N_2 = 62: 36.5: 1.5, 1 gram of Fe/Zn/Cu/K catalyst in the 1st FT stage at 240ºC, 1 gram of 1.0 wt. % Pd/ASA catalyst in the 2nd hydrocracking/isomerization stage at 330 ºC, system pressure = 35 bar.

Normal paraffins are the predominant species in the liquid product obtained from SC-FTC, as shown in Figure 4.11. Very low percentages of branched paraffins and cyclo-paraffins were obtained from SC-FTC. The olefin and oxygenate contents were also quite negligible. This result demonstrates that the hydrocracking/isomerization stage provided an aggressive level of hydrogenation activity under supercritical phase conditions. Previous investigations of SC-FTS in our laboratory demonstrated that significant amounts of aldehyde products were generated over a broad range of carbon numbers (as discussed in chapter 3). However, negligible amounts of the aldehyde species were detected in SC-FTC, illustrated that the aldehydes produced in the first SC-FTS stage are readily converted to other chemical constituents in the subsequent hydrocracking/isomerization bed under these supercritical fluids conditions. The likely pathway is that the aldehyde product generated in SC-FTS is initially converted into an olefin, which is a thermodynamically favored conversion (Durham *et al*. 2010), which is then readily hydrogenated

into paraffinic products in the hydrocracking/isomerization stage. This result indicates that the hydrogenation capability of the hydrocracking/isomerization stage using this 1.0 wt. % Pd/ASA catalyst is greatly enhanced under supercritical phase conditions. Furthermore, the selectivity towards C_{13+} range paraffins is elevated. This stems from the heavy wax species (that are generated in the upstream SC-FTS stage) being cracked into middle distillate compounds in the hydrocracking/isomerization bed. This results in an intensified product slate of hydrocarbons in the fuel range. It is also noted that the weight percentage of paraffins in Figure 4.11 exhibits a local maxima between C_{14} and C_{18}, illustrating that products larger than these carbon numbers can be cracked (shortened) into this range, while the products within this carbon number range are less readily converted into even smaller species. As such, a maximum in the product distribution is generated within the fuel range in SC-FTC. Bearing in mind that the product distribution for SC-FTS was shifted towards heavier hydrocarbons compared to GP-FTS, it would expected that the SC-FTC selectivity towards C_{20+} products would be distinguishably higher than that in GP-FTC. Indeed, the product distribution for SC-FTC is heavier than GP-FTC, and the additional cracking in the second stage appears to be less impactful under the supercritical conditions when comparing the change in the product distributions for SC-FTS versus SC-FTC and GP-FTS versus GP-FTC. As such, further improvements in the effectiveness of the cracking stage under supercritical fluid conditions are needed. This could be achieved by modification of the catalyst, addition of more catalyst, or an adjustment in operating conditions as discussed in the future work section of this dissertation.
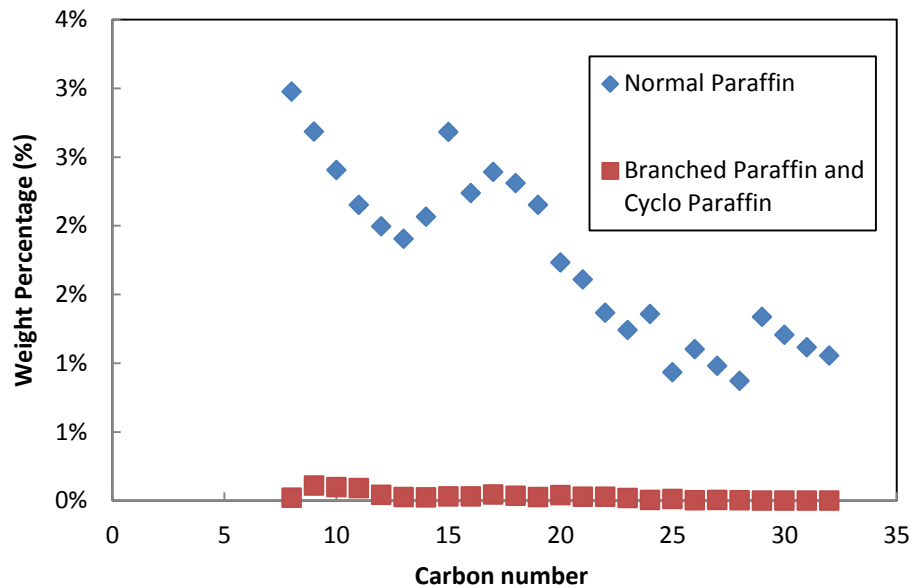
Figure 4.11 Paraffin distribution from supercritical phase FTS plus hydrocracking/isomerization (SC-FTC). Syngas flow rate was 50 SCCM with a ratio of H_2: CO: N_2 = 62: 36.5: 1.5, 1 gram of Fe/Zn/Cu/K catalyst in the 1st FT stage at 240ºC, 1 gram of 1.0 wt. % Pd/ASA catalyst in the 2nd hydrocracking/isomerization stage at 330 ºC, hexanes flow rate was 1.0 ml/min, system pressure = 76 bar.

Characterization studies have been performed on the catalysts that were used in these FTC and FTO systems including measurement of the BET surface area before and after reaction, as well as their analysis using scanning electronic microscopy (SEM). The surface area (BET) test was performed by Micromeritics Inc and these results are listed in Table 4.1. The following nomenclature has been used to identify the different catalysts that were analyzed both before and after the experimentation. The iron-based FTS catalyst that was analyzed before use in the reactor is labeled as FeB. The iron-based FTS catalyst that was analyzed after use in the GP-FTS is labeled FeAG, while the iron based FTS catalyst that was analyzed after use in the SC-FTS is labeled Fe-AS. The ASA oligomerization catalyst that was analyzed before use in the reactor is labeled as ASAB. The ASA catalyst that was analyzed after use in the GP-FTO operation is

labeled as ASAG, while the ASA catalyst that was analyzed after use in the SC-FTO experiment is designated as ASAS. The Pd/ASA hydrocracking/isomerization catalyst that was analyzed before use in the reactor is named PdB. The Pd/ASA hydrocracking/isomerization catalysts that were analyzed after use in GP-FTC and SC-FTC are labeled as PdAG and PdAS, respectively.

Table 4.1   BET results of unused and used catalysts employed in FTC and FTO experiments

	FeB	FeAG	FeAS	ASB	ASAG	ASAS	PdB	PdAG	PdAS
Surface Area	33.460	8.03	0.46	466.67	245.78	170.84	411.87	131.40	28.75

The surface area of each of the catalysts (Fe-based FTS catalyst, ASA oligomerization catalyst, and the Pd/ASA hydrocracking/isomerization catalyst) has been significantly reduced after the gas phase reactions. Interestingly, the surface area of each of these catalysts is even smaller after the supercritical operation compared to those from the gas phase operations. At first blush, this seems contradict to what has been previously suggested that the use of the supercritical solvent in the FTS reactions can act to maintain the catalyst performance by preventing accumulation of products on the surface of the catalyst and by improving the heat management in the catalyst bed (thereby reducing the formation of catalytic hot spots and undesired side products such as coke). However, the CO conversion results indicate that the activity under the supercritical conditions was indeed much higher than that under gas phase conditions, illustrating that despite the results in Table 4.1 the active site accessibility was not diminished by the presence of the supercritical fluid solvent or the products formed therein. It is also noted that the product distribution from the supercritical experiments were significantly higher in molecular weight than that obtained from gas phase operation. This combined with the higher CO conversion in the supercritical phase illustrates that the supercritical environment is

effective in providing effective transport of the heavy products from the catalyst pore in the supercritical phase in-situ. It is very important to note that the catalysts that were analyzed after reaction were collected from the reactor and analyzed ex-situ and do not necessarily depict the nature of the catalyst during use. In fact, the manner in which the catalysts were collected from the reactor during the shutdown of each experiment may have played a very significant role in impacting the final state of the catalyst, and as such, the pore volume and surface area as described in the following text. One likely scenario is that when an experiment was being shut down in order to collect the catalyst, the flow of syngas was exchanged for inert helium gas with the same flow rate in order to terminate the reactions. However, this inert gas significantly changes the solvating power of the reaction medium (in both gas phase and supercritical phase) where the solubility of heavy products would be expected to be diminished considerably and their removal from the catalyst bed would be instantaneously lower than during the actual reaction period. Since the supercritical FTS process produces a heavier product slate, these very heavy molecules would be even more effectively precipitate onto the surface of the catalyst within the reactor catalyst bed upon introduction of the helium. This could result in the instantaneous buildup of product on the catalyst surface such that the surface area and pore volume would be decreased (i.e. covered active sites and blocked catalyst pores). To further examine this possibility, additional experiments should be performed where the produced hydrocarbons are flushed from the catalyst bed prior to collection of the catalyst. The could be done where the introduction of helium is not performed prior to collection of the catalyst from the reactor, and the catalyst is only collected after a long period of solvent washing with pure hexanes. In short, it is important to point out that while the data in Table 4.1 represents the analysis of the catalysts after the reaction (and after the shutdown process was employed), it does

not represent the state of the catalyst in situ. One telling feature of the data in Table 4.1 is that each of the three catalyst systems shown the same trend when collected in this same fashion after the shutdown process with helium, further indicating that caution should be taken in drawing conclusion from these catalysts post reaction analysis.

Figures 4.12, 4.13 and 4.14 present the SEM images of the FTS catalysts before and after the reactions in both gas phase and supercritical phase operation (please note that these catalysts were collected post reaction in the same manner as described above). The iron-based FTS catalyst has a chip-like porous appearance before the reaction. The iron-based catalysts exhibit a more consolidated appearance upon their collection after the gas phase reaction. This may indicate that under the gas phase conditions, the catalyst can be sintered by the local overheating (from insufficient heat removal). It is also noted that Energy Dispersive Spectroscopy (EDS) analysis was performed during the SEM testing (spectra not shown) where significant amounts of surface carbon was detected on the used catalyst, while no surface carbon was detected on the unused catalyst. The iron-based catalyst obtained after supercritical phase operation exhibited the appearance of a loose powder, as opposed to the more consolidated nature of the catalyst obtained after gas phase operation. Again, EDS analysis revealed that significant surfaced carbon was present in the used catalyst after supercritical operation. Unfortunately, it cannot be determined from this set of experiments if the surface carbon derives from residual hydrocarbon products on the catalyst surface or from iron carbide which is widely believed to be the active form of the iron catalyst for FTS that is generated from in-situ reduction processes.
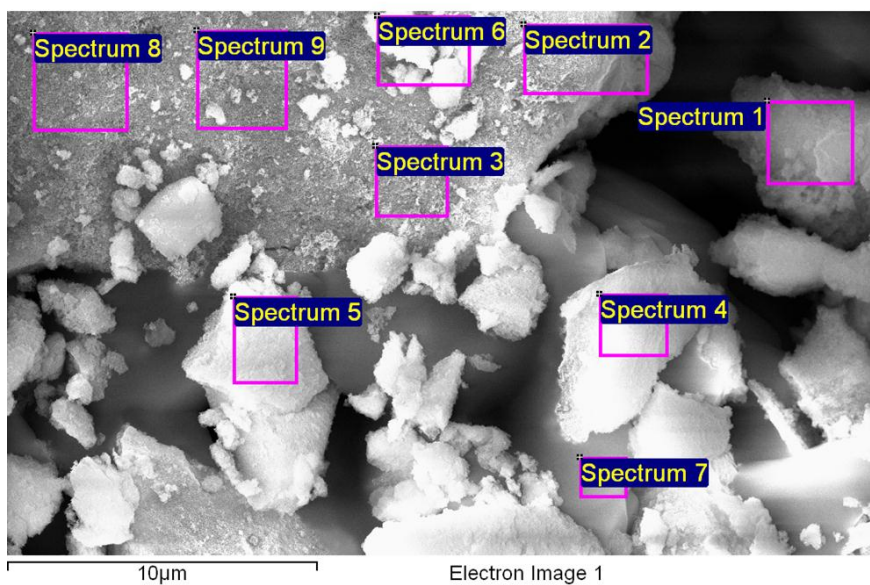
Figure 4.12   SEM of Iron-based FTS catalyst before reaction
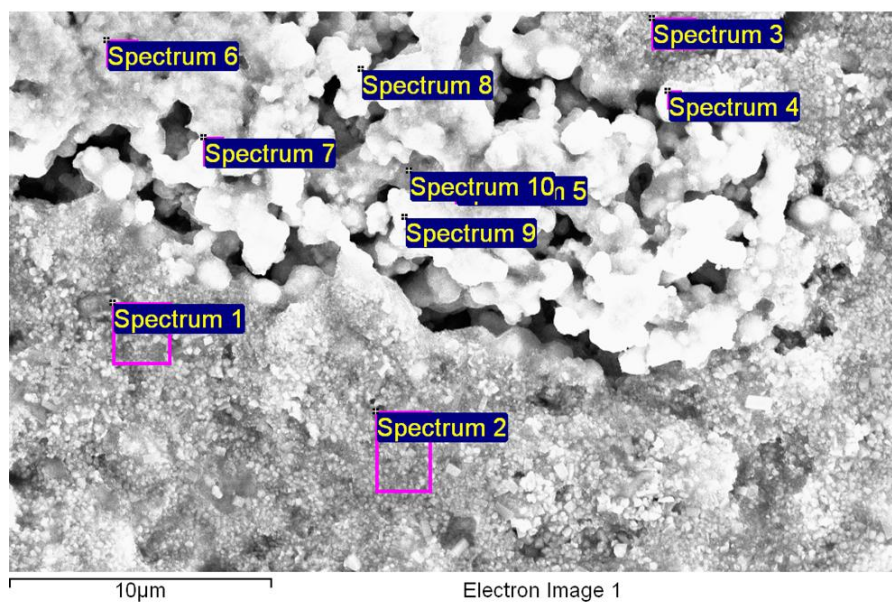
Figure 4.13   SEM image of Iron-based FTS catalyst after collection from the reactor after gas phase operation

146
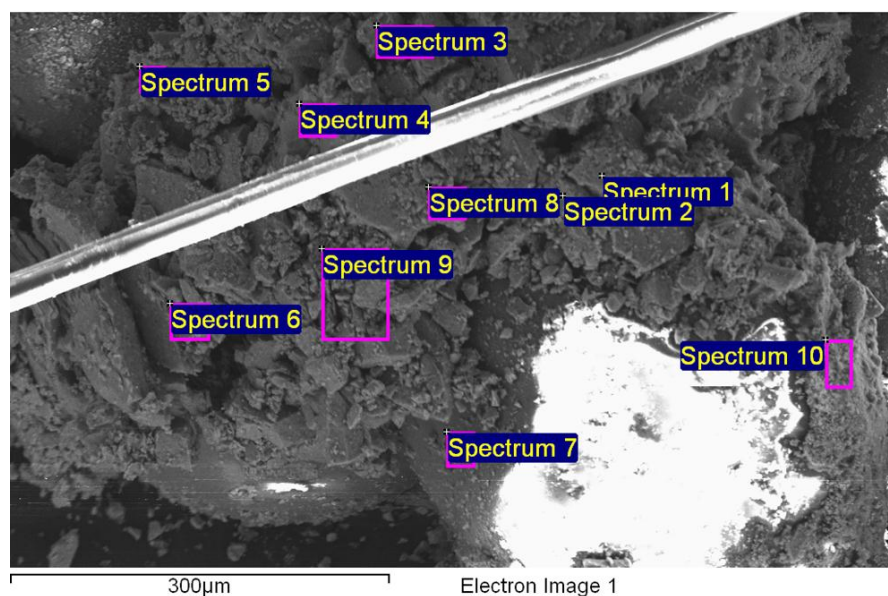
Figure 4.14 SEM image of Iron-based FTS catalyst after collection from the reactor after supercritical phase operation

4.4 Conclusions

This study demonstrates that Fischer-Tropsch synthesis with subsequent oligomerization (FTO) and Fischer-Tropsch synthesis with hydrocracking/isomerization stages (FTC) can be effectively performed using a dual-bed catalytic reactor system, separately. Using 1g iron-based FTS catalyst in the first FTS stage, 1g ASA catalyst in the second oligomerization stage, significantly improved CO conversion has been observed in supercritical phase FTO (SC-FTO) compared to the CO conversion that was obtained from gas phase FTO (GP-FTO). Similarly, using 1g iron-based FTS catalyst in the first FTS stage, 1g of 1.0 wt.% Pd/ASA catalyst in the hydrocracking/isomerization stage, greatly enhanced CO conversion has been shown to occur in supercritical phase (SC-FTC) compared to the value of CO conversion that was obtained from the gas phase FTC operation (GP-FTC). Moreover, the selectivity toward CO_2 and CH_4 was

greatly reduced under supercritical phase conditions compared to gas phase operation which is consistent with previously documented observations for the use of a supercritical solvent in FTS. The liquid product distribution obtained from GP-FTC exhibited a substantial enhancement in the amount of branched hydrocarbon products generated as well as a markedly decreased heavy wax selectivity. This result indicates that the isomerization and cracking activity is significant in the hydrocracking/isomerization stage in GP-FTC. Analysis of the liquid products that were obtained from SC-FTC also reveals that a high degree of activity towards the hydrogenation reaction occurred in the hydrocracking/isomerization stage by the observation of high paraffin selectivity. SEM microscopy pictures indicated that under supercritical phase conditions, the used iron-based FTS catalysts exhibited a less consolidating appearance than those iron-based FTS catalysts collected after the gas phase operation, suggesting that under the gas phase conditions, the catalyst can be sintered by the local overheating from insufficient heat removal.

Chapter 5 Evaluation of Critical Points and Phase Boundaries in Simulated Mixtures of Hexanes Solvent plus Fischer-Tropsch Reactants and Products

This chapter focuses on the collaborative efforts between Sihe Zhang and Rui Xu to examine the phase behavior of mixtures relevant to supercritical Fischer Tropsch Synthesis and mixed alcohol synthesis from syngas. The author expresses her sincere gratitude to Rui Xu for his fruitful collaboration in every aspect of this work and this chapter presents the collective results of this entirely shared effort.

5.1 Introduction

A considerable amount of research has been performed in order to enable the utilization of supercritical fluids (SCF) in a wide variety of applications, including: reactions (Elbashir 2010, Subramaniam 1986), extractions and separations (Chester 1998) and material processing (Kazarian 1999).

A supercritical fluid is defined as a substance (or mixture) that is heated above its critical temperature and compressed beyond its critical pressure (where it is a single phase in this supercritical region). For a pure substance, the supercritical region begins at the critical point, which lies at the terminus of the vapor-liquid equilibrium curve. Beyond this critical point is where the most dramatic changes in solvent properties can be achieved. In the supercritical regime, the thermo-physical properties are highly adjustable with simple changes in temperature and pressure and are intermediate between those of a liquid and a vapor, such as liquid-like densities and vapor-like transport properties. Several of the major advantages of using a SCF as a reaction medium include: (1) offering single phase operation, (2) high concentrations of reactants and products can be achieved due to high miscibility of gases in SCFs compared to liquid

solvents, (3) The ability of a SCF to dissolve non-volatile materials is similar as that of liquid solvents, (4) superior mass transfer and heat transfer properties can be obtained in SCFs compared to gas phase due to high diffusivity and low viscosity, (5) large variations in density (and density dependent properties) in the near-critical range can be imparted by modest temperature and/or pressure changes, thereby enabling the feasibility of tuning the reaction environment and enabling easy separation of dissolved chemicals from the SCFs, (6) in situ extraction of non-volatile materials and low-volatility products from catalyst pores as a result of the low surface tensions of SCFs (Abbaslou *et al*. 2009, Lang, *et al*. 1995, Subramaniam 2001, Frew *et al*. 1988, Baiker 1999). These unique and highly tunable properties make supercritical solvent media ideal for certain heterogeneous catalytic reactions, such as Fischer Tropsch synthesis.

Fischer-Tropsch synthesis (FTS) is a typical heterogeneous reaction, involving CO, H_2, CO_2 and light hydrocarbons in the gas phase, with heavier hydrocarbon products in the liquid phase and catalysts in the solid phase. Traditional gas phase fixed-bed FTS reactors are susceptible to catalytic "hotspots" which result from excessive heat released by the FT reactions leading to local overheating of the catalyst and increased methane formation (Lang *et al*. 1995, Steynberg & Dry 2004, Elbashir *et al*. 2010). Blockage of the catalyst surface and pores by heavy product and carbon condensation is another issue for fixed bed FTS. In combination, these two issues result in low conversion and catalyst deactivation.

The concept of utilizing supercritical fluids as reaction media in FTS was initially proposed by Kaoru Fujimoto in the late 80's and has since drawn researchers' attention due to the benefits it can bring. One benefit is that supercritical solvents can enhance the mass transport in the FTS reaction mixture, for both the gaseous reactants and the liquid products. Enhanced

wax selectivity and olefin selectivity were observed in supercritical phase (SC) FTS compared to gas phase (GP) FTS. Another benefit is that supercritical solvents can assist in the maintenance of thermal uniformity within the reactor to prevent catalytic hot spots and smaller scale temperature variations. This will allow for using larger diameter reactor tubes and simpler heat-exchange designs. A third benefit is that supercritical solvents can help maintain catalyst performance and yield less CH_4 and CO_2 during the reaction due to better heat management compared to gas phase operations. In addition, increased aldehyde selectivity at higher carbon number has been reported, as well as higher diesel/wax selectivity.

Researchers have performed many studies using different SCF media for FTS and related catalytic reactions: propane (Abbaslou *et al*. 2001, Bukur *et al*. 1997, Yan *et al*. 1998), pentane (Fan & Fujimoto 1999, Yan *et al*. 1998, Tsubake *et al.* 2002, Jacobs, *et al.* 2003, Linghu *et al.* 2004, Huang *et al*. 2004, Shi, *et al.* 2005, Irankhah & Haghtalab 2008), hexane (Yokota & Fujimoto 1989, Fan & Fujimoto 1999, Linghu *et al*. 2004, Huang *et al*. 2004, Yokota & Fujimoto 1991, Huang & Roberts 2004, Elbashir & Roberts 2005, Elbashir *et al*. 2005, Bukur 2006), heptanes (Linghu *et al*. 2004, Irankhah, A. Haghtalab 2008), octane (Liu *et al.* 2006, Tang *et al.* 2008), decane (Linghu *et al*. 2004, Liu *et al*. 2006), dodecane (Liu *et al*. 2006), hexadecane (Yokota & Fujimoto 1989, 1991, Yokota *et al*. 1991, Liu *et al*. 2006). Hydrocarbons with carbon number of 5 and 6 are widely considered to be the most viable compounds to be used as solvents in the supercritical Fischer-Tropsch synthesis (SC-FTS) process when considering their consistency with the criteria proposed by Fujimoto (Yokata & Fujimoto 1989) for selection of an appropriate solvent. These criteria are as follows: 1) The critical point (temperature and pressure) of the supercritical reaction media should be slightly lower than the operation temperature and pressure (especially when aiming for single phase operation). 2) The

151

supercritical reaction media should be stable under the reaction conditions and should be inert in the reaction and to the catalysts. 3) The supercritical reaction media should exhibit high solubility for hydrocarbons, which will enhance the extraction of products (e.g. wax) from the surface of the catalysts and also enhance the readsorption of reaction intermediates.

In the sub-critical and supercritical region, a small change in temperature or pressure of the fluid can result in significant property changes. The operation of fixed-bed catalytic reactors for these highly exothermic reactions (i.e. with controlled temperature rise) requires that the bulk reaction mixture (reactants, products and media) can be flexibly controlled with respect to the phase behavior. Roberts' group reported that the phase behavior of the SC-FTS reaction mixture (composed of reactants and SCF media) is quite different from the pure SCF media, and the critical temperature and pressure are both higher in the reactor effluent than those of the neat media (Elbashir & Roberts 2005). However, only a few studies have dealt with the phase behavior of the supercritical phase FTS reaction mixture (Joyce *et al*. 1999, Joyce *et al*. 2000, Gao *et al*. 2001, Polishuk *et al*. 2004, Elbashir & Roberts 2005, Mogalicherla & Elbashir 2011). Thus, knowledge of the critical point of the reaction mixture (or the location of the phase boundary beyond which a single phase exists) will allow for the determination of the necessary operation parameters (such as temperature or pressure) in order to achieve single phase FTS operation, and thus the appropriate design of the reactor.

Table 5.1 shows the critical data for mixtures of hexane and synthesis gas (at different mixing ratios) that were previously obtained by Roberts' group using a high-pressure, variable-volume view cell system (VVVC), as performed by Nimir Elbashir and Deborah Bacik (Bacik 2011, Elbashir 2005). This preliminary phase behavior investigation involved the mixing of only hexane and synthesis gas (syngas) at three different molar ratios, namely 3:1, 4.3:1 and 6:1.

Table 5.1 Critical data for mixtures of synthesis gas and hexane obtained in a variable volume view cell system (Bacik 2011)

Ratio (H$_2$: CO: hexane)	Mole Fraction Of Syngas	Measured Critical Point	
		T$_c$ (ºC)	P$_c$ (bar)
Mixture 1 (2:1:9)	0.25	225.9	86.5
Mixture 2 (2:1:13)	0.19	229.0	72.8
Mixture 3 (2:1:18)	0.14	231.3	63.4

However, in FTS, the mixture in the reactor is much more complicated than the simplified scenario of syngas plus hexane, especially when considering the presence of the products paraffins, olefins, oxygenates, CO$_2$ and water. The significant variation in the physicochemical properties of the chemical constituents involved (i.e. syngas, hexanes solvent, hydrocarbon products of varying molecular weight, oxygenate products of varying molecular weight, and water) significantly affects the critical properties and phase behavior of these reaction mixtures compared to their pure component properties. As such, this more complex thermodynamic mixture can also affect other reaction parameters including the transport properties, solubilities and kinetics. To make things more complicated, the composition of the reaction system changes throughout the course of the reaction (or down the length of the reactor in the case of a plug flow packed bed reactor) as the syngas is sequentially converted into the various reaction products. As such, a better understanding of the phase behavior of the syngas plus solvent (i.e. reactor inlet) and the syngas plus solvent plus products system (i.e. reactor outlet) is warranted. This underscores the need for reliable knowledge of phase boundary curves of the reaction mixtures,

and the measurement of mixture critical points where applicable. Reliable knowledge of the supercritical FTS reaction system is essential for rational supercritical phase FTS process design and optimization. Thus, to better evaluate the phase behavior of the reaction mixture in the reactor during operation, it is important to include more chemical components in the study of the phase behavior of the supercritical phase FTS mixture. To be specific, the products (hydrocarbons, oxygenated hydrocarbons, H_2O and CO_2) should be added into the studied mixture. To somewhat simplify this particular investigation, a representative hydrocarbon product of a fixed carbon number (normal C_{14} paraffin) and water, were added into the syngas + solvent mixture. The amount of each of these species that were added to the mixture was calculated based on the assumption of a 50% CO conversion where the only products were the C_{14} paraffin and water. It is noted that this is still a very simplified scenario. The polymerization nature of the FTS reaction is ignored in this case as well as the products of CO_2 as an additional reaction product. Nonetheless, investigation of the phase boundaries of this syngas + hexanes + C_{14} paraffin + water mixture will provide better insight into the thermodynamic properties of the supercritical FTS reaction system.

Table 5.2 presents the molar rations of the mixtures that have been examined in order to offer a better understanding of these simulated reaction mixtures.

Table 5.2   Simulated mixtures of synthesis gas, hexane and FT products

Mixture	Molar Ratio
H_2: CO: C_6	2 : 1 : 9
H_2: CO: C_6	2 : 1 : 13
H_2: CO: C_6	2 : 1 : 18
H_2: CO: C_6	2 : 1 : 27
H_2: CO: N_2: C_6 : C_{14}	2 : 1 : 0.126: 9 : 0.071*
H_2: CO: N_2: C_6 : C_{14}: H_2O	2 : 1 : 0.126: 9 : 0.071: 1*

*The amount of C_{14} and H_2O added was based on the assumption of a CO conversion of 50%. The amount of N_2 added corresponds to the concentration used in prior FTS experiments performed in the Roberts laboratory, where N_2 was used as an internal analytical standard.

5.2   Methods and Materials

5.2.1   Variable Volume View Cell System and Experimental Apparatus

To evaluate and examine the phase behavior of supercritical fluids and supercritical FTS reaction mixtures, an easy-to-control, high pressure variable volume view cell (VVVC) apparatus with live video monitoring has been designed and assembled in the Roberts' laboratory to allow for the analysis of phase boundaries and critical points in situ [Bacik 2011, Elbashir 2005]. The annular space (sample chamber) within a stainless steel cylindrical view cell is

equipped with a quartz window that allows for observation of the phase state of various fluid mixtures of interest to supercritical FTS, including real time observation of phase changes within the system. This is achieved by the use of a new, highly advanced, auto-focusing, auto-light-compensating monitoring system. A stainless steel piston with four surface sealing O-ring grooves is placed within the stainless steel cylinder to separate the material being studied from a hydraulic pressurizing liquid in the pressure generator system (as shown in Figure 5.1). The temperature of the sample is monitored using a resistive temperature device (RTD) that is implanted in the front sample chamber of the cylinder. A metal membrane pressure transducer is placed next to the thermal probe to detect real-time system pressure. A pressure generator system (i.e. pressure controlled hydraulic fluid in a movable piston system) is connected to the back of the view cell, which provides precise control over, and incremental changes to, the sample side pressure (via piston movement) when approaching phases change boundaries of interest.
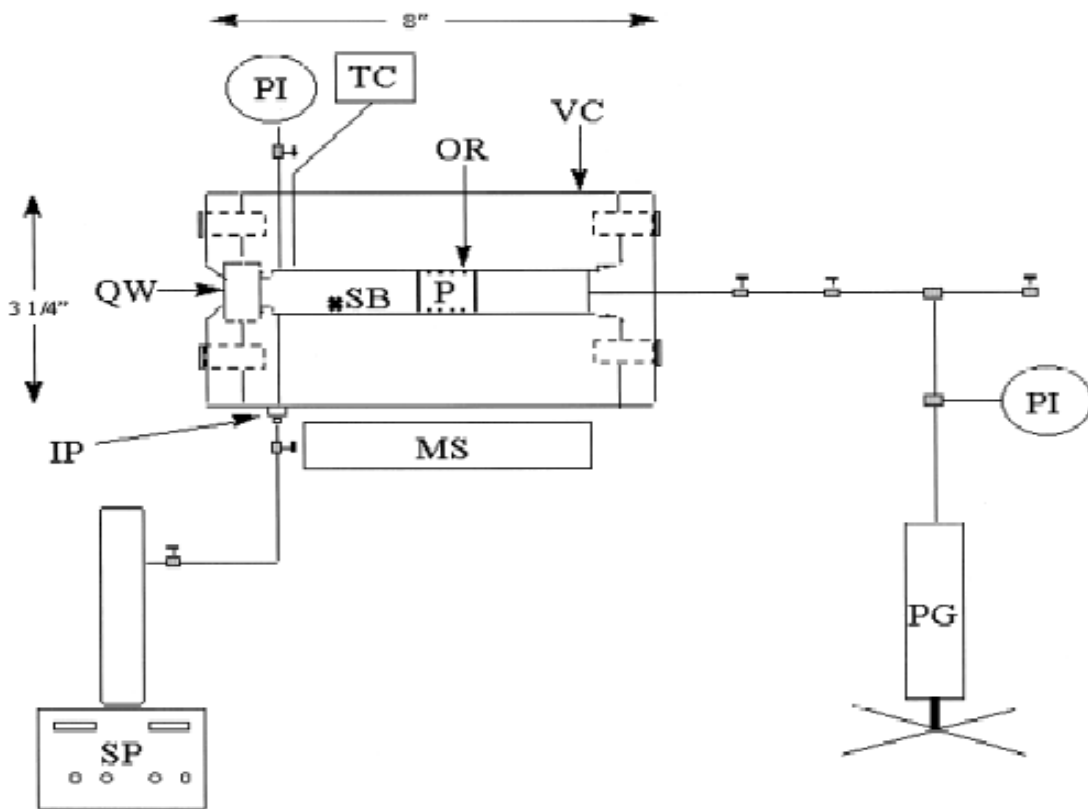
Figure 5.1 High pressure variable volume view cell phase behavior experimental apparatus

(IP, injection port; MS, magnetic stirrer; OR, O-ring; P, piston; PG, pressure generator; PI, pressure indicator; QW, quartz window; SB, stir bar; MP, metering pump; RTD, resistive temperature detector; VC, view cell; PC, personal computer; VCa, video camera) [Bacik 2011, Elbashir 2005]

5.2.2   Modification of Variable Volume View Cell System

When starting to collect data on the phase equilibrium of the reactant mixture (simulated with syngas and supercritical solvent only), we discovered some system design defects which affected the consistency of the phase behavior experiments under high temperature and pressure operation. One of these defects involved the fact that the movable piston met great resistance when being inserted into the core of the view cell cylinder. The other design issue involved an inability to maintain the desired location of an O-ring that is placed between the quartz window

and the front surface of the view cell cylinder. Accordingly, we engineered new features into this view cell system to eliminate these system design drawbacks. In figure 5.2, the rectangles highlight the locations of the modifications that were performed. One was made at the rear of the cylinder which was machined to provide a "V" shaped opening with an angle of c.a. 5 degrees. This modification allowed the insertion of the piston with high durometer O-rings into the cylinder more easily while also eliminating the abrasion that occurred between the edge of inside wall of the cylinder and the O-rings on the inserted piston. Another modification to the vessel involved machining an angled groove between the window and the cylinder into a concave seat.

The chamber is sealed from the front (lid) side by tightening bolts that bring the lid into contact with the body of the chamber where a quartz window is held in place between the lid and the chamber body with an O-ring placed on both sides of the window. The vessel was machined to have an angled O-ring groove such that the O-ring that placed on the interior side of the window will be pulled into the machined groove (rather than slipping into the interior of the chamber's annual space) upon tightening of the lid bolts.
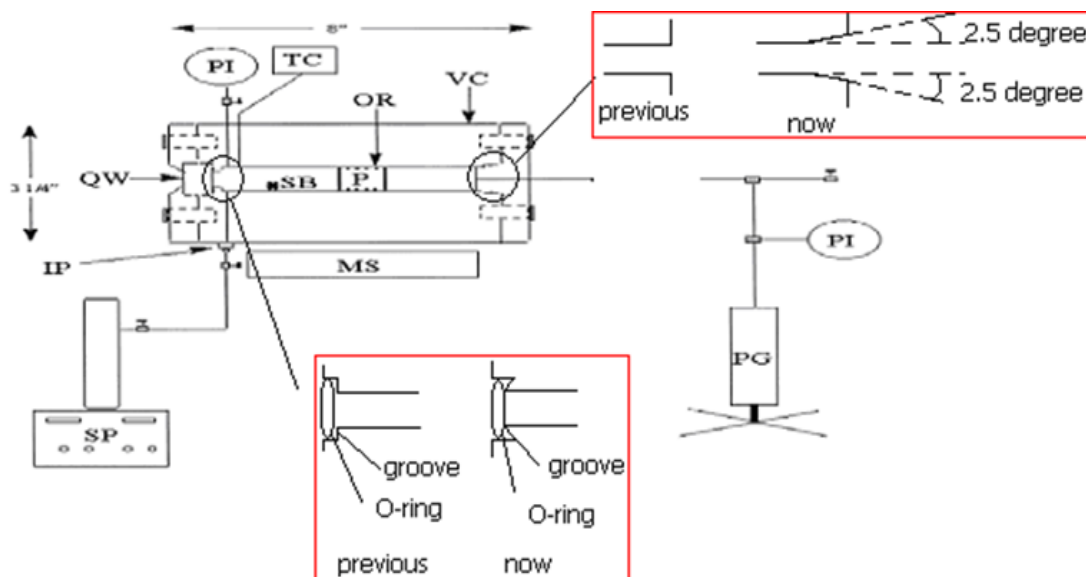
**Figure 5.2** Modifications of the high pressure phase behavior experimental apparatus (IP, injection port; MS, magnetic stirrer; OR, O-ring; P, piston; PG, pressure generator; PI, pressure indicator; QW, quartz window; SB, stir bar; MP, metering pump; RTD, resistive temperature detector; VC, view cell)

After having replicated the phase behavior measurements for hexane, pentane, and various syngas + hexane mixtures of different molar ratios, we continued to further examine the phase behavior of the syngas + hexane + products systems as listed in Table 5.2 above.

From time to time, we experienced sealing failure across the piston seals (O-rings) and it was found that the O-rings on the piston were degraded by the combination of heat, pressure, chemicals (CO and H_2), and abrasion. Several types of O-ring materials were examined, including Buna, Viton, FEP-Viton, Aflas, Kelraz, etc. as well as various combinations of the same. This dynamic seal is necessary in order to properly isolate the studied material mixtures from the hydraulic fluid used in increasing the chamber pressure in the back part of the view cell chamber. In addition, we found that several grooves engraved by the movement of the piston were created in the vessel walls after experiments. These grooves adversely affect the ability to create a dynamic seal between the separated chambers (divided by the movable piston). Upon

this observation, we had to re-polish the internal surface of the view cell to increase its smoothness and continuity. After carefully sanding and measuring (to keep the cross sections constantly round with the same diameter), the internal surface was regenerated free of any grooves, concavities or scratches thereby allowing better sealing during the back and forth movement of the piston during the phase behavior experiments. However, an inherent issue came about with this improvement of the internal cylinder surface, i.e. the internal diameter of this view cell was increased during this resurfacing process. As such, the original piston and O-rings could not provide an adequate seal with the cylinder surface due to creation of a gap between the outer diameter of the piston + O-ring and the internal surface of the view cell. In order to improve the accuracy of our results, we engineered several modifications to the design of the piston and remanufacture the piston with a larger radial diameter (keeping the same piston axial length), and widen the grooves on the piston as shown in figure 5.3. Thus, the "gap" was filled by enlarging the piston radially. In addition, we have used a thicker and wider O-ring with a size number 114, instead of the previous size 18 O-rings.

Figure 5.3   Piston with smaller radial diameter (left) and piston with larger diameter (right)

After several tests involving the phase behavior of mixtures of syngas + hexane + tetradecane, it was determined that additional leakage was observed either through the quartz window from the mixture side of the piston, or, leakage across the movable piston from the mixture side to the side containing the pressure-increasing-hydraulic fluid. To locate the exact

location of leakage, the whole view cell chamber was submerged in a water bath while pressurized to 2000 psig (much higher than the critical pressure for hexane and the mixture) with helium. It was determined that no gas leaked out of the view cell after a 4 hour observation period. This indicated that the leakage happened across the piston such that the solvent mixture escaped at high temperature and pressure from the studied mixture side to the hydraulic fluid side. In addition, to further confirm this hypothesis, we examined the hydraulic fluid on the back side of the view cell and analyzed its composition using gas chromatography. Hexane was detected in the gas chromatograph of the hydraulic fluid sample, confirming that significant leakage occurred across the piston. This, unfortunately, required further re-design of the VVVC system in order to obtain better phase behavior results. This time, rather than enlarge the radial diameter of the piston, we redesigned the piston with shallower grooves to ensure a better compression of the O-ring material to create an effective dynamic seal, as shown in figure 5.4. We were also concerned about truncation of the O-ring when placing the piston into the back side of the view cell. The previous design involving a sloped entrance, shown in figure 5.2, helped such that the O-rings on the piston were not severely damaged when inserted.
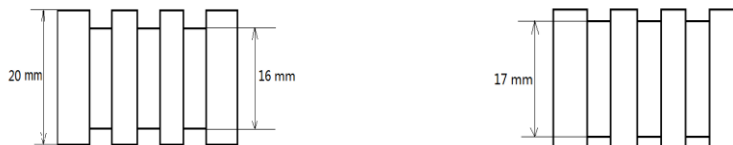
Figure 5.4   Piston with deeper grooves (left) and piston with shallower grooves (right)

However, when we started to investigate the phase behavior of mixture made of syngas, hexane, tetradecane and water, we still found sealing failure across piston seals and the O-rings (Kelraz, which is the most anti-degradation material with considerate durometer we found in all)

161

on piston had also been degraded by combination of heat, pressure, chemicals (CO and water), and abrasion. To solve this problem, we decide to change the material of O-ring from Kelraz to PTFE, which is more chemical/heat/abrasion resistant but with higher durometer and low elasticity (very hard to be put into the grooves on the piston, and overly stiff which prevented the piston from fitting properly in the view cell.). Thus, to utilize this hard PTFE O-ring without stretching it too much (so that it will not shrink back to the original size), we had to redesign the piston. Figure 5.5 shows a new piston design that we have also employed in this study. There is a center piece of the piston which has two slopes at both ends of it. After putting this center body of piston into the annular cylinder of the VVVC, two PTFE O-rings are cautiously pushed into the cylinder from the front side and the back hydraulic fluid side. After placing the center piece of the piston into the annual space of the chamber, the two O-rings are placed against each end of center piece of the piston and then the two end pieced are threaded into the center piece of the piston from both ends. When tightening the end pieces of the piston onto the piston center piece using allen wrenches, the O-rings are pushed towards each other, sliding along the slopes of the piston center piece until they are put in contact with the inner wall of chamber cylinder in order to form a seal.
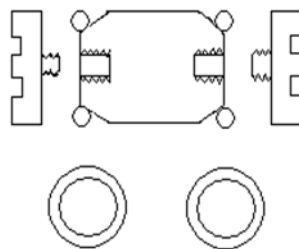
Figure 5.5   New piston design

These vessel modifications took a considerable amount of time.   Unfortunately, the net result is a piston system that did not work any better than the previously described piston system due to deformation of the PTFE O-rings when in use in this new geometry. Other types of O-ring materials should be examined with this piston design in future studies.

5.2.3   Procedures for measuring critical points and determination of phase boundary loci.

We periodically calibrated the pressure transducer (both in our lab and at the manufacture's facility), which ensured accuracy of the pressure measurements recorded. A carefully controlled phase behavior study was performed to determine the critical point of pure hexane (HPLC grade) in order to compare the performance of this new system to previous measurements in our lab and to verify these measurements against reference literature values. A typical experimental procedure for measuring the critical point of pure n-hexane (Alfa Aesar #L09938, CAS# 110-54-3) was as follows: Hexane was injected into the view cell and was heated uniformly from room temperature to 210°C at a rate of 5°C/min, and was then heated to 225°C at a rate of 2°C/min. During this heating process, the pressure of the system correspondingly increased and was monitored. The system was then held at 225°C for 10min and was then heated to 235°C at a rate of 1°C to allow temperature uniformity/equilibrium to be achieved while taking the system temperature (and corresponding pressure) above the critical point of the system up to 239°C at this rate of 1°C/min. While doing so, the phase behavior of the system (two phases below the critical point, and one phase above the critical point) was observed and recorded. After a single phase was reached, the system was maintain at the current temperature and pressure for further observation for another 10 min, and then the heating was stopped and pressure was dropped accordingly until the studied material reenters the two phase appearance. The heating was started again when the material vapor liquid equilibrium was

obtained again at about 5℃ below the temperature where the single phase was obtained. Then, as the temperature and pressure of the studied material was as high as the single phase was obtained again, the temperature and pressure was recorded. In addition, the temperature and pressure where the two phases appear when decrease the temperature and pressure from the supercritical phase was recorded as well.

To measure the phase behavior of mixtures of supercritical solvent and FTS syngas reactants, we examined the phase behavior of mixtures of n-hexane, carbon monoxide, and hydrogen using four different molar compositions that are relevant to our previous supercritical phase FTS investigations. The hydrogen and carbon monoxide were delivered in a 2:1 molar ratio, respectively. The H_2 : CO : Hexane ratios under investigation were: Mixture 1 (2:1:9), Mixture 2 (2:1:13), Mixture 3 (2:1:18), and Mixture 4 (2:1:27). The corresponding syngas to hexane ratios were (1:3), (1:4.33), (1:6) and (1:9), respectively.

To initiate the phase behavior investigations of the supercritical FTS reaction mixtures, we have measured the critical points for a simulated SCF-FTS mixture with syngas, hexane, tetradecane and water. Given the product distribution obtained in supercritical FTS (Huang et al. 2004), tetradecane was chosen as a representative (model) product compound to simulate the heavy FTS product. In addition, water was also added to the system in the second set of experiments, since it is a necessary byproduct generated by water-gas shift and hydrogenation in the FTS reactions. Assuming a syngas conversion of 50% in the reactor, the representative syngas + hexane + hydrocarbon product mixture was calculated to have a molar ratio of (2.02 H_2 : 1 CO : 0.126 N2 : 9 Hexane : 0.071 Tetradecane). In the case with addition of water as an oxygenate FTS product, syngas conversion is also 50% with the representative syngas + hexane + hydrocarbon product + water molar ratio of (2.02 H_2: 1 CO : 0.126 N_2 : 9 Hexane : 0.071

Tetradecane : 1 H$_2$O).

The composition of the tested syngas cylinder is CO 31.83%, H$_2$ 64.17%, N$_2$ 3.999%. The reason for using this particular composition is that it represents the syngas mixture that has previously been used in our laboratory for supercritical phase Fischer-Tropsch synthesis investigations. It should be noted that all of the following test results are to be considered preliminary (due to the leakage issues described above when adjusting the T or P in order to duplicate the critical point observations). All of these experiments were performed separately and repeated over five times for each of the mixtures to confirm the reproducibility.

5.3   Results and Discussion

For the evaluation the critical point of hexane, figure 5.6 presents a digital image that was captured of the hexane at a vapor-liquid equilibrium state below the critical point (note the distinct presence of a two phase meniscus at the center line of the vessel). Figure 5.7 presents an image that was collected as the hexane in the system approached its critical point (note the disappearance of the two phase meniscus and the critical opalescence phenomena). Figure 5.8 presents an image collected above the critical temperature of the hexane which indicates a homogeneous single phase system. In approaching the critical point, the contents of the vessel becomes cloudy and the interface between the two phases vanishes with increasing temperature and as the temperature is raised beyond the critical temperature, a clear, colorless single phase is observed for the supercritical state. Movies of these phenomena are available from the Roberts laboratory upon request. The critical point data (the temperature and pressure upon observation of the phase change) were measured several times using both increasing and decreasing temperature pathways and the resultant critical point measurement for pure hexane is Tc = 235.0°C and Pc = 30.88 bar, respectively using this system. This corresponds very well with

reported literature data (Smith and Van Ness: Tc = 234.5°C and Pc = 30.25 bar) where the critical temperature is within 0.2% and the critical pressure is within 2.1%. This data also corresponded well with previous measurements in our laboratory.

Figure 5.6   Subcritical phase of pure n-hexane

Figure 5.7   At critical point of pure n-hexane
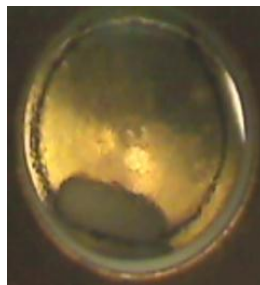
Figure 5.8   Supercritical phase of pure n-hexane

Table 5.3 and table 5.4 shows the critical point measurements of pure pentane and hexane.

Table 5.5 shows the critical point measurements of syngas and hexane mixtures with variation in the syngas/hexane molar ratio (1:3, 1:4.3, 1:6, 1:9, respectively). Table 5.6 shows the critical point measurements of the mixture of syngas + hexane + tetradecane. Table 5.7 shows the critical point measurements of the mixture of syngas + hexane + tetradecane + water.

Table 5.3   Critical point data for pentane

Pentane	Measured	Literature[*]	Error (%)
T_C (°C)	197	196.68 ± 0.5	0.16
P_C (bar)	35.39	33.6 ± 0.6	5.33

Table 5.4   Critical point data for hexane

Hexane	Measured	Literature[*]	Error (%)
T_C (°C)	235.0	234.5	0.2
P_C (bar)	30.88	30.25	2.1

Table 5.5   Critical point data for the hexane + syngas mixture

Ratio (H$_2$: CO: hexane)	Mole Fraction of Syngas	Previous Observation		Current Observation	
		T$_c$ (ºC)	P$_c$ (bar)	T$_c$ (ºC)	P$_c$ (bar)
Mixture 1 (2:1:9)	0.25	225.85	86.5	228.4	86.38
Mixture 2 (2:1:13)	0.19	229.0	72.8	231.5	74.58
Mixture 3 (2:1:18)	0.14	231.25	63.4	232.8	59.58
Mixture 4 (2:1:27)	0.10	-	-	237.5	41.32

Table 5.6   Experimental data obtained for phase behavior studies of simulated supercritical FTS mixtures (syngas conversion 50%)

Ratio (H$_2$: CO: N$_2$: C$_6$: C$_{14}$) = (2.02 :1 : 0.126: 9 : 0.071)	Observation	
	T$_c$ (ºC)	P$_c$ (bar)
Test 1	238.5	70.7
Test 2	241.0	72.5
Test 3	240.5	71.3

Table 5.7   Experimental data obtained for phase behavior studies of supercritical FTS mixtures with water (syngas conversion 50%)

Ratio (H_2: CO: N_2: C_6 : C_{14} : H_2O) = (2.02 :1 : 0.126: 9 : 0.071: 1)	Observation	
	T_c (°C)	P_c (bar)
Test 1	252.0	76.2
Test 2	253.4	77.0
Test 3	251.1	75.1

Figure 5.9 shows the experimental results of the detected temperature and pressure where the studied material (either the pure pentane, hexane or the FTS mixture) entered into a single phase status. With the enhancement of the syngas concentration in the syngas + hexane mixture, the pressure where the mixtures entered a single phase increase monotonically. The temperature where these syngas + hexane mixtures entered a single phase decrease slightly when the syngas to hexane ratio increased. When adding C_{14} into the syngas + hexane mixture, the temperature of the mixture where a single phase was obtained was higher than the temperature of the syngas + hexane mixture with the same syngas/hexane ratio (1: 3), while the pressure is lower. In addition, when introducing water into the syngas + hexane + tetradecane system, the single phase point locus was approached with higher temperature and higher pressure compared to the syngas + hexane + tetradecane mixture system.
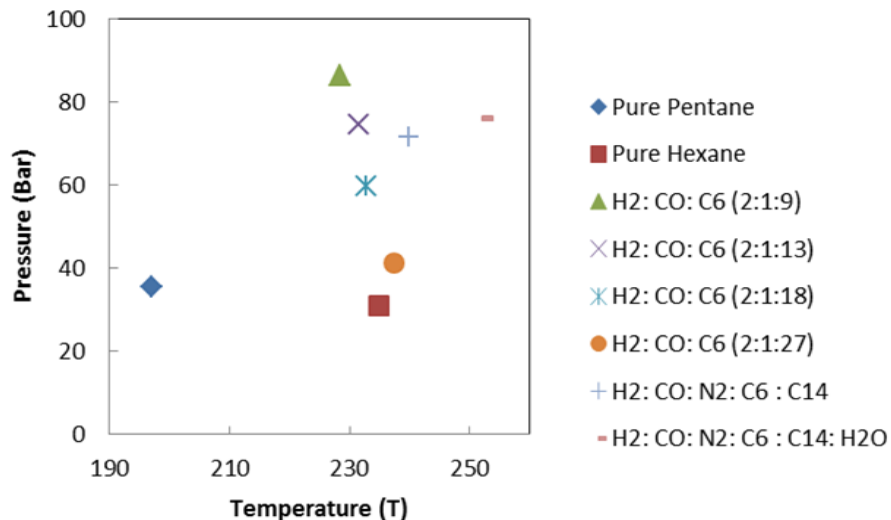
Figure 5.9 Critical point loci for pure pentane, pure hexane and model FTS mixture using VVVC system

5.4 Conclusions

A high pressure variable volume view cell system has been developed in order to investigate the phase behavior and to approach the critical points for model supercritical FTS reaction mixtures. Specifically, the critical point loci of the mixtures of syngas (CO and H_2 and inert internal standard N_2) + hexane (with different syngas/hexane ratios), syngas + hexane + tetradecane (which serves as a typical FTS paraffin product), and syngas + hexane + tetradecane + H_2O (which is an important FTS side product that can significantly affect the phase behavior of the SC-FTS reaction mixture) have been carefully measured in order to understand the effects of these FTS reaction and product species on the phase behavior of these highly nonideal mixtures.

From the experimental results of the phase behavior of the reaction feed mixture, we determined that the temperature where a single phase was obtained decreases as the mole fraction of syngas was increased. The pressure where a single phase was obtained for the

170

mixtures increases as the mole fraction of syngas is increased. In addition, FTS paraffin product and side product (water) distinguishably affected the operation temperature and pressure where a single phase can be approached.

Chapter 6   Recommendations

The work presented in this chapter explores additional avenues of investigation that could further advance the themes of this dissertation. These topical areas for future investigation involve: 1) Optimization of the operational parameters for this multi-bed reactor system in order to controllably produce a variety of desired products, 2) Investigation of the feasibility of using a cobalt-based FT catalyst in the first bed of this multi-bed reactor system, 3) Further modification of the catalysts employed in this system in order to optimize the FT fuel production, 4) Detailed evaluation of the fuel properties of the derived FT products.

6.1   Investigation of the Effect of Reaction Parameters on the Performance on the Multi-bed Reactor System

The choice of reaction parameters employed can significantly impact the catalytic reactions that occur in each of the reactor beds within the three bed reactor system. The reaction temperature, pressure, the amount of catalyst loading, the catalyst reduction procedure, etc. have been shown to profoundly influence the reaction and catalyst activity (Dry 2003, Dry 1999, Steynberg & Dry 2004, Schulz 1999, Botes 2008).

Operation temperature can significantly affect catalyst performance. In a certain temperature range, higher operation temperature can result in a higher catalytic kinetic coefficient, thus higher reaction activity. However, at too-high of a temperature, the catalyst particles can be fused together and the porous structure of the catalyst can be destroyed by the combination of high temperature and high pressure, which will inherently result in the loss of catalytic active sites, and thus catalyst deactivation (Morale 2003). As such, investigations to find an optimum operation temperature are necessary in order to provide a balance between the initial

catalyst activity and the catalyst activity maintenance. For FTS, there are two operation modes: high temperature FT (HTFT, 300 - 350 ºC) and low temperature FT (LTFT, 220 - 250 ºC). For LTFT, cobalt FT catalysts are normally operated in the range of 220 - 240 ºC. Previous investigations in our group that used iron LTFT catalysts have indicated that the operation temperature of 240 ºC is optimal, and as such, this temperature was used throughout this study. For the oligomerization and hydrocracking/isomerization stages, the operation temperatures used in this study, as discussed in chapter 2 and chapter 3, were determined based on literature information. However, considering the specific product distribution of the FTS products which is generated in the first FTS stage using the previously-mentioned iron-based FTS catalyst, the optimal operation temperatures for the oligomerization and hydrocracking/isomerization in the second and third catalytic reaction beds, respectively, should be examined in this three bed reactor system in the future work.

Operation pressure has been shown to affect the performance of the reactions in this three bed reactor system. Specifically, for oligomerization in the second reaction bed and hydrocracking/isomerization in the third reaction bed, the operation pressure can influence the activity of the catalyst employed. Thus, future work should involve investigation of the optimal operation pressure. It is noted that the design of this 3-bed reactor system requires that this multi-bed system is operated at a single pressure throughout, and as such, the determination of an "optimal" pressure will involve a trade-off in performance in each individual bed to yield an overall "optimal" system performance.

The effect of syngas flow rate should also be incorporated into the future work. The syngas flow rate can directly influence the CO conversion in the FTS step (since FTS is kinetically controlled). The composition of the outlet mixture from the first bed, which exits the FTS stage

and enters the consecutive product upgrading stages as the feed, is affected by the inlet syngas flow rate. As a result, the product upgrading reactions and the consequent product selectivity is impacted. In addition, in order to further study the feasibility of recycling a portion of the products (and unreacted syngas), a fundamental understanding of the effect that syngas flow rate has on the product distribution is important. Moreover, very low residence time can be accomplished by maintaining the syngas flow rate at a very high value. Under low residence time conditions, the products largely consist of the primary products, the analysis of which will be critical in determining the underpinning reaction mechanisms.

A great amount of work in the literature has been focused on examining the reduction steps of each of these catalysts prior to reaction. For iron-based FTS, the active sites consist of iron carbide, in which CO can be a good carbon source. Different reduction gases, such as pure H_2, pure CO, and mixtures of CO and H_2 have been investigated by several different researchers (Bukur et al. 1995, Bukur et al. 1996, Bukur et al. 1999, O'Brien et al. 1996). Bukur reported that using H_2 at 250 ℃, the reduced catalyst exhibited higher activity and lower selectivity towards long chain hydrocarbons when compared with reduction that using CO at 280 ℃ (Bukur et al. 1999). Davis reported that CO or CO rich syngas can lead to higher activity than using hydrogen rich syngas for the reduction (O'Brien et al. 1996). For the upgrading reactor beds, the reduction temperature and gas can possibly result in a significant difference in the catalysts' activity and selectivity as well. However, in this three bed reactor system, due to the consecutive nature of the reactor bed layout, the reduction gas is a mixture of the inlet reduction gas and the FTS reduction products when it enters the upgrading beds. In this case, the reduction of the upgrading catalyst can be consequently affected and can be different from the results obtained from the single bed reactor operations that are predominantly described in literature. Thus, the

174

investigation of the reduction process for each bed in this three bed reactor system is necessary in the future work.

Enhancement in heat transfer (which is helpful to prevent catalytic "hot spots" and thermal runaway) and mass transport (which is supportive to prevent diffusion resistance build-up) have been observed indirectly (from analysis of CO conversion and product distributions, etc.) in supercritical phase operation. Nonetheless, supplementary characterization of the catalysts should also be involved in the future work to confirm the benefits that have been derived from the use of the SC solvents. The scanning electron microscopy (SEM) analysis and the measurement of BET surface area and pore volume that were reported in Chapter 4 were only performed on the catalysts at two points in time: 1) before loading the catalysts into the reactor system and 2) after the complete "shut-down" of the reactor system was achieved. However, it can be more important to evaluate the catalyst at additional points in time, including: 1) after reduction, 2) during or right after the reaction, 3) after operation at each of the various pressure levels in both gas phase and supercritical phase. Further characterization of the catalysts would allow us to better understand and interpret the observed enhancement in catalyst activity. However, it is noted that removal of the catalyst from the reactor for further analysis can result in changes in the catalyst active sites and the catalyst being "re-oxygenated." As such, ex-situ analysis of the catalysts is fraught with challenges, while in-situ catalyst characterization can be equaly difficult (but not impossible) to achieve.

6.2   Investigation of the Catalytic Performance of a Co-Based FT Catalyst in the Three Bed Reactor System

As introduced in chapter 1, the iron FT catalysts generate more olefins (predominately linear 1-olefins) than cobalt FT catalysts, even at the same operation conditions and in the same

type of reactor. The cobalt FT catalysts are more hydrogenating and the extent of the water-gas-shift is almost negligible. Cobalt LTFT catalysts generate significant amount of water in the FTS process, which would have a significant influence on the composition of the mixture inside the reactor, and inherently affect the product upgrading reactions. Supported cobalt FT catalysts have been synthesized and investigated previously in our group (Huang et al. 2003, Huang et al. 2004, Elbashir et al. 2004, Elbashir & Roberts 2005). Thus, examinations of the three bed reactor system performance using a cobalt FT catalyst as the FTS catalyst in the first bed should be included in the future work. In addition, cobalt FT catalysts typically produce more long chain hydrocarbons, i.e. the carbon chain growth factor (α) is normally higher than that using iron FT catalysts. In this case, an enhancement in the activity of the hydrocracking/isomerization step should be integrated as well to accommodate the heavier products (i.e. wax) that would be fed into the third bed because of the cobalt FT catlayst.

6.3   Investigation of Different Catalyst Systems in the Three-Bed Reactor System

The types of catalysts that are employed in the reaction system are crucial to the performance of the whole reaction process. The choice of the catalyst synthesis method, the type and concentration of the active metal (or non-metal), catalytic promoters, etc. can all impact the catalytic productivity and selectivity. These factors determine the catalyst particle size, surface area, structure confinement, reducibility, active site distribution and accessibility, chemical surface affinity, stability, etc. and thus the catalytic performance. The catalyst employed for each reaction bed has not been modified in the work described in this dissertation, i.e. common precipitated iron-based FTS catalysts were employed in the FTS stage, a commercially obtained amorphous silica alumina (ASA) catalyst was used in the oligomerization stage, and a 1.0 wt.% Pd/ASA (wetness impregnation method) catalyst was used in the hydrocracking/isomerization

stage. Further development of the catalysts employed in this system is necessary for further optimization of this three-bed reactor process.

There are quite a few research opportunities with respect to modification of the catalyst system. One example involves the introduction of nano-scale metal/metal-oxide particles as catalysts (supported or unsupported with catalytic supports). Davis and coworkers reported alumina-supported iron oxide nanoparticles as active FTS catalysts (Park et al. 2010). Significant expertise exists in the Roberts laboratory for the synthesis of iron-oxide nanoparticles, cobalt nanoparticles, and palladium nanoparticles, and this should be very helpful in future investigations. In addition, bimetallic nanoparticle and nano-sized catalytic supports can also be investigated in order to optimize the catalytic performance.

Another meaningful topic is to explore involves the use of other solid acid catalysts (instead of ASA) as the catalyst in the oligomerization stage, and as the support for the hydrocracking/isomerization catalyst. The type, structure confinement, surface acidity, etc. can be investigated in order to yield the desired product distribution using the three-bed reactor system.

6.4   Investigation of Fuel Properties of the Products

While the FTS product distributions have been evaluated in chapter 3 and chapter 4, the specific fuel properties that these products possess have not been examined. Cold flow properties (cloud point, pouring point, and cold filter plugging point), fuel density, fuel energy density, octane number, etc. should be examined for the products obtained from this three bed system. Standard testing method, such as ASTM D2699-12, should be used to evaluate the product performance.

Reference

M. E. Dry, The Fischer–Tropsch Process: 1950–2000, *Catalysis Today* 71 (2002) 227 - 241

A. de Klerk, Can Fischer-Tropsch Syncrude Be Refined to On-Specification Diesel Fuel, *Energy Fuels* 23 (2009), 4593 - 4604

P. Steynberg, M. E. Dry (Editors), Fischer-Tropsch Technology, ISBN 978-0-444-51354-0, 2004

N. Hamelinck, A. P.C. Faaij, H. D. Uil, H. Boerrigter, Production of FT Transportation Fuels from Biomass: Technical Options, Process Analysis and Optimisation, and Development Potential. *Energy* 29 (2004), 1743 - 1771

D.J. Wilhelm, D.R. Simbeck, A.D. Karp, R.L. Dickenson, Syngas Production for Gas-To-Liquids Applications: Technologies, Issues and Outlook, *Fuel Processing Technology* 71 (2001) 139 - 148

Christopher Higman, Maarten van der Burgt, Gasification. ISBN-13 978-0-750-67707-3, 2003

M. J.A. Tijmensen, A. P.C. Faaij, C. N. Hamelinck, M. R.M. van Hardeveld, Exploration of the Possibilities for Production of Fischer Tropsch Liquids and Power via Biomass Gasification, *Biomass and Bioenergy* 23 (2002) 129 – 152

W. Keim, Catalysis in C1 Chemistry. ISBN 978-9-027-71527-2, 1983

Y. Khodakov, W. Chu, P. Fongarland, Advances in the Development of Novel Cobalt Fischer Tropsch Catalysts for Synthesis of Long-chain Hydrocarbons and Clear Fuels, *Chemical Reviews* 107 (2007), (5) 1692 - 1744

http://www.sasol.com/sasol_internet/frontend/navigation.jsp?navid=700003&rootid=2

http://sasol.investoreports.com/sasol_sf_2011/technology-and-production/gtl-and-ctl-technology

P. Steynberg, R. L. Espinoza, B. Jager, A. C. Vosloo, High Temperature Fischer–Tropsch Synthesis in Commercial Practice, *Applied Catalysis A: General* 186 (1999) 41 - 54

B. Jager, M. E. Dry, T. Shingles and A. P. Steynberg, Experience with a New Type of Reactor for Fischer - Tropsch Synthesis, *Catalysis Letter* 7 (1990) 293 - 302

R. L. Espinoza, A. P. Steynberg, B. Jager, A. C. Vosloo, Low Temperature Fischer–Tropsch Synthesis from a Sasol Perspective, *Applied Catalysis A: General* 186 (1999) 13 - 26

B. Jager, R. L. Espinoza, Advances in Low Temperature Fischer-Tropsch Synthesis, *Catalysis Today* 23 (1995) 17 - 28

H. Kolbel, M. Ralek, The Fischer - Tropsch Synthesis in the Liquid Phase, *Catalyst Reviews* 21 (1980) (2) 225 - 274

J. Duvenhage, T. Shingles, Synthol Reactor Technology Development, *Catalysis Today* 71 (2002) 301 - 305

K. Agee, R. L. Espinoza, Future Role and Characteristics of the Fischer - Tropsch Technology, *Presentation - AIChE Spring Meeting* (2010): Coal, Biomass, and Natural Gas to Liquids I, 10a

E. Iglesia, Design, synthesis, and Use of Cobalt-Based Fischer-Tropsch Synthesis Catalysts (Review), *Applied Catalysis A: General* 161 (1997) 59 - 78

M. E. Dry, Commercial Conversion of Carbon Monoxide to Fuels and Chemicals, *JournaI of Organometallic Chemistry* 372 (1989) 117-127

P. J. van Berge, R. C. Everson, Cobalt as an Alternative Fischer- Tropsch Catalyst to

Iron for the Production of Middle Distillates, Natural Gas Conversion IV, p207-212, ISBN 978-0-444-82352-6, 1997

D. Schanke, A. M. Hilmen, E. Bergene, K. Kinnari, E. Rytter, E. Adnanes, and A. Holmen, Reoxidation and Deactivation of Supported Cobalt Fischer-Tropsch Catalysts, *Energy to Fuels* 10 (1996) 867 - 878

M. Hilmen, D. Schanke, K. F. Hanssen, A. Holmen, Study of the Effect of Water on Alumina Supported Cobalt Fischer–Tropsch Catalysts, *Applied Catalysis A: General* 186 (1999) 169 - 188

P. J. van Berge, J. van de Loosdrecht, S. Barradas, A. M. van der Kraan, Oxidation of Cobalt Based Fischer–Tropsch Catalysts as a Deactivation Mechanism, *Catalysis Today* 58 (2000) 321 - 334

G. Jacobs, T. K. Das, Y. Zhang, J. Li, G. Racoillet, B. H. Davis, Fischer–Tropsch Synthesis: Support, Loading, and Promoter Effects on the Reducibility of Cobalt Catalysts, *Applied Catalysis A: General* 233 (2002) 263 - 281

H. Xiong, Y. Zhang, K. Liew, J. Li, Fischer–Tropsch Synthesis: The Role of Pore Size for Co/SBA-15 Catalysts, *Journal of Molecular Catalysis A: Chemical* 295 (2008) 68 - 76

A. Martínez, C. López, F. Márquez, I. Díaz, Fischer–Tropsch Synthesis of Hydrocarbons over Mesoporous Co/SBA-15 Catalysts: The Influence of Metal Loading, Cobalt Precursor, and Promoters, *Journal of Catalysis* 220 (2003) 486 - 499

F. Morales, B. M. Weckhuysen, Promotion Effects in Co-Based Fischer-Tropsch Catalysis, *Catalysis* 19 (2006) 1 - 40

R. Oukaci, A. H. Singleton, J. G. Goodwin, Comparison of Patented Co F-T Catalysts Using Fixed-Bed and Slurry Bubble Column Reactors, *Applied Catalysis A: General* 186

(1999) 129 - 144

E. Iglesia, S. L. Soled, R. A. Fiato, G. H. Via, Bimetallic Synergy in Cobalt Ruthenium Fischer-Tropsch Synthesis Catalysts, *Journal of Catalysis* 143 (1993) 345 - 368

M. K. Niemela, A.O. Krause, T. Vaara, J. J. Kiviaho, M. K. Rienikainen, The Effect of the Precursor on the Characteristics of Co/SiO$_2$ Catalysts, *Applied Catalysis A*: *General* 147 (1996) 325 - 345

C. H. Bartholomew, R. C. Reuel, Cobalt-support Interactions, Their Effects on Adsorption and CO Hydrogenation Activity and Selectivity Properties, *Industrial Engineering Chemical Production Research* 24 (1985) 56 - 61

G. L. Bezemer; J. H. Bitter, H. P. C. E. Kuipers, H. Oosterbeek, J. E. Holewijn, X. Xu, F. Kapteijn, A. J. van Dillen, K. P. de Jong, Cobalt Particle Size Effects in the Fischer-Tropsch Reaction Studied with Carbon Nanofiber Supported Catalysts, *Journal of the American Chemical Society* 128 (2006) 3956 - 3964

J. Wilson, C. de Groot, Atomic-scale Restructuring in High-Pressure Catalysis, *Journal of Physical Chemistry* 99 (1995) 7860 - 7866

M. Adachi, K. Yoshii, Y. Z. Han, K. Fujimoto, Fischer - Tropsch Synthesis with Supported Cobalt Catalyst. Promoting Effects of Lanthanum Oxide for Cobalt/silica Catalyst, *Bulletin of the Chemical Society of Japan* 69 (1996) 1509 - 1516

F. Rohr, O. A. Lindvåg, A. Holmen, E.A. Blekkan, Fischer-Tropsch Synthesis over Cobalt Catalysts Supported on Zirconia-modified Alumina, *Catalysis Today* 58 (2000) 247 - 254

G. L. Bezemer, P. B. Radstake, U. Falkb, H. Oosterbeek, H. P. C. E. Kuipers, A. J. van Dillen, K. P. de Jong, Investigation of Promoter Effects of Manganese Oxide on Carbon

Nanofiber-Supported Cobalt Catalysts for Fischer–Tropsch Synthesis, *Journal of Catalysis* 237 (2006) 152 - 161

B. Cornils, W. A. Herrmann, R. Schlogl, C. H. Wong (Editors), Catalysis from A to Z, A Concise Encyclopedia, Wiley-VCH, Weinheim, ISBN 3-527-29855-X, 2000

S. Sun, K. Fujimoto, Y. Yoneyama, N. Tsubaki, Fischer-Tropsch Synthesis Using Co/SiO_2 Catalysts Prepared from Mixed Precursors and Addition Effect of Noble Metals, *Fuel* 81 (2002) 1583 - 1591

S. M. Kim, J. W. Bae, Y. J. Lee, K. W. Jun, Effect of CO_2 in the Feed Stream on the Deactivation of $Co/\gamma-Al_2O3$ Fischer–Tropsch Catalyst, *Catalysis Communication* 9 (2008) 2269 - 2273

H. Pichler, Review of 25 Years Research on the Fischer-Tropsch Synthesis and Related Processes, with Especial Attention to the Reaction Mechanism Involved, *Brennstoff-Chemie* 1 (1952) 89-96

T. K. Das, G. Jacobs, P. M. Patterson, W. A. Conner, J. l. Li, B. H. Davis, Fischer-Tropsch Synthesis: Characterization and Catalytic Properties of Rhenium Promoted Cobalt Alumina Catalysts, *Fuel* 82 (2003) (7) 805 - 815

J. G. Chen, H. W. Xiang, H. Y. Gao, Y. H. Sun, Study on Deactivation of $Co/ZrO_2/SiO_2$ Catalyst for Fischer Tropsch Synthesis, *Reaction Kinetics Catalysis Letters* 73 (2001) 169 - 177

O. Ducreux, J. Lynch, B. Rebours, M. Roy, P. Chaumette: In Situ Characterization of Cobalt Based Fischer-Tropsch Catalysts: a New Approach to the Active Phase, Natural Gas Conversion V p125, ISBN 978-044-482-9672, 1998

G. P. Van Der Laan, A. A. C. M. Beenackers, Kinetics and Selectivity of the Fischer-

Tropsch Synghesis: A Literature Review. *Catalysis Reviews* 41 (1999), 255 - 318

H. Schulz, Short History and Present Trends of Fischer-Tropsch Synthesis, *Applied Catalysis A: General* 186 (1999) 3 - 12

S. Z. Li, S. Krishnamoorthy, A. W. Li, G. D. Meitzner, E. Iglesia, Promoted Iron-based Catalysts for the Fischer–Tropsch Synthesis: Design, Synthesis, Site Densities, and Catalytic Properties, *Journal of Catalysis* 206 (2002) 202 - 217

M. E. Dry, The Fischer-Tropsch Synthesis, *Catalysis*, J.R. Anderson and M. Boudart (Editors), ISBN 978-038-710-353-21981, 1981

B. H. Davis, Fischer-Tropsch Synthesis: Relationship Between Iron Catalyst Composition and Process Variables, *Catalysis Today* 84 (2003) 83 - 98

W. Ngantsoue-Hoc, Y. Q. Zhang, R. J. O'Brien, M. S. Luo, B. H. Davis, Fischer-Tropsch Synthesis: Activity and Selectivity for Group I Alkali Promoted Iron-based Catalysts, *Applied Catalysis A: General* 236 (2002) 77 - 89

M. S. Luo, B. H. Davis, Fischer-Tropsch Synthesis: Group II Alkali-earth Metal Promoted Catalysts, *Applied Catalysis A: General* 246 (2003) 171 - 181

R. J. O'Brien, L. G. Xu, R. L. Spicer, S. Q. Bao, D. R. Milburn, B. H. Davis, Activity and Selectivity of Precipitated Ion Fischer-Tropsch Catalysts, *Catalysis Today* 36 (1997) 325 - 334

M. S. Luo, R. O'Brien, B. H. Davis, Effect of Palladium on Iron Fischer-Tropsch Synthesis Catalysts, *Catalysis Letters* 98 (2004) 17 - 22

H. N. Pham, A. K. Datye, The Synthesis of Attrition Resistant Slurry Phase Iron Fischer-Tropsch Catalysts, *Catalysis Today* 58 (2000) 233 - 240

D. B. Bukur, C. Sivaraj, Supported Iron Catalysts for Slurry Phase Fischer - Tropsch

Synthesis, *Applied Catalysis A: General* 231 (2002) 201 - 214

A. A. Adesina, Hydrocarbon Synthesis via Fischer-Tropsch Reaction: Travails and Triumphs, *Applied Catalysis A: General* 138 (1996) 345 - 367

R. J. Madon, S. C. Reyes, E. Iglesia, Primary and Secondary Reaction Pathways in Ruthenium-catalyzed Hydrocarbon Synthesis, *Journal of Physical Chemistry* 95 (1991) 7795 - 7804

E. Durham, S. H. Zhang, C. Roberts, Diesel-length Aldehydes and Ketones via Supercritical Fischer Tropsch Synthesis on an Iron Catalyst, *Applied Catalysis A: General* 386 (2010) 65 - 73

J. T. Kummer, P. H. Emmett, Hydrogen Exchange Reactions over Iron Synthetic Ammonia Catalysts at 195º, *Journal of Physical Chemistry* 56 (1952) 258 - 261

A. T. Bell, Catalytic Synthesis of Hydrocarbons over Group VIII Metals. A Discussion of the Reaction Mechanism, *Catalysis Reviews* 23 (1981) 203 - 232

J. T. Kummer, P. H. Emmett, Fischer-Tropsch Synthesis Mechanism Studies. The Addition of Radioactive Alcohols to the Synthesis Gas, *Journal of American Chemistry Society* 75 (1953) (21) 5177-5183

W. K. Hall, R. J. Kokes, P. H. Emmett, Mechanism Studies of the Fischer- Tropsch Synthesis: the Incorporation of Radioactive Ethylene, Propionaldehyde and Propanol, *Journal of American Chemical Society* 82 (1960) (5) 1027-1037

G. Blyholder, M. Lawless, Hydrogen-assisted Dissociation of CO on a Catalyst Surface, *Langmuir* 7 (1991) 140 - 141

O. R. Inderwildi, S. J. Jenkins, D. A. King, Fischer-Tropsch Mechanism Revisited: Alternative Pathways for the Production of Higher Hydrocarbons from Synthesis Gas.

Journal of Physical Chemistry C Letter 112 (2008) 1305 - 1307

X. P. Dai, C. C. Yu, H$_2$-Induced CO Adsorption and Dissociation over Co/Al$_2$O$_3$ Catalyst, *Journal of Natural Gas Chemistry* 17 (2008) 365 - 368

M. K. Zhuo, K. F. Tan, A. Borgna, M. Saeys, Density Functional Theory Study of the CO Insertion Mechanism for Fischer Tropsch Synthesis over Co Catalysts, *Journal of Physical Chemistry C* 133 (2009) 8357 - 8365

H. C. Long, M.L. Turner, P. Fornasiero1, J. Ka, M. Graziani1, P. M. Maitlis, Vinylic Initiation of the Fischer–Tropsch Reaction over Ruthenium on Silica Catalysts, *Journal of Catalysis* 167 (1997) 172 - 179

Z. P. Liu, P. Hu, A New Insight into Fischer-Tropsch Synthesis, *Journal of the American Chemical Society* 124 (2002) 11568 - 11569

B. H. Davis, Fischer–Tropsch Synthesis: Current Mechanism and Futuristic Needs, *Fuel Processing Technology* 71 (2001) 157 - 166

L. M. Tau, H. A. Dabbahg, B. H. Davis, Fischer-Tropsch Synthesis: Comparison of [14]C Distributions When Labeled Alcohol is Added to the Synthesis Gas, *Energy Fuels* 5 (1991) 174 - 179

R. Srinivasan, L. G. Xu, R. L. Spicer, F. L. Tungate, B. H. Davis, Fischer-Tropsch Catalysts. Attritions of Carbided Iron catalyst in the Slurry Phase, *Fuel Science and Technology International* 14 (1996) 1337 - 1359

C. M. Masuku, D. Hildebrandt, D. Glasser, Olefin Pseudo-equilibrium in the Fischer-Tropsch Reaction, *AIChE Spring Meeting* (2010) Presentation 33c.

X. J. Lu, D. Hildebrandt, D. Glasser, A Termodynamic Approach to the Olefin Products Distribution in Fischer-Tropsch Synthesis, *AIChE Spring Meeting* (2010) Presentation 10c

K. P. Johnston and J. M. L. Penninger, Eds, Supercritical Fluid Science and Technology, ISBN 0841216789, 1989

W. H. Hauthal, Advances with Supercritical Fluids (review), *Chemosphere* (2001) (43) 123 - 135

R. M. M Abbaslou, J. S. S. Mohammadzadeh, A. K. Dalai, Review on Fischer-Tropsch Synthesis in Supercritical Media, *Fuel Processing Technology* 90 (2009) 849-856

X. Lang, A. Akgerman, D. B. Bukur, Steady State Fischer-Tropsch Synthesis in supercritical Propane, *Industrial & Engineering Chemistry Research* 34 (1995) 72-77

B. Subramaniam. Enhancing the Stability of Porous Catalysts with Supercritical Reaction Medi,. *Applied Catalysis A: General* 222 (2001) 199-233

K. Yokota, K. Fujimoto, Supercritical Phase Fischer-Tropsch Synthesis Reaction, *Fuel* 68 (1989) 255 - 256

L. Fan, K. Fujimoto, Fischer-Tropsch synthesis in Supercritical Fluids: Characteristics and Application, *Applied Catalysis A: General* 186 (1999) 343 - 354

N. O. Elbashir, D. B. Bukur, E. Durham, C. B. Roberts, Advancement of Fischer-Tropsch Synthesis via Utilization of Supercritical Fluid Reaction Media, *AIChE Journal* 56 (2010) (4), 997-1015

J. Benoit, Supercritical Phase Fischer-Tropsch Synthesis Inhibition of CO_2 Selectivity for Enhanced Hydrocarbon Production, Theses, 2008

D. B. Bukur, X. S. Lang, A. Akgerman, Z. T. Feng, Effect of Process Conditions on Olefin Selectivity during Conventional and Supercritical Fischer-Tropsch Synthesis, *Industrial & Engineering Chemistry Research* (1997) 36 (7), 2580-2587

S. R. Yan, L. Fan, Z. X. Zhang, J. L. Zhou, K. Fujimoto, Supercritical Phase Process for

Selective Synthesis of Heavy Hydrocarbons from Syngas on Cobalt Catalysts, *Applied Catalysis A: General* 186 (1998) 247-254

N. Tsubaki, K. Yoshii, K. Fujimoto, Anti-ASF Distribution of Fischer-Tropsch Hydrocarbons in Supercritical-Phase Reactions. *Journal of Catalysis* 207 (2002) 371-375

G. Jacobs, K. Chaudhari, D. Sparks, Y. Q. Zhang, B. C. Shi, R. Spicer, T. K. Das, J. L. Li, B. H. Davis, Fischer-Tropsch Synthesis: Supercritical Conversion Using a Co/Al$_2$O$_3$ Catalyst in a Fixed Bed Reactor, *Fuel* 82 (2003) 1251-1260

W. S. Linghu, X. Li, K. Asami, K. Fujimoto, Supercritical Phase Fischer-Tropsch synthesis over Cobalt Catalyst, *Fuel Processing Technology* 85 (2004) 1121-1138

X. W. Huang, N. O. Elbashir, C. B. Roberts, Supercritical Solvent Effects on Hydrocarbon Product Distributions from Fischer Tropsch Synthesis over an Alumina-Supported Cobalt Catalyst, *Industrial & Engineering Chemistry Research* 43 (2004) 6369-6381

B. C. Shi, G. Jacobs, D. Sparks, B. H. Davis, Fischer- Tropsch Synthesis: C^{14} labeled 1-Alkene conversion Using Supercritical Conditions with Co/Al$_2$O$_3$, *Fuel* 84 (2005) 1093-1098

A. Irankhah, A. Haghtalab, Fischer- Tropsch Synthesis Over Co-Ru/γ-Al$_2$O$_3$ Catalyst in Supercritical Media, *Chemical Engineering & Technology* 31 (2008) 525-536

K. Yokota, K. Fujimoto, Supercritical-Phase Fischer-Tropsch Synthesis Reaction. 2. The Effective Diffusion of Reactant and Products in the Supercritical-Phase Reaction, *Industrial & Engineering Chemistry Research* 30 (1991) 95-100

K. Yokota, Y. Hanakata, K. Fujimoto, Supercritical-Phase Fischer-Tropsch Synthesis Reaction. 3. Extraction Capability of supercritical Fluids, *Fuel* 70 (1991) 989-994

X. W. Huang, C. B. Roberts, Selective Fischer-Tropsch Synthesis over an Al$_2$O$_3$

Supported Cobalt Catalyst in Supercritical Hexane, *Fuel Processing Technology* 83 (2003) 81-99

N. O Elbashir, P. Dutta, A. Manivannan, M. S. Seehra, C. B. Roberts, Impact of Cobalt-Based Catalyst Characteristics on the Performance of Conventional Gas-Phase and Supercritical-Phase Fischer Tropsch Synthesis, *Applied Catalysis A: General* 285 (2005) 169-180

N. O Elbashir, C. B. Roberts, Enhanced Incorporation of α-Olefins in the Fischer-Tropsch Synthesis Chain-growth Process over and Alumina-supported Cobalt Catalyst in Near-Critical and supercritical Hexane Media, *Industrial & Engineering Chemistry Research* 44 (2005) 505

D. B. Bukur, X. S. Lang, L. Nowicki, Comparative Study of an Iron Fischer-Tropsch Catalyst Performance in Stirred Tank Slurry and Fixed-Bed Reactors, *Industrial & Engineering Chemistry Research* 44 (2005) 6038-6044

W. S. Linghu, X. H. Li, K. Asami, K. Fujimoto, Process Design and Solvent Recycle for the Supercritical Fischer-Tropscher Syntheis, *Energy and Fuels* 20 (2006) 7-10

X. H. Liu, W. S. Linghu, X. H. Li, K. Asami, K. Fujimoto, Effect of Solvent on Fischer-Tropsch Synthesis, *Applied Catalysis A: General* 303 (2006) 251-257

W. S. Linghu, X. H. Li, K. Fujimoto, Supercritical and Near-Critical Fischer-Tropsch Syntheis: Effects of Solvents, *Journal of Fuel Chemistry and Technology* 35 (2007) (1) 51-56

A. Irankhah, A. Haghtalab, E. V. Farahani, K. sadaghianizadeh, Fischer-Tropsch Reaction Kinetics of Cobalt Catalyst in supercritical Phase, *Journal of Natural Gas Chemistry* 16 (2007) (2) 115-120

H. D. Tang, H. Z. Liu, X. Z. Yang, Y. Li, Supercritical Phase Fischer-Tropsch Synthesis

Reaction over Highly Active Fused Iron Catalyst at Low Temperature, *Journal of Chemical Engineering of Chinese Universities* 22 (2008) (2) 259

E. Durham, S. Zhang, C. B. Roberts, Supercritical Reactivation of Fischer Tropsch Catalysts, *AIChE Annual Meeting* (2008) 678d

E. E. Elmalik, E. Tora, M. El-Halwagi, N. O. Elbashir*,* Solvent Selection for Commercial Supercritical Fischer-Tropsch Synthesis Process, Fuel Processing Technology, 92 (2011) 1525-1530

N. O. Elbashir, B. P. Bao, M. M. El-Halwagi, An Approach to the Design of Advanced Fischer-Tropsch Reactor for Operation in Near-Critical and Supercritical Phase Media, *Advances in Gas Processing: Proceedings of the 1ˢᵗ Annual symposium on Gas Processing Symposium* 1 (2009) 423-433

A. de Klerk, Hydroprocessing Peculiarities of Fischer-Tropsch Syncrude, *Catalysis Today* 130 (2008) 439-445

N. M. Prinsloo, Solid Phosphoric Acid Oligomerization: Manipulating Diesel Selectivity by Controlling Catalyst Hydration, *Fuel Processing Technology* 87 (2006) 437-442

R. F. Jameson, The Composition of the "Strong" Phosphoric Acids, *Journal of the Chemical Society* (1959) 752-759

E. H. Brown, C. D. Whitt, Vapor Pressure of Phosphoric Acids, *Industrial & Engineering Chemistry* 44 (1952) 615-618

Directive 98/69/EC of the European Parliament and of the Council of 13 October 1998

T. L. Alleman, R. L. McCormick, Fischer-Tropsch Diesel Fuels - Properties and Exhaust Emissions: A Literature Review, SAE Paper 2003-01-0763, 2003

K. Nakakita, H. Ban, S. Takasu, Y. Hotta, K. Inagaki, W. Weissman, J. T. Farrell, Effect

of Hydrocarbon Molecular Structure in Diesel Fuel on In-Cylinder Soot Formation and Exhaust Emissions, SAE Paper 2003-01-1914, 2004

X. Dupain, R. A. Krul, M. Makkee, Are Fischer–Tropsch Waxes Good Feedstocks for Fluid Catalytic Cracking Units?, *Catalysis Today* 106 (2005) 288-292

A. de Klerk, thermal Cracking of Fischer-Tropsch Waxes, *Industrial & Engineering Chemistry Research*, 46 (2007) 5516-5521

S. T. Sie, M. M. G. Senden, H. M. H. Van Wechem, Conversion of Natural Gas to Transportation Fuels via the Shell Middle Distillate Synthesis Process (SMDS), *Catalysis Today* 8 (1991) 371-394

D. O. Leckel, D. Liwanga-Ehumbu, Diesel-Selective Hydrocracking of an Iron-Based Fischer−Tropsch Wax Fraction (C15−C45) Using a MoO3-Modified Noble Metal Catalyst, *Energy & Fuels* 20 (2006) 2330-2336

V. Calemma, C. Gambaro, W. O. Parker Jr., R. carbone, R. giardino, P. Scorletti, Middle Distillates from Hydrocracking of FT Waxes: Composition, Characteristics and Emission Properties, *Catalysis Today* 149 (2010) (1-2) 40-46

V. Calemma, S. Peratello, S. Pavoni, , Hydroconversion of a Mixture of Long Chain n-Paraffins to Middle Distillate: Effect of the Operating Parameters and Products Properties, in: E. Iglesia, J.J. Spivey, T. H. Fleisch (Editors), *Studies of Surface Science Catalysis, Elsevier,* vol. 136, 2001

J. Abbot, P. R. Dunstan, Catalytic Cracking of Linear Paraffins: Effect of Chain Length, *Industrial & Engineering Chemistry Research,* 36 (1997) 76-82

I. Rossetti, C. Gambaro, v. Calemma, Hydrocracking of Long Chain Linear Paraffins, *Chemical Engineering Journal* 154 (2009) 295-301

H. Deldari, Suitable Catalysts for Hydroisomerization of Long-chain Normal Paraffins, *Applied Catalysis A: General* 293 (2005) 1-10

Z. W. Liu, X. H. Li, K. Asami, K. Fujimoto, Syngas to Isoparaffins over Co/SiO$_2$ Combined with Metal/Zeolites Catalyst, *Fuel Processing Technology* 88 (2007) 165-170

Z. W. Liu, X. H. Li, K. Asami, K. Fujimoto, High Performance Pd/beta Catalyst for the Production of Gasoline-Range Iso-Praffins via a Modified Fischer-Tropsch Reaction, *Applied Catalysis A: Gen*eral 300 (2006) 162-169

F. G. Botes, W. Bohringer, The Addition of HZSM-5 to the Fischer Tropsch Process for Improved Gasoline Production, *Applied Catalysis A: General* 267 (2004) 217-225

W.H. Lee, S. M. Jeong, J. H. chae, J. H. Kang, W. J. Lee, Coke Formation on KVO3−B2O3/SA5203 Catalysts in the Catalytic Pyrolysis of Naphtha, *Industrial & Engineering Chemistry Research* 43 (2004) 1820-1826

M. Golombok, J. de Bruijn, Dimerization of n-Butenes for High Octane Gasoline Components, *Industrial & Engineering Chemistry Research* 39 (2000) 285-291

PEP Report 248, Steam Cracking for Olefins Production, 2003

R. Mukhopadhyay, G. V. R. Rao, Thermodynamic Modeling for Supercritical Fluid Process Design, *Industrial & Engineering Chemistry Research* 32 (1993) 1914-1920

J. Towfighi, H. Zimmermann, R. Karimzadeh, M. M. Akbarnejad, Steam Cracking of Naphtha in Packed Bed Reactors, *Industrial & Engineering Chemistry Research* 41 (2002) 1419-1424

Z. Dardas, M. G. Suer, Y. H. Ma, W. R. Moser, A Kinetic Study of n-Heptane Catalytic Cracking over a Commercial Y-Type Zeolite under Supercritical and Subcritical Conditions, *Journal of Catalysis* 162 (1996) 327-338

A. de Klerk, Hydrotreating in a Fischer-Tropsch refinery, 2nd Sub-Saharan Africa Catalyst Symposium, Swakopmund, Namibia 5-7 Nov (2001)

J. Stell, Worldwide catalyst report, Oil Gas J., 99:41 (2001) 56-76

M. E. Dry, Fischer–Tropsch reactions and the environment, *Applied Catalysis A: General* 189 (1999) 185 - 190

D. B. Bukur, M. Koranne, X. Lang, K. R. P. M. Rao, G. P. Huffman, Pretreatment Effect Studies with a Precipitated Iron Fischer-Tropsch Catalyst, *Applied Catalysis A: General,* 126 (2005) 85-113

M. E. Dry, High Quality Diesel via the Fischer–Tropsch Process – a Review, *Journal of Chemical Technology and Biotechnology* 77 (2002) 43-50

D. B. Bukur, C. Sivaraj, Supported Iron Catalysts for Slurry Phase Fischer–Tropsch Synthesis, *Applied Catalysis A: General* 231 (2002) 201-214

S. A. Elaison, C. H. Bartholomew, Reaction and Deactivation Kinetics for Fischer–Tropsch Synthesis on Unpromoted and Potassium-promoted Iron Catalysts, *Applied Catalysis A: General186 (1999) 229-243*

A. Bisio, C. Atkinson, Shouldn't we know the molecular composition of Fischer-Tropsch diesel fuels, *Fuel Chemistry Division Preprints* 47 (2002) 496 - 497

V. Calemma, S. Peratello, S. Pavoni, G. Clerici, C. Perego, Hydroconversion of a mixture of long chain n-paraffins to middle distillate: effect of the operating parameters and products properties, Studies on Surface Science Catalysis 136 (2001) 307

W. A. Dietz, Response factors for gas chromatographic analyses, *Journal of Gas Chromatography* 5 (1967) 68

D. Leckel, Noble metal wax hydrocracking catalysts supported on high-siliceous

alumina Industrial Engineering Chemistry Research 46 (2007) 3505 – 3512

A. de Klerk, Effect of Oxygenates on the Oligomerization of Fischer-Tropsch Olefins over Amorphous Silica-Alumina, *Energy & Fuels* 21 (2007) 625 – 632

J. H. Gary, G. E. Handwerk, Petroleum Refining Technology and Economics, 4th ed. ISBN 978-082-470-4827, Marcel Dekker, Inc. (New-York) 2001

T. G. Kaufmann, A. Kaldor, G. F. Stuntz, M. C. Kerby, L. L. Ansell, Catalysis science and technology for cleaner transportation fuels, *Catalysis Today* 62 (2000) 77 – 90

V. M. Akhmedov, A. Khowaiter, H. Soliman, Recent advances and future aspects in the selective isomerization of high n-Alkanes, *Catalysis Reviews* 49 (2007) 33 – 139

J. A. Martens, P. A. Jacobs, J. Weitkamp, Attempts to rationalize the distribution of hydrocracked products: I. qualitative description of the primary hydrocracking modes of long chain paraffins in open zeolites, *Applied Catalysis* 20 (1986) 239 – 281

J. Weitkamp, Isomerization of long-chain n-alkanes on a Pt/CaY zeolite catalyst, *Industrial and Engineering Chemistry Product Research and Development* 21 (1982) 550 - 558

Y. Liu, C. Liu, C. Liu, Z. J. Tian, L. Lin, Sn-modified Pt/SAPO-11 catalysts for selective hydroisomerization of n-paraffins, *Energy and Fuels* 18 (2004) 1266 - 1271

F. Alvarez, F.R. Ribeiro, G. Perot, C. Thomazeau, M. Guisnet, Hydroisomerization and hydrocracking of alkanes: 7. Influence of the balance between acid and hydrogenating functions on the transformation of n-decane on PtHY catalysts, *Journal of Catalysis* 162 (1996) 179 – 189

J.M. Campelo, F. Lafont, J.M. Marinas, Hydroconversion of n-dodecane over Pt/SAPO-11 catalyst, *Applied Catalysis A: General* 170 (1998) 139 - 144

J. Walendziewski, B. Pniak, Synthesis, physicochemical properties and hydroisomerization activity of SAPO-11 based catalysts, *Applied Catalysis A: General* 250 (2003) 39 - 47

K.C. Park, S.K. Ihm, Comparison of Pt/zeolite catalysts for n-hexadecane hydroisomerization, Applied Catalysis A: General 203 (2000) 201 - 209

V. Calemma, S. Peratello, C. Perego, Hydroisomerization and hydrocracking of long chain n-alkanes on Pt/amorphous SiO_2–Al_2O_3 catalyst, *Applied Catalysis A: General* 190 (2000) 207 – 218

D. M. Brouwer, H. Hogeveen, Electrophilic substitutions at alkanes and in alkylcarbonium ions, A. Streitwieser (Editor), R. W. Taft (Editor), Progress in Physical Organic Chemistry ISBN: 978-0-470-17209-4 1972

M. A. Baltanas, K. K. Van Raemdonck, G. F. Froment, S. R. Mohedad, Fundamental kinetic modeling of hydroisomerization and hydrocracking on noble-metal-loaded faujasites. 1. Rate Parameters for Hydroisomerization, *Industrial and Engineering Chemical Research* 28 (1989) 899 - 910

R. J. Taylor, R. H. Petty, Selective hydroisomerization of long chain normal paraffins, *Applied Catalysis A: General* 119 (1994) 121-138

J. L. Carter, J. A. Cusumano, J. H. Sinfelt, Hydrogenolysis of n-heptane over unsupported metals, *Journal of Catalysis* 20 (1971) 223-229

Z. W. Liu, X. H. Li, K. Asami, K. Fujimoto, Iso-paraffins synthesis from modified Fischer–Tropsch reaction Insights into Pd/beta and Pt/beta catalysts, *Catalysis Today* 104 (2005) 41 - 47

A. Forney, W. P. Heynes, J. J. Elliott, A. C. Zarochak, Fischer-Tropsch process: gasoline

from coal, *ACS Division of Fuel* 20 (1975) 171 – 181

S. R. Yan, L. Fan, Z. X. Zhang, J. L. Zhou, K. Fujimoto, *Applied Catalysis* A 171 (1998) 247-254

A de Klerk, Oligomerization of Fischer-Tropsch Olefins to Distillates over Amorphous Silica-Alumina, *Energy & Fuels* 20 (2006) 1799-1805

D. M. Brouwer, The mechanism of double-bond isomerization of olefins on solid acids, *Journal of Catalysis* 1 (1962) 22-31

P. J. van Berge, R. C. Everson, Cobalt as an alternative Fischer-Tropsch catalyst to iron for the production of middle distillates, in: M. de Pontes, *et al*. (Eds.), Natural Gas Conversion IV, *Elsevier* (1997) 207-212

N. Tsubakia, Y. Yoneyamaa, K. Michikib, K. Fujimoto, Three-component Hybrid Catalyst for Direct Synthesis of Isoparaffin via Modified Fischer–Tropsch Synthesis, *Catalysis Communications* 4 (2003) 108 - 111

F.G. Botes, W. Böhringer, The Addition of HZSM-5 to the Fischer–Tropsch Process for Improved Gasoline Production, *Applied Catalysis A: General* 267 (2004) 217 - 225

F. G. Botes, The Effect of a Higher Operating Temperature on the Fischer–Tropsch/ HZSM-5 Bifunctional Process, *Applied Catalysis A: General* 285 (2005) 21 - 29

J. J. He, Y. Yoneyama, Bo. Xu, N. Nishiyama, N. Tsubaki, Designing a Capsule Catalyst and Its Application for Direct Synthesis of Middle Isoparaffins, *Langmuir* 21 (2005) 1699 - 1702

T. Nowitzki, A. F. Carlsson, O. Martyanov, M. Naschitzki, V. Zielasek, T. Risse, M. Schmal, H. J. Freund, M. Ba1umer, Oxidation of Alumina-Supported Co and Co-Pd Model catalysts for the Fischer-Tropsch Reaction, *Journal of Physical Chemistry* 111(2007) 8566 -

8572

V. M. Mysov, K. G. Ione, Bifunctional Catalysts for the Production of Motor Fuels and Aromatic Hydrocarbons from Synthesis Gas, Natural gas conversion VII: proceedings of the 7th Natural Gas Conversion, Studies in Surface Science and Catalysis (volume 147), X. Bao and Y. Xu (Ed.) Elsevier 2004

A. Martinez, G. Prieto, A. Garcia-Trenco, E. Peris, Advanced Catalysts Based on Micro- and Mesoporous Molecular Sieves for the conversion of Natural Gas to Fuels and Chemicals, *Zeolites and Catalysis*, J. Cejka, S. Zones, A. Corma (Eds.), Wiley-VCH, ISBN: 978-3-527-32514-6 (2010)

S. Bessell, Investigation of Bifunctional Zeolite Supported Cobalt Fischer-Tropsch Catalysts, *Applied Catalysis A: General* 126 (1995) 235 - 244

M. A. Marvast, M. sohrabi, S. Zarrinpashne, G. Baghmisheh, Fischer-Tropsch Synthesis: Modeling and Performance Study for Fe-HZSM5 Bifunctional Catlayst, *Chemical Engineering & Technology*, 28 (2005) 78 - 86

Q. J. Ge, X. H. Li, H. Kaneko, K. Fujimoto, Direct Synthesis of LPG from Synthesis Gas over Pd-Zn-Cr/Pd-β Hybrid Catalysts, *Journal of Molecular Catalysis A: Chemical* 278 (2007) 215 - 219

X. H. Li, X. L. Feng, Q. J. Ge, K. Fujimoto, Direct Synthesis of Iso-paraffins from Syngas with Slurry Phase Reaction, *Fuel* 87 (2008) 534 - 538

W. O. Haag, T. J. Huang, U.S. Patent 4,159,995 (1979)

W.O. Haag, T.J. Huang, U.S. Patent 4,279,830 (1981)

Kyung Min Cho, Sun young Park, Jeong Gil Seo, Min Hye Youn, Sung-Hyeon Baeck, Ki-Won Jun, Jin Suk Chung, In Kyu Song, Production of Middle Distillate in a Dual-bed

Reactor from Synthesis Gas through Wax Cracking: Effect of Acid Property of Pd-loaded Solid Acid Catalysts on the Wax Conversion and Middle Distillate Selectivity, *Applied Catalysis B: Environmental* 83 (2008) 195 - 201

V. Udaya, S. Rao, Robert J. Gormley, Bifunctional Catalysis in Syngas Conversions, *Catalysis Today* 6 (1990) 207 - 234

J. A. Brennan, P. D. Caesar, J. C. Pitman, W. E. Garwood, U.S. Patent 4,304,871 (1981)

D. B. Bukur, L. Nowicki, R.K. Manne, X. Lang, Activation Studies with a Precipitated Iron Catalyst for Fischer-Tropsch Synthesis II. Reaction Studies, *Journal of Catalysis* 155 (1995) 366- 375

D. B. Bukur, L. Nowicki, S.A. Patel, Activation Studies with an Iron Fischer-Tropsch Catalyst in Fixed Bed and Stirred Tank Slurry Reactors, *Canadian Journal of Chemical Engineering* 74 (1996) 399 - 404

D. B. Bukur, X. Lang, Y. Ding, Pretreatment effect studies with a precipitated iron Fischer−Tropsch catalyst in a slurry reactor, *Applied Catalysis A: General*, 186 (1999) 255

R. J. O'Brien, L.G. Xu, R. L. Spicer, B. H. Davis, Activation Study of Precipitated Iron Fischer-Tropsch Catalysts, *Energy & Fuels*, 10 (1996) 921-926

P. C. Joyce, B. E. Leggett, M. C. Thies, Vapor−liquid Equilibrium for Model Fischer−Tropsch Waxes (Hexadecane, 1-Hexadecene, and 1-Hexadecanol) in supercritical hexane, *Fluid Phase Equilibria* 158-160 (1999) 723 -731

P. C. Joyce, J. Gordon, M. C. Thies, Vapor−Liquid Equilibria for the Hexane + Tetracosane and Hexane + Hexatriacontane Systems at Elevated Temperatures and Pressures, *Journal of Chemical & Engineering Data* 45 (2000) 424-427

L .Gao, Z. S. Hou, H. F. Zhang, J. He, Z. M. Liu, X. G. Zhang, B. X. Han, Critical

Parameters of Hexane + Carbon Monoxide + Hydrogen and Hexane + Methanol + Carbon Monoxide + Hydrogen Mixtures in the Hexane-Rich Region, *Journal of Chemical & Engineering Data* 46 (2001) 1635-1637

Ⅰ. Polishuk, J. Wisniak, H. Segura, Estimation of Liquid−Liquid−Vapor Equilibria in Binary Mixtures of n-Alkanes, Industrial & Engineering chemistry Research 43 (2004) 5957-5964